Second species orbits of negative action and contact forms in the circular restricted three-body problem

Dissertation

zur Erlangung des akademischen Grades

Dr. rer. nat.

eingereicht an der

Mathematisch-Naturwissenschaftlich-Technischen Fakultät

der Universität Augsburg

von

Robert Nicholls

Augsburg, Mai 2021

Gutachter:	Prof. Dr. Urs Frauenfelder, Universität Augsburg Prof. Dr. Kai Cieliebak, Universität Augsburg Prof. Dr. Otto van Koert, Seoul National University
Tag der mündlichen Prüfung:	28.07.2021

Acknowledgements

During the work on this thesis I have been most kindly assisted in various ways by many people, who I want to thank with all my heart for their generous support.

First and foremost I would like to thank my supervisor Urs Frauenfelder for overseeing my work. You very patiently and readily took your time to help me with your infallible intuition and precise reasoning while at the same time letting me figure things out for my self and allowing me to follow my own ideas freely. I am tremendously grateful for your mathematical support as well as your extremely kind and benevolent manner in which you taught me many lectures, took me along to conferences and suggested further research.

I would also like to thank the international mathematical community and my colleagues at the mathematical department in Augsburg for creating an enjoyable and productive working environment. My special thanks go to Kai Cieliebak, Alexandru Doicu, Pavel Hájek, Soengchan Kim, Otto van Koert, Bowen Liu, Miguel Pereira, Elena Perfilev, Felix Schlenk and Lei Zhao.

For their life-long encouragement and unwavering belief, as well as their overall support and love, I would like to thank my mother Ursula and my sister Julia. You have both always been there for me and I very much appreciate everything you have done for me.

Last but not least I want to thank my girlfriend Lisa for her love and support throughout. You have been a great emotional pillar to me through difficult phases of the project, shared the good times and endured my sometimes unorthodox working times at home.

There are many more great friends, teammates and colleagues who have supported me along the way and though it is impossible for me to list them all here and put my gratitude into words I want to acknowledge all of your gestures, which often went a long way.

Abstract

The restricted three-body problem is the study of the motion of a particle in the gravitational force field of two heavier bodies encircling their common centre of mass. This is a very old mathematical problem which goes back to Euler, Lagrange, Poincaré and others. Since those times many new theoretical fields related to dynamical systems have arrived. Often, a contact structure is required, which is in the case of the restricted three-body problem defined on an energy level set. Such contact structures have been shown to exist in the restricted three-body problem for the bounded component of the regularised energy hypersurface when the energy is below or slightly above the first critical value. This was done by Albers, Frauenfelder, van Koert and Paternain in [AFvKP12] in the planar case and Cho, Jung and Kim in [CJK20] in the spatial case. Above the energy value zero the canonical Liouville 1-form becomes a contact form. But in between these two values it was as yet unknown whether or not the corresponding energy level sets admit contact structures.

We show in this work that the restricted three-body problem is in general not of contact type. More explicitly, sequences of generating orbits with increasingly negative action and energies between $-\sqrt{2}$ and zero are constructed. Using results from [BM00], it is shown that these generating orbits extend to periodic solutions of the restricted three-body problem for small mass ratios and the action remains within a small neighbourhood. These orbits obstruct the existence of contact structures for energy level sets Σ_c of the mentioned values and small mass ratios of the spatial problem. In the planar case the constructed orbits are noncontractible even in the Moser-regularised energy hypersurface $\overline{\Sigma}_c$. Here, the constructed orbits still obstruct the existence of contact structures in certain relative de Rham classes of $\overline{\Sigma}_c$ to the Liouville 1-form. Numerical results are additionally given to visualise the computations and give evidence for the existence of these orbits for higher mass ratios.

Contents

Chapter 1

Historical background and overview

In 1687 Isaac Newton published his famous Philosophiæ Naturalis Principia Mathematica, in which he describes the laws of motion and the inverse square law for gravitational force, thus laying the foundation for modern classical mechanics. In his work he proceeded to solve the old problem of the motion of two point masses being attracted to one another in frictionless space. This problem is known as the two-body problem or the Kepler problem. It's laws of motion were first described by Johannes Kepler in 1609 and 1619 after analysing the very accurate observations by Danish astronomer Tycho Brahe. The main quest in all this research was to understand the motion of our solar system. Consequently, the next logical step after having solved the two-body problem was to introduce a third mass into the equation and try to solve the new system using Newton's laws. However, this proved to be too hard and until today there are only very few exact solutions to the general three-body problem. Famous examples of periodic solutions are Euler's solution from 1767, where all bodies remain collinear and encircle their common centre of mass, Lagrange's solution in 1772, where all bodies remain at the vertices of a rotating triangle, and, more recently, the figure of eight choreography by Chenciner and Montgomery in [CM00].

In order to better understand the three-body problem, some simplified models have been proposed. One of the first was Leonhard Euler who suggested to assume that one body has negligible mass compared to the other two and thus does not influence their motion. Additionally, he fixed the two primaries in space, resulting in what is now known as Euler's problem of two centres. This models for example the classical motion of an electron in the electric field of two fix protons, i. e. the classical dynamics inside a positively charged Hydrogen molecule H_2^+. A variant more adapted to planetary motion is the restricted three-body problem where, similarly, one of the bodies is assumed to have negligible mass but the other two continue to move according to Kepler's laws. The special case which is at the centre of study here is the version where the primaries move in exact circles. This is in full terms referred to as the circular restricted three-body problem but will from now on simply be called the restricted three-body problem. The case where the motion of the particle is confined to the same plane as the primaries will be called the planar case, while we refer to the spatial case if we allow the particle to

move in all of the surrounding three-dimensional space.

The first extensive work on this problem was done by Henry Poincaré in 1892 to 1899 in a series of publications called the 'New methods of Celestial Mechanics', [Poi92, Poi93, Poi99]. He predicted the existence of what he calls second species orbits. These are supposed to be periodic orbits generated by special kinds of collision orbits. However, he does not give a rigorous proof for these second species orbits in the restricted or the full three-body problem, where he conjectured them to exist. First full proofs of their existence in the restricted three-body problem were given by Gomez and Olle in [GO91], Marco and Niedermann in [MN95] and for more general settings by Bolotin and McKay in [BM00].

Since the time of Poincaré, splitting off from the dynamic systems approach, more theoretical structures have been discovered and developed with the aim of solving dynamical problems. These structures arise from works in fields like symplectic and contact geometry, Floer homology and holomorphic curves. In the mentioned fields there are results on the existence of periodic orbits for certain dynamical systems, which have to meet specific requirements. Examples are Floer's work on the Arnold conjecture [Flo88], Hofer's paper on the Weinstein conjecture [Hof93], the existence of disc-like global surfaces of section by Hofer, Wysocki, Zehnder [HWZ98] and by Hryniewicz, Salomão [HSa11], and the usage of holomorphic curves to find a new family of periodic orbits by Belbruno, Frauenfelder, van Koert in [BFvK19b] and [BFvK19a]. But checking these requirements, in particular the contact condition, can be very hard if one is given an explicit dynamical system. Still, a connection between these theoretical fields and dynamical systems looks very promising so far.

For the restricted three-body problem, one hopes to solve the over 100 year old Birkhoff conjecture. In [Bir14] Birkhoff proved the existence of a retrograde periodic orbit and conjectured that it bounds a disc-like global surface of section. That is an embedded disc into the energy level set where the Hamiltonian flow is tangential on the boundary and transversal on the interior of the disc while always returning back to the interior in both forward and backward time. The retrograde orbit is conjectured to be the boundary of such a disc and the return map of the interior would be forced by Brouwer's fixed point theorem of area-preserving maps to have a fixed point. Consequently, another simple periodic orbit must exist, as sketched in figure 1.1. This orbit is then thought to be the direct periodic orbit.

Our earth's moon is moving in the direct—or prograde—direction, that is when the direction of the moon around the earth is the same as earth's around the sun. The other direction is called retrograde, where the bodies rotate in opposite motion. As most moons in our solar system are prograde, there is a very natural and historical interest particularly in the study of direct orbits.

A first step to connecting the restricted three-body problem to these powerful new theories was done by Albers, Frauenfelder, van Koert and Parternain in [AFvKP12], showing that the bounded components of the Moser-regularised energy hypersurface of the planar restricted three-body problem is of contact type below the first critical energy level and also slightly above this value. The same result for the spatial problem

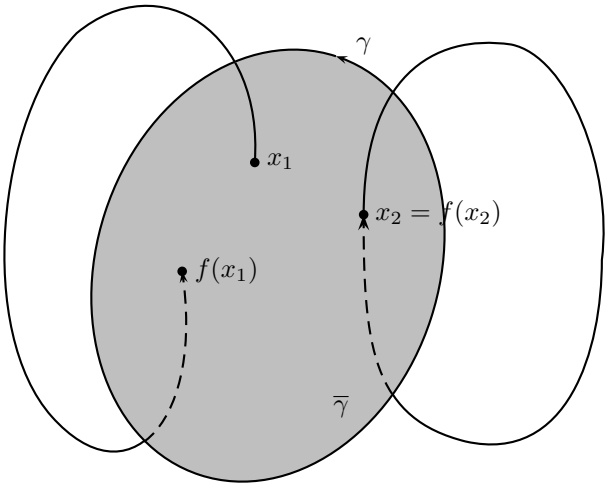

Figure 1.1: Simple periodic orbit arising as the fixed point of the return map on a disclike global surface of section.

was proven by Cho, Jung and Kim in [CJK20]. Although the spatial case has more physical relevance, for example in space mission design, some results on contact manifolds currently only work for three-dimensional manifolds, e.g. energy level sets inside a four-dimensional phase space of a two-dimensional configuration space. For energies above zero the restricted three-body problem again admits a contact structure as the canonical Liouville 1-form becomes a contact form. So the question remains: What happens for energies in between these two values? There are three critical values of the gravitational potential left, so the areas between those and the area between the highest critical value and zero are still open. This present work focuses on the region between the highest critical energy value and zero, and the main statement is the following:

Theorem 1.1:
The spatial restricted three-body problem is in general not of contact type.

Theorem 1.2:
If the planar restricted three-body problem is of contact type between $-\sqrt{2}$ and zero, then the de Rham class of the contact form minus the Liouville 1-form must become infinitely bad for small mass ratios μ.

A more detailed version of the statements can be found in theorem 8.3. In order to explain the result more explicitly, let μ bet the mass ratio of the two primaries M_1 and M_2 of the circular restricted three-body problem. The Hamiltonian is given by

$$H_\mu(q,p) = \frac{1}{2}\left((p_1+q_2)^2 + (p_2-q_1)^2 + p_3^2\right) - \frac{1-\mu}{\|q-M_1\|} - \frac{\mu}{\|q-M_2\|} - \frac{q_1^2+q_2^2}{2},$$

where q are the position coordinates in $\mathbb{R}^3 \setminus \{M_1, M_2\}$ and p are the momentum coordinates in $T_q^*(\mathbb{R}^3 \setminus \{M_1, M_2\})$. The planar case is recovered by setting $q_3 = p_3 = 0$. By the conservation of energy, solutions to this Hamiltonian system with energy $H_\mu = c$ stay in their own energy level set $\Sigma_{\mu,c}$ for all time. For all energies the hypersurface $\Sigma_{\mu,c}$ can be regularised at collision with the primaries using the Moser regularisation. We will denote the regularised energy hypersurface by $\overline{\Sigma}_{\mu,c}$. The question is whether one can find a contact structure α on $\overline{\Sigma}_{\mu,c}$ that is compatible with the symplectic structure ω on $T^*(\mathbb{R}^n \setminus \{M_1, M_2\})$ in the sense that $\mathrm{d}\alpha = \omega$ and orientations are preserved. If that is the case, we can compute the integral of α along an orbit γ by

$$0 < \int \gamma^* \alpha = \int \gamma^* \lambda + \sum \left(r_i \int \gamma^* \beta_i \right),$$

where λ is the canonical Liouville 1-form on the cotangent bundle, β_i are de Rham generators and r_i are the corresponding coefficients of the de Rham class of $\alpha - \lambda$ in $\overline{\Sigma}_c$. The integral $\int \gamma^* \lambda$ is called the action of the orbit. If one now has a contractible periodic orbit with negative action there can not exist a contact structure. The action of noncontractible orbits, on the other hand, only obstructs the existence of contact structures in certain relative de Rham classes.

In the course of this work we will construct orbits with negative action that are contractible even in the original energy hypersurfaces of the spatial problem but noncontractible in the regularised hypersurfaces of the planar problem. The construction happens in the limit case where $\mu = 0$, which is also called the rotating Kepler problem. These generating orbits are shown to continue over to the restricted three-body problem with small mass ratios while maintaining the same energy. Generating orbits of this kind are found for energies between $-\sqrt{2}$ and 0.

The remaining work will be structured as follows: In the second chapter we will explain the theoretical foundations which we will be working with. We will explain some required definitions from symplectic geometry, Hamiltonian mechanics and contact topology, and all the statements that will be used in later chapters. Chapter 3 introduces all the Hamiltonian systems which we will encounter along the way and gives first insights into periodic orbits. Two different methods of how to regularise collisions will be shown in chapter 4 and the computation of the topology of Moser-regularised energy hypersurfaces in chapter 5. Generating orbits in a notation following [Hén97] are introduced in chapter 6 with all their categorising names, and each of their action is computed in chapter 7. In that chapter we will also select the orbits which are needed for the main statement. Finally, in chapter 8 everything is put together and the main statement is proven.

Chapter 2

Symplectic geometry, Hamiltonian mechanics and contact topology

We begin by explaining our notation and presenting standard results without proofs from symplectic geometry, Hamiltonian mechanics and contact topology. All results are well known and can be read up for example in [FvK18] and [Gei08], where most of the definitions and statements are taken from. The remainder comes from [Fra17] and [Fra18].

Definition 2.1:
A *symplectic manifold* (M, ω) is a smooth manifold M equipped with a closed and nondegenerate 2-form ω, called the *symplectic structure* or the *symplectic form*, i. e.

i) $\mathrm{d}\omega = 0$ and

ii) $\forall x \in M, v \in T_xM \backslash \{0\}\ \exists w \in T_xM \colon \omega(v, w) \neq 0$.

If $\omega = \mathrm{d}\alpha$ is exact, we call (M, α) an *exact symplectic manifold*.

A first and simple to prove property is

Lemma 2.2:
Let (M, ω) *be a symplectic manifold, then* $\dim_{\mathbb{R}} M$ *is even.*

This can be seen either by Darboux's theorem 2.8 or by the fact that there do not exist real invertible antisymmetric matrices of odd dimension, which describe ω in the tangent space at a point.

Remark 2.3:
The nondegeneracy of a symplectic form means that $\omega^{\wedge n} \neq 0$ defines a volume form and therefore an orientation on M.

Definition 2.4:
We call a submanifold L of (M, ω) a *Lagrangian* if the symplectic form $\omega|_L = 0$ vanishes on L and it has half the dimension $\dim_{\mathbb{R}} M = 2 \dim_{\mathbb{R}} L$.

Remark 2.5:
A Lagrangian is a submanifold of the maximal dimension where the symplectic form vanishes. For an alternative definition one could first define the symplectic orthogonal complement V^ω of a linear subspace $V \subset T_xM$ as the set

$$V^\omega := \{w \in T_xM : \omega_x(v, w) = 0 \ \forall v \in V\}.$$

One can then easily show by identifying V^ω with the dual of T_xM/V that the dimensions add up to $\dim_{\mathbb{R}} V + \dim_{\mathbb{R}} V^\omega = \dim_{\mathbb{R}} T_xM = \dim_{\mathbb{R}} M$. Then one can define a linear Lagrangian subspace L_x by $L_x^\omega = L_x$. It is obvious then that a linear Lagrangian subspace is half-dimensional and one calls a submanifold L Lagrangian if at every point x the tangent space $T_xL \subset T_xM$ is a linear Lagrangian subspace.

We will look at two examples of symplectic manifolds in the following and also point out some Lagrangian submanifolds within them.

Example 2.6:
The easiest example is the Euclidean space $\mathbb{R}^{2n}$ with the standard symplectic form, defined by

$$\omega_0(v, w) := \langle v, Jw \rangle$$

for tangent vectors $v, w \in T_{(x,y)}\mathbb{R}^{2n} \cong \mathbb{R}^{2n}$, where

$$J := \begin{pmatrix} 0 & -\mathbb{1}_n \\ \mathbb{1}_n & 0 \end{pmatrix}$$

is the canonical invertible antisymmetric matrix and $\langle \cdot\,, \cdot \rangle$ is the Euclidean inner product on $\mathbb{R}^{2n}$. In the standard basis $(x_1, \ldots, x_n, y_1, \ldots y_n)$ of $\mathbb{R}^{2n}$ the symplectic structure then has the form

$$\omega_0 = \sum_{i=1}^{n} \mathrm{d}y_i \wedge \mathrm{d}x_i =: \mathrm{d}y \wedge \mathrm{d}x. \tag{2.1}$$

Lagrangian subspaces in this setting are for example $\mathbb{R}^n \times \{0\}$ and $\{0\} \times \mathbb{R}^n$. In the case $n = 1$ actually every linear subspace is Lagrangian, hence every smooth one-dimensional submanifold is Lagrangian in $(\mathbb{R}^2, \omega_0)$.

Example 2.7:
Most physical settings are defined on the symplectic manifold of a cotangent bundle where the base is a smooth manifold N, called the *configuration space*, which can be thought of as the space of all possible positions. The cotangent bundle T^*N becomes the *phase space* which is the space of all possible states with position and momentum. On T^*N there is a canonical 1-form called the *Liouville 1-form* λ:

In the coordinate-free definition we assign to the tangent vector $\xi \in T_eT^*N$ of the cotangent bundle at the point $e \in T^*N$ the value

$$\lambda(e)\xi := e(\mathrm{d}\pi_N(e)\xi),$$

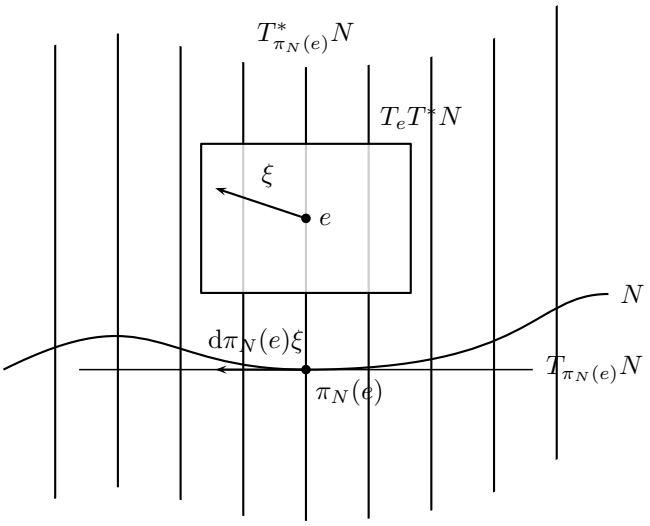

Figure 2.1: Cotangent bundle and footpoint projection of a smooth manifold.

where $\pi_N \colon T^*N \to N$ is the footpoint projection of the bundle.

If $(q_1, \dots q_n)$ are local coordinates of N, then we can write a cotangent vector as $\sum_{i=1}^n p_i \,\mathrm{d}q_i$ and a point in the cotangent bundle becomes $e = (q, p)$. The Liouville 1-form assigns to a tangent vector $(\hat{q}, \hat{p}) \in T_eT^*N$ in these coordinates the value $\lambda(q,p)(\hat{q},\hat{p}) = \sum_{i=1}^n p_i\hat{q}_i$, so the local presentation of λ is

$$\lambda = \sum_{i=1}^n p_i \,\mathrm{d}q_i = p \,\mathrm{d}q.$$

We get a symplectic form on T^*N by taking the exterior derivative of λ,

$$\omega := \mathrm{d}\lambda = \sum_{i=1}^n \mathrm{d}p_i \wedge \mathrm{d}q_i = \mathrm{d}p \wedge \mathrm{d}q.$$

Obviously, ω is closed since it is exact and it is also nondegenerate, as one can easily check, so it defines an exact symplectic structure on T^*N. Examples of Lagrangians here are the base manifold N as the zero section of the cotangent bundle or every fibre T^*_xN.

Both these examples are exact symplectic manifolds with locally the same presentation of the symplectic form. No closed manifold can be exact, since then by Stokes' theorem

$$\int_M \omega^{\wedge n} = \int_{\partial M} \alpha \wedge \omega^{\wedge n-1}$$

would be zero. The local presentation of the symplectic form, however, is nothing special and in fact every symplectic form can be presented by (2.1).

Theorem 2.8 (Darboux):
Every $2n$-dimensional symplectic manifold (M, ω) admits a local chart ϕ with coordinates $(x_1, \dots x_n, y_1, \dots y_n)$ such that $\phi^*\omega = \omega_0$.

For a proof see for example [MZ05].

So in contrast to Riemannian geometry, where there is curvature, symplectic manifolds have no local invariant except dimension.

We next want to define maps between symplectic manifolds that preserve the respective symplectic structures.

Definition 2.9:
Let (M, ω_M) and (N, ω_N) be symplectic manifolds. We call a diffeomorphism $\Phi\colon M \to N$ *symplectic* or a *symplectomorphism* if $\Phi^*\omega_N = \omega_M$. Furthermore, we call Φ *conformally symplectic* with *conformal factor* $c \neq 0$ if $\Phi^*\omega_N = c\omega_M$. If (M, α_M) and (N, α_N) are exact symplectic manifolds, we call Φ *exact symplectic* or an *exact symplectomorphism* if $\Phi^*\alpha_N = \alpha_M$ and *exact conformally symplectic* if $\Phi^*\alpha_N = c\alpha_M$ for some conformal factor $c \neq 0$.

Remark 2.10:
Note that if Φ is (exact) symplectic then so is Φ^{-1}, and if Φ_c is (exact) conformally symplectic with factor c then Φ_c^{-1} is (exact) conformally symplectic with factor $1/c$.

For our first example of a symplectomorphism we want to extend a change of coordinates on a base manifold to a symplectomorphism on the cotangent bundle with the symplectic structure from example 2.7.

Definition 2.11:
Let $\Phi\colon M \to N$ be a diffeomorphism on smooth manifolds and $\pi_M\colon T^*M \to M$ the footpoint projection of the cotangent bundle over M. The *pushforward* of Φ onto the cotangent bundles is defined as

$$\begin{aligned} \mathrm{d}_*\Phi\colon T^*M &\to T^*N \\ e &\mapsto \left(\mathrm{d}\Phi\left(\pi_M(e)\right)^*\right)^{-1}(e), \end{aligned}$$

where $\mathrm{d}\Phi(x)^*$ is the dual of the tangent map at $x \in M$.

Proposition 2.12:
The pushforward of a diffeomorphism onto the cotangent bundles is an exact symplectomorphism regarding the respective Liouville 1-forms, i. e.

$$\left(\mathrm{d}_*\Phi\right)^* \lambda_N = \lambda_M.$$

A proof can be found in [FvK18].

The second example of a symplectomorphism is on the cotangent bundle of the Euclidean space $T^*\mathbb{R}^n$:

Example 2.13:
The switch map $\sigma\colon T^*\mathbb{R}^n \to T^*\mathbb{R}^n$ which maps $(q,p) \in T^*\mathbb{R}^n$ to $\sigma(q,p) = (-p,q)$ is a linear symplectomorphism regarding the canonical symplectic structure from example 2.7. Note that this is not a physical transformation as in the previous proposition, since the coordinates q in the configuration space—which can be interpreted as position coordinates—get mapped into the fibre—which can be interpreted as the momentum. So this transformation essentially switches position and momentum.

Next, we want to define dynamics on symplectic manifolds by introducing the Hamiltonian formalism:

Definition 2.14:
Let (M,ω) be a symplectic manifold and $H\colon M \to \mathbb{R}$ a smooth function, called a *Hamiltonian* in this context. The *Hamiltonian vector field* X_H is defined implicitly by

$$\mathrm{d}H = \omega(\,\cdot\,, X_H)$$

and it is well defined due to the symplectic structure ω being nondegenerate. The *Hamiltonian flow*

$$\phi_H^t := \phi_{X_H}^t \colon M \to M$$

is the time-t flow of the Hamiltonian vector field.

The main point of symplectic transformations in this context is that they preserve the Hamiltonian flow, i. e. for a symplectic diffeomorphism $\Phi\colon M \to N$ between two symplectic manifolds (M,ω_M) and (N,ω_N) and a Hamiltonian H on N, we have

$$\omega_M(\,\cdot\,, \Phi^* X_N) = \mathrm{d}\,(\Phi \circ H)\,.$$

For a conformal symplectic diffeomorphism Φ_c with conformal factor c, we get

$$\omega_M(\,\cdot\,, \Phi_c^* X_N) = c\,\mathrm{d}(\Phi_c \circ H),$$

i. e. the vector fields are parallel and rescaled by $c \neq 0$.

We will in general also consider nonautonomous Hamiltonians $H\colon M \times \mathbb{R} \to \mathbb{R}$. However, if H is indeed autonomous, we get

Proposition 2.15 (Conservation of energy):
The value of an autonomous Hamiltonian $H\colon M \to \mathbb{R}$ is conserved along its Hamiltonian flow $\phi_H^t(x)$, i. e. $H(\phi_H^t(x))$ is independent of time.

One can prove this easily by differentiating $H(\phi_H^t(x))$.

Remark 2.16:
If we have a symplectic manifold (M,ω) and an autonomous Hamiltonian H, this proposition now allows us to decompose M into energy level sets $\Sigma_c := H^{-1}(c)$ which are invariant under the flow of H. Since ω provides an orientation on M, a regular energy hypersurface Σ_c is naturally oriented within M by the gradient of H.

A level set Σ_c of a regular energy value c together with the closed 2-form $\omega|_{\Sigma_c}$ on their own become what is known as a Hamiltonian manifold:

Definition 2.17:
A *Hamiltonian manifold* (Σ, ω) is an odd-dimensional smooth manifold Σ together with a closed 2-form ω, called the *Hamiltonian structure*, such that $\ker \omega$ defines a one-dimensional smooth subbundle of $T\Sigma$.

In the example of a regular value energy hypersurface Σ_c from above we can see that for a point $x \in \Sigma_c$ and a tangent vector $v \in T_x\Sigma_c$ we have

$$\omega(X_H, v) = -\,\mathrm{d}H(v) = 0,$$

so the kernel of ω is spanned by the Hamiltonian vector field at every point.

Nonetheless, we need an autonomous Hamiltonian to start with for the above example to work. A method to convert a nonautonomous Hamiltonian is provided by the following proposition:

Proposition 2.18:
Let (M, ω) be a symplectic manifold and $H, L \in C^\infty(M \times \mathbb{R}, \mathbb{R})$ possibly nonautonomous Hamiltonians. Assume for convenience of notation that the Hamiltonian flows ϕ_H^t and ϕ_L^t are defined for all time $t \in \mathbb{R}$. Then

$$\begin{aligned} L \diamond H \colon M \times \mathbb{R} &\to \mathbb{R} \\ (x,t) &\mapsto L(x,t) + H\left((\phi_L^t)^{-1}(x), t\right) \end{aligned}$$

satisfies

$$\phi_{L\diamond H}^t = \phi_L^t \circ \phi_H^t \quad \forall t \in \mathbb{R}.$$

A proof can again be found in [FvK18].

Consequently, we can compose the flow of a Hamiltonian H by the flow of a vector field generated by L. This can yield the flow of an autonomous Hamiltonian from nonautonomous Hamiltonians and vice versa.

We can find the Hamiltonian that generates a given vector field X on a base manifold N by

$$H_X(e) := e(X(\pi_N(e)))$$

as the dual pairing of the cotangent vector $e \in T^*N$ at $\pi_N(e)$ with the vector of X at that point.

Another property of a Hamiltonian flow is that it defines a symplectomorphism for every time-t map:

Proposition 2.19:
Let (M, ω) be a symplectic manifold and ϕ_H the flow of some Hamiltonian H on M. Suppose the flow exists for all time $t \in \mathbb{R}$. Then $(\phi_H^t)^*\omega = \omega$ for every $t \in \mathbb{R}$.

A consequence of this proposition is that a Hamiltonian flow is area preserving, since by the commutativity of pull back and wedge product the flow also preserves the volume form $\omega^{\wedge n}$.

If we are in a Darboux chart, where the symplectic form is given by the standard symplectic form ω_0, we can more explicitly compute the Hamiltonian flow:

Proposition 2.20 (Hamilton's equations of motion):
Let $(q_1, \dots, q_n, p_1, \dots, p_n) \in \mathbb{R}^{2n}$ be canonical coordinates, $\omega_0 = \mathrm{d}p \wedge \mathrm{d}q$ the standard symplectic form and $H \colon \mathbb{R}^{2n} \times \mathbb{R} \to \mathbb{R}$ a Hamiltonian function (not necessarily autonomous). Then the components of the Hamiltonian vector field are given by the first order ODE

$$\frac{\mathrm{d}p_i}{\mathrm{d}t} = -\frac{\partial H}{\partial q_i} \qquad \textit{and} \qquad \frac{\mathrm{d}q_i}{\mathrm{d}t} = \frac{\partial H}{\partial p_i} \qquad \textit{for } i = 1, \dots n.$$

This can be checked easily be plugging a vector field in the given coordinates into the symplectic form and comparing coefficients with the exterior derivative of H.

Additionally to symplectic manifolds there is also an odd-dimensional analogue:

Definition 2.21:
A *contact manifold* (Σ, α) is a $2n+1$-dimensional smooth manifold Σ together with a 1-form α, such that

$$\alpha \wedge (\mathrm{d}\alpha)^{\wedge n} \neq 0$$

is a volume form on Σ. The kernel of α is a hyperplane distribution $\xi = \ker \alpha$ and is called the *contact structure*. We define the *Reeb vector field* R implicitly by

$$\begin{aligned} \mathrm{d}\alpha(R, \,\cdot\,) &= 0 \quad \text{and} \\ \alpha(R) &= 1. \end{aligned}$$

Remark 2.22:
A contact form uniquely defines a contact structure, but a contact structure ξ does not uniquely define a contact form α with $\xi = \ker \alpha$. More precisely, if α is a contact form for ξ, then so is $f\alpha$ for every smooth and nonvanishing function f. Different contact forms to the same contact structure in general give nonparallel Reeb vector fields.

The tangent space of a contact manifold splits into the Reeb direction R and the hyperplane ξ:

$$T\Sigma = \langle R \rangle \oplus \xi.$$

Analogously to theorem 2.8, all contact manifolds locally look the same and we have a standard local presentation:

Theorem 2.23 (Darboux):
Let (Σ, α) be a $2n+1$-dimensional contact manifold and $p \in \Sigma$. Then there exists a local chart ϕ around p with coordinates $(x_1, \dots x_n, y_1, \dots y_n, z)$ such that

$$\phi^* \alpha = \mathrm{d}z + \sum_{i=1}^{n} x_i \, \mathrm{d}y_i.$$

For a proof see for example [Gei08].

In order to create a bridge between contact manifolds and Hamiltonian manifolds, we define the following:

Definition 2.24:
Let (Σ, ω) be an oriented Hamiltonian manifold. Then we call a contact form α on Σ to be *compatible* if $\mathrm{d}\alpha = \omega$ and the orientation of Σ coincides with the orientation given by α. If $\Sigma = \Sigma_c := H^{-1}(c)$ arises as a regular level set of a Hamiltonian H on a $2n$-dimensional symplectic manifold (M, ω), we want the orientation of Σ given by the contact form α to match the orientation given by the symplectic form ω and the Hamiltonian H. We write this condition as

$$\alpha \wedge (\mathrm{d}\alpha)^{\wedge n-1} > 0.$$

Remark 2.25:
If one has such an ω-compatible contact hypersurface Σ_c, one can use results on Reeb flows for the Hamiltonian flow on that energy level since both X_H and R span the one-dimensional $\ker \omega = \ker \mathrm{d}\alpha$ at every point, i. e. R and X_H are parallel. Since we also assumed the orientations to match, we get that they even point in the same direction

$$X_H(x) = c(x)R(x) \quad \text{for } c(x) > 0 \quad \forall x \in \Sigma$$

and the Reeb flow is only a positive reparametrisation of the Hamiltonian flow.

The usual way to find contact structures on hypersurfaces of symplectic manifolds is to look for transverse Liouville vector fields:

Definition 2.26:
Let (M, ω) be a symplectic manifold and $\Sigma \subset M$ a smooth codimension one submanifold. Assume X is a smooth vector field defined in a neighbourhood of Σ. We say X is a *Liouville vector field* if it satisfies

$$\mathcal{L}_X \omega = \omega,$$

where $\mathcal{L}_X$ is the Lie derivative with respect to X. We get a 1-form λ_X by

$$\lambda_X := \omega(X, \ \cdot \ ).$$

Remark 2.27:
Conversely, also every primitive α of ω defines a Liouville vector field X_α implicitly by

$$\alpha = \omega(X_\alpha, \ \cdot \ ),$$

where $\mathcal{L}_{X_\alpha}\omega = \omega$ can be checked by Cartan's formula.

As mentioned above, we get a contact structure if we find a transverse Liouville vector field per the following statement:

Proposition 2.28:
Let (M, ω) be a symplectic manifold, $\Sigma \subset M$ a smooth hypersurface and X a Liouville vector field defined on a neighbourhood of Σ. If the vector field X is transverse to Σ, i. e. $T_pM = T_p\Sigma \oplus X(p)$ for every $p \in \Sigma$, then the 1-form $\lambda_X|_\Sigma$ is a contact form on Σ.

Remark 2.29:
In the case that the hypersurface $\Sigma = \Sigma_c$ is given by a regular energy level set we get an orientation of Σ_c from the Hamiltonian and the symplectic form as in remark 2.16. Then $\lambda_X|_{\Sigma_c}$ becomes an ω-compatible contact form on Σ_c in the sense of definition 2.24 if this first orientation of Σ_c agrees with the orientation given by ω and X. In other words: We need X and ∇H to point in the same direction with respect to Σ_c to get a positive reparametrisation of the Reeb flow and the Hamiltonian flow on Σ_c.

Definition 2.30:
We call such a hypersurface $\Sigma \subset M$ of a symplectic manifold (M, ω), where there exists a coorientend Liouville vector field X, to be of *contact type*.

For the next two examples we will use in advance the Hamiltonian of the restricted three-body problem

$$H_\mu(q,p) = \frac{\|p\|^2}{2} + p_1q_2 - p_2q_1 - \frac{1-\mu}{\|q - M_1\|} - \frac{\mu}{\|q - M_2\|}$$

which is the main object of study in this work and which will be explained in more detail in chapter 3.4.

Example 2.31:
It was shown in [AFvKP12] for the planar case $(q,p) \in T^*(\mathbb{R}^2 \setminus \{M_1, M_2\})$ that the bounded components of the energy hypersurface $\Sigma_{\mu,c} := H_\mu^{-1}(c)$ is of contact type below and slightly above the first critical energy level. The same was shown for the spatial case $(q,p) \in T^*(\mathbb{R}^3 \setminus \{M_1, M_2\})$ by [CJK20]. The Liouville vector field which was used is the radial vector field from each of the primaries M_1 and M_2, which gives the ω-compatible contact form

$$\lambda = -(q - M_i)\,\mathrm{d}p.$$

Example 2.32:
We will now show that above the energy value zero the Liouville 1-form becomes a contact form for the energy hypersurface of the restricted three-body problem. The Liouville vector field for $\lambda = p\,\mathrm{d}q$ is the fibrewise radial vector field

$$X_\lambda = p\frac{\partial}{\partial p}.$$

We show that $\mathrm{d}H_\mu|_{\Sigma_{\mu,c}}(X_\lambda) > 0$ for $c > 0$ and thus $\Sigma_{\mu,c}$ is of contact type:

$$\begin{aligned}\mathrm{d}H_\mu\big|_{\Sigma_{\mu,c}}(X_\lambda) &= \|p\|^2 + p_1q_2 - p_2q_1 \\ &= c + \frac{\|p\|^2}{2} + \frac{1-\mu}{\|q - M_1\|} + \frac{\mu}{\|q - M_2\|} > 0\end{aligned}$$

Remark 2.33:
Every contact manifold (Σ, α) defines a Hamiltonian manifold by setting $\omega := \mathrm{d}\alpha$, which is obviously a Hamiltonian structure. On the other hand, not every Hamiltonian manifold is necessarily of contact type or admits a contact structure. An obvious obstruction is that the Hamiltonian structure ω—which is necessarily closed—needs to be exact as well, i. e. it needs to represent the trivial second de Rham class $[\omega] = 0 \in H^2_{\mathrm{dR}}(\Sigma)$.

Another obstruction can be found via the action of orbits, which is defined as follows:

Definition 2.34:
Let $(T^*N, \mathrm{d}\lambda)$ be the symplectic manifold defined by a cotangent bundle and the Liouville 1-form λ as in example 2.7 and let H be a Hamiltonian on T^*N. For an interval between $a \in \mathbb{R} \cup \{-\infty\}$ and $b \in \mathbb{R} \cup \{\infty\}$, let $\gamma\colon (a, b) \to T^*N$ be a solution of the Hamiltonian flow, i. e.

$$\dot{\gamma}(t) = X_H(\gamma(t)) \quad \forall t \in (a, b).$$

The *action* $\mathcal{A}(\gamma)$ is then defined by

$$\mathcal{A}(\gamma) := \int_a^b \gamma^*\lambda.$$

If γ is closed with period τ, then we simply integrate from $a = 0$ to $b = \tau$ to define the action of a periodic orbit.

Remark 2.35:
In a general symplectic manifold (M, ω) the action of a closed γ is often defined alternatively by

$$\mathcal{A}(\gamma) = \int_{\mathbb{D}} \bar{\gamma}^*\omega,$$

where $\bar{\gamma}\colon \mathbb{D} := \{x \in \mathbb{R}^2 : \|x\| \leq 1\} \to M$ is a smooth *filling disc* for γ, i. e. $\bar{\gamma}|_{\partial\mathbb{D}} = \gamma$. For this definition of the action to make sense and be well-defined, we firstly need M to have trivial fundamental group $\pi_1(M) = 1$ such that every orbit γ is contractible and admits a filling disc. Secondly, we need the symplectic form ω to vanish on $\pi_2(M)$, i. e. for every embedded 2-sphere $s\colon S^2 \to M$ we have

$$\int_{S^2} s^*\omega = 0.$$

If this is the case, then M is said to be *symplectically aspherical* and then the definition of the action as above is independent of the choice of the filling disc. In the situation of definition 2.34, the symplectic manifold is exact and therefore automatically symplectically aspherical by Stokes's theorem.

Remark 2.36:
Let $(T^*N, \mathrm{d}\lambda)$ be the symplectic manifold from example 2.7 and H a Hamiltonian on T^*N. Assume $\Sigma_c := H^{-1}(c) \neq \emptyset$ is of contact type with contact form α and let γ be a solution of the Hamiltonian system with energy c. Then by remark 2.25 the Reeb flow of α on Σ_c is just a positive reparametrisation of the Hamiltonian flow. From this we get that the integral of the contact form along γ is

$$\int_a^b \gamma^*\alpha = \int_a^b \alpha\left(X_H\left(\gamma(t)\right)\right)\mathrm{d}t = \int_a^b c\left(\gamma(t)\right)\alpha\left(R\left(\gamma(t)\right)\right)\mathrm{d}t = \int_a^b c\left(\gamma(t)\right)\mathrm{d}t > 0 \quad (2.2)$$

and needs to be strictly positive.

Assume now additionally that γ is closed and contractible. Then we can find a filling disc $\bar{\gamma}$ as in the previous remark 2.35 and by Stokes' theorem the action is then

$$\mathcal{A}(\gamma) = \int_{S^1} \gamma^*\lambda = \int_{\mathbb{D}} \bar{\gamma}^*\omega = \int_{S^1} \gamma^*\alpha > 0. \quad (2.3)$$

If γ is only closed but not contractible in Σ, let β_i for $i \in \{1, \dots b_1(\Sigma)\}$ be generators of the first de Rham cohomology $H^1_{\mathrm{dR}}(\Sigma)$. Since both λ and α are primitives of ω, we can write the closed 1-form $\lambda - \alpha = \sum_{i=1}^{b_1(\Sigma)} r_i\beta_i + \mathrm{d}f$, for some real coefficients r_i and a smooth function f. Consequently, we then have

$$\mathcal{A}(\gamma) = \int_{S^1} \gamma^*\lambda = \int_{S^1} \gamma^*\alpha + \sum_{i=1}^{b_1(\Sigma)} \left(r_i \int_{S^1} \gamma^*\beta_i\right).$$

These computations give obstructions for Hamiltonian manifolds to be of contact type: A primitive α of ω can not be an ω-compatible contact form on Σ_c if

1) the integral $\int_a^b \gamma^*\alpha$ over its pullback along any part of a Hamiltonian solution with energy c is nonpositive,

2) the action of a closed orbit minus the integral over a de Rham representative of the relative de Rham class with the Liouville 1-form $\mathcal{A}(\gamma) - \sum_{i=1}^{b_1(\Sigma)} \left(r_i \int_{S^1} \gamma^*\beta_i\right)$ is nonpositive, or

3) the action for any contractible orbit is nonpositive.

This concludes the theoretical foundations for the present work. In the subsequent chapters we next want to introduce the specific Hamiltonians we well be working with and then start to construct orbits that obstruct the existence of compatible contact structures in the restricted three-body problem as shown above.

Chapter 3

Hamiltonian systems

In this chapter we introduce various Hamiltonians that will either be studied in detail during the course of this work or will be useful at some steps in the process. The first we will discuss is the free particle on a manifold. This is the only Hamiltonian which is defined on a somewhat more general symplectic manifold, namely on the cotangent bundle of a general manifold as described in example 2.7. All other Hamiltonians—the Harmonic oscillator, the Kepler problem and the restricted three-body problem—are defined on the cotangent bundle of a subset of the Euclidean space $\mathbb{R}^n$. In general, they can also be defined on other cotangent bundles, like the cotangent bundle on a sphere, and they pose interesting problems there as well.

We will discuss some proofs and computations more explicitly since we want to refer back to them at later stages. More on these Hamiltonians can be found in [FvK18], [MHO09] and [AM78].

Before we start with the first Hamiltonian we want to categorise different types of Hamiltonians on a cotangent bundle. We can think of the Hamiltonian as an energy function and according to this view, we can model mechanical systems by describing the composition of the energy.

Definition 3.1:
Let (N, g) be a Riemannian manifold, $(T^*N, \mathrm{d}\lambda)$ the symplectic manifold consisting of the cotangent bundle of N and the exterior derivative of the Liouville 1-form $\lambda = p\,\mathrm{d}q$, where q are local coordinates on N and p the corresponding coordinates on the cotangent fibre. We call a Hamiltonian H of the form

$$H(q,p) = \frac{1}{2}\|p\|^2_{g_q^*} + V(q)$$

a *mechanical Hamiltonian*. Here, $\|\cdot\|_{g_q^*}$ is the norm on T_q^*N induced by the inner product g_q on T_qN, and $V\colon N \to \mathbb{R}$ is a smooth function on N called the *potential energy*. The first term $\|p\|^2/2$ is called the *kinetic energy*.

By Hamilton's equations 2.20 we then have

$$\frac{\mathrm{d}q}{\mathrm{d}t} = p \qquad \text{and} \qquad \frac{\mathrm{d}p}{\mathrm{d}t} = -\nabla V(q),$$

so the acceleration of q is the negative gradient of V. Mechanical Hamiltonians thus model physical systems of the kind where a particle has kinetic energy and moves in a conservative force field generated by a potential function. Examples include a pendulum with gravitational potential, a spring system with elastic potential, a classical electron moving in an electrical Coulomb potential force field and similar settings.

In more general systems one might like to add a velocity dependent force like the Coriolis force or the magnetic Lorentz force:

Definition 3.2:
We call a Hamiltonian of the form

$$H(q,p) = \frac{1}{2}\|p + A_q\|^2_{g_q^*} + V(q)$$

a *magnetic Hamiltonian* where, additionally to definition 3.1, $A \in \Omega^1(N)$ is a 1-form on N, i. e. $A_q \in T_q^*N$.

These are the two general types of Hamiltonian systems which we will encounter. The following sections each discuss one specific Hamiltonian system in more detail.

3.1 The free particle

The easiest case for a mechanical Hamiltonian is the free particle on a Riemannian manifold (N, g). Here, we have no potential energy and the Hamiltonian is solely given by kinetic energy

$$H_{\text{kin}}(q,p) := \frac{1}{2}\|p\|^2_{g_q^*}. \tag{3.1}$$

For this Hamiltonian one can show explicitly that the Hamiltonian flow is just the geodesic flow on N. To write this statement down more precisely, let $q \in N$ and $v \in T_qN$. Assume for simplicity of notation that N is geodesically complete. Then there exists a unique geodesic $q_v \colon \mathbb{R} \to N$ through $q = q_v(0)$ with velocity $\dot{q}_v(0) = v$. The geodesic flow

$$\begin{aligned} \Psi_g^t &\colon TN \to TN \\ &(q,v) \mapsto (q_v(t), \dot{q}_v(t)) \end{aligned}$$

is a map on the tangent bundle. Composing with the isomorphism of vector bundles

$$\begin{aligned} \Phi_g &\colon TN \to T^*N, \\ &(q,v) \mapsto (q, g_q(v, \,\cdot\,)) \end{aligned}$$

we can define the co-geodesic flow

$$\phi_g^t := \Phi_g \circ \Psi_g^t \circ \Phi_g^{-1}$$

as a map on the cotangent bundle. The claim is now that this flow is the same as the Hamiltonian flow of the kinetic energy on T^*N.

Theorem 3.3:
The Hamiltonian flow of H_{kin} and the co-geodesic flow ϕ_g^t coincide for all time $t \in \mathbb{R}$.

The proof is done by computing the differential equations of the co-geodesic flow in terms of metric coefficients and comparing to the Hamiltonian vector field of the kinetic energy. The detailed computations can be found in [FvK18, theorem 2.3.1].

3.2 The harmonic oscillator

The next Hamiltonian describes the motion of a harmonic oscillator. We define it straight away on $T^*\mathbb{R}^n \ni (q,p)$ which leads to a system of n uncoupled harmonic oscillators. By Hook's law the force is directly proportional to its displacement, so we want

$$\ddot{q}_k = a_k q_k \tag{3.2}$$

for constants $a = (a_1, \dots a_n) \in \mathbb{R}^n$. The Hamiltonian

$$H_a(q,p) := \frac{1}{2}\|p\|^2 - \sum_{k=1}^{n} \frac{a_k}{2} q_k^2, \tag{3.3}$$

where $\|\cdot\|$ is the standard Euclidean norm on $T_q\mathbb{R}^n$, thus provides the desired dynamics. We call each of the oscillators *attractive* if $a_k < 0$, and *repulsive* if $a_k > 0$. For $a_k = 0$ we just get solutions of the free particle in that direction. Furthermore, the system is called *isotropic* if $a_k = a_l$ for all $k, l \in \{1, \dots n\}$.

As a special case we will now discuss solutions of the two-dimensional isotropic system: For $a < 0$ we can check by differentiating twice that in complex notation $q \in \mathbb{C} \cong \mathbb{R}^2$ the curves

$$q(t) = Ae^{i\sqrt{-a}t} + Be^{-i\sqrt{-a}t} \tag{3.4}$$

are solutions to the Hamiltonian system for any $A, B \in \mathbb{C}$.

Lemma 3.4:
Traces of solutions to the system of two uncoupled attractive isotropic harmonic oscillators in the configuration space are ellipses with centre at the origin.

Proof: Firstly, without loss of generality we can assume that both $A, B \in \mathbb{R}$: Traces of solutions are invariant under time-shift and the property of being an ellipse with centre at the origin is invariant under rotations. A solution rotated by the angle ϑ and time-shifted by τ can be written as

$$e^{i\vartheta}q(t+\tau) = Ae^{i(\vartheta+\sqrt{-a}\tau)}e^{i\sqrt{-a}t} + Be^{i(\vartheta-\sqrt{-a}\tau)}e^{i\sqrt{-a}t}.$$

Obviously, we can find for every $A, B \in \mathbb{C}$ some ϑ and τ such that $Ae^{i(\vartheta+\sqrt{-a}\tau)}$ and $Be^{i(\vartheta-\sqrt{-a}\tau)}$ are real.

Finally, we use Euler's formula and we have a parametrised ellipse

$$q(t) = (A+B)\cos(\sqrt{-a}t) + i(A-B)\sin(\sqrt{-a}t)$$

which proves the lemma. □

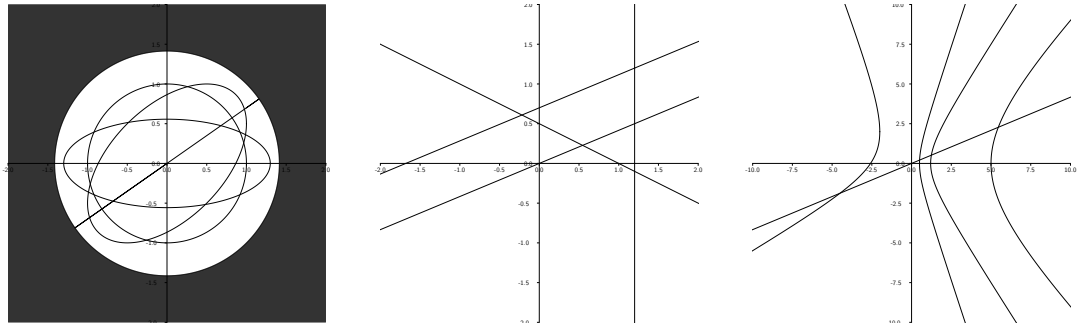

(a) $a = -4$ (b) $a = 0$ (c) $a = 4$

Figure 3.1: Orbits for a system of two uncoupled isotropic harmonic oscillators for the same energy $c = 4$ and different Hook's constants a.

The case $a = 0$ has been covered by the free particle example above and solutions are geodesics in the plane. For the remaining case $a > 0$ we see again by differentiating twice that solutions of the Hamiltonian system are given by

$$q(t) = Ae^{\sqrt{a}t} + Be^{-\sqrt{a}t}$$

for $A, B \in \mathbb{C}$ in complex notation. We can again describe the shape:

Lemma 3.5:
Traces of solutions to the system of two uncoupled repulsive harmonic oscillators in the configuration space are hyperbolas with centre at the origin.

Proof: As in the previous proof we use time-shift and rotation, which leaves the property of being a hyperbola with centre at the origin invariant. Solutions become

$$e^{i\vartheta}q(t+\tau) = e^{i\vartheta+\sqrt{a}\tau}Ae^{\sqrt{a}t} + e^{i\vartheta-\sqrt{a}\tau}Be^{-\sqrt{a}t}$$

and we see that a time-shift scales the coefficients in opposite directions and a rotation rotates the coefficients. We can therefore assume without loss of generality that $A = \overline{B}$.

Using the decomposition of e^x and e^{-x} into hyperbolic sine and cosine we find that for $A = \overline{B}$ we have

$$q(t) = 2\mathrm{Re}(A)\cosh(\sqrt{a}t) + 2i\mathrm{Im}(A)\sinh(\sqrt{a}t),$$

which is a standard parametric equation of a hyperbola with centre at the origin as claimed. □

3.3 The Kepler problem

The Kepler problem is the simplest system in celestial mechanics other than the free particle in empty space. It models the dynamics of two bodies attracted to one another

by Newtonian gravitation. The configuration space can either be thought of as relative position coordinates for two bodies with mass or as the position of a particle in the gravitational force field of one heavy body at the origin. We will use $\mathbb{R}^2 \setminus \{0\}$ and $\mathbb{R}^3 \setminus \{0\}$ as configuration spaces, although other base manifolds are also possible. We will also use the slightly different notation of (Q, P) for the coordinates on $T^*(\mathbb{R}^n \setminus \{0\})$ for $n = 2$ and 3 because we want to distinguish between different coordinates later on. The Kepler problem is a very well studied Hamiltonian system, so we will not deduce every statement here. For more details and derivation of the formulae stated here, see for example [AM78, chapter 9] or [MHO09].

The Newtonian gravitational force

$$\ddot{Q} = -\frac{Q}{\|Q\|}\frac{1}{\|Q\|^2} \tag{3.5}$$

is directed towards the point mass at the origin with an inverse square magnitude. Therefore, the Hamiltonian of the Kepler problem becomes

$$H_{\text{fix}}(Q, P) = \frac{1}{2}\|P\|^2 - \frac{1}{\|Q\|}. \tag{3.6}$$

Periodic solutions, as we will also check later, are ellipses that adhere to Kepler's famous laws of planetary motion:

1) The focus of the ellipse is at the origin,

2) the area swept by a line segment connecting the particle Q to the origin is constant for equal time intervals and

3) the period T of the orbit can be computed by

$$T = 2\pi\sqrt{a^3}, \tag{3.7}$$

where a is the semi-major axis of the ellipse.

We define the angular momentum L as the cross product

$$L(Q, P) := P \times Q$$

for $Q, P \in \mathbb{R}^3$, and as only the last component

$$L(Q, P) = P_1Q_2 - P_2Q_1$$

for $Q, P \in \mathbb{R}^2$. For all central forces $V(\|q\|)$ the angular momentum L is invariant under the flow of $H = \|p\|^2/2 + V(\|q\|)$. In particular the Kepler potential is a central force, and so we have that $L(\phi^t_{H_{\text{fix}}}(x))$ is constant in time for all $x \in T^*(\mathbb{R}^n \setminus \{0\})$. We call such a conserved quantity an *integral of motion*.

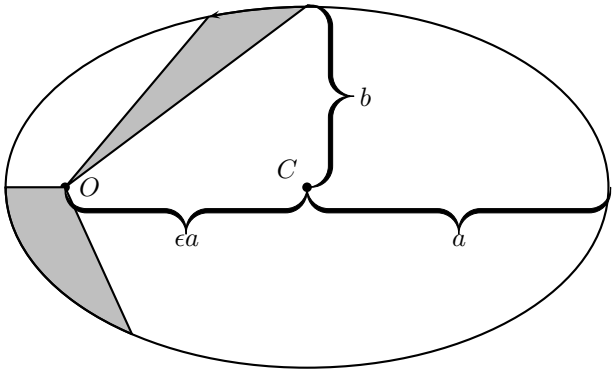

Figure 3.2: Elliptical Kepler orbit and Kepler's laws of planetary motion.

More explicitly, one can show that solutions to the Kepler problem with energy $H_{\text{fix}} = c < 0$ are ellipses with semi-major axis

$$a = -\frac{1}{2c}$$

and eccentricity

$$e = \sqrt{1 + 2cL^2}.$$

Therefore, one can recover the energy and the angular momentum from the geometry of the ellipse by

$$c = H_{\text{fix}} = -\frac{1}{2a} \quad \text{and} \tag{3.8}$$

$$L = -\epsilon' \sqrt{a(1-\epsilon^2)}, \tag{3.9}$$

where ϵ' is the direction of rotation defined by

$$\epsilon' := \begin{cases} +1 & \text{for anti-clockwise motion and} \\ -1 & \text{for clockwise motion.} \end{cases} \tag{3.10}$$

We call the case of $\epsilon' = +1$ *direct* or *prograde motion* and $\epsilon' = -1$ *retrograde*.

To describe the motion of the particle along the ellipse more precisely we write the angular momentum

$$L = r^2 \dot{\varphi}$$

in polar coordinates (r, φ) and get that the angular velocity is

$$\frac{\mathrm{d}\varphi}{\mathrm{d}t} = \frac{L}{\|Q\|^2}, \tag{3.11}$$

which is in general nonconstant along a solution.

For later reference we will do an explicit computation in the one-dimensional Kepler problem or, equivalently, for Kepler solutions with zero angular momentum: Assume we let go the particle with zero initial velocity at time $t_0 = 0$ at a height $Q_0 > 0$. We want to compute how long it takes to fall down to $0 < Q_1 \leq Q_0$. The one-dimensional second order ODE reduces to

$$\ddot{Q} = -\frac{1}{Q^2}$$

with initial conditions

$$\dot{Q}(0) = 0 \qquad \text{and} \qquad Q(0) = Q_0.$$

Multiplying both sides by $\mathrm{d}Q/\,\mathrm{d}t$ and integrating once, we get

$$\frac{1}{2}\left(\frac{\mathrm{d}Q}{\mathrm{d}t}(t)\right)^2 - \frac{1}{2}\left(\frac{\mathrm{d}Q}{\mathrm{d}t}(0)\right)^2 = \frac{1}{Q(t)} - \frac{1}{Q_0}.$$

Solving for $\mathrm{d}t$, we have

$$\mathrm{d}t = -\sqrt{\frac{QQ_0}{2Q_0 - 2Q}}\,\mathrm{d}Q.$$

Integrating again from Q_0 to Q_1, this gives the free-fall time

$$t_{Q_0}(Q_1) = \sqrt{\frac{Q_0^3}{2}}\left(\sqrt{\frac{Q_1}{Q_0}\left(1 - \frac{Q_1}{Q_0}\right)} + \arccos\left(\sqrt{\frac{Q_1}{Q_0}}\right)\right) \tag{3.12}$$

of a particle falling from a height $Q_0 > 0$ down to $0 < Q_1 \leq Q_0$. In the original system we had to exclude $Q = 0$ because the potential has a singularity there. We can still compute the finite free-fall time to this singularity from a given height $Q_0 > 0$. Inserting $Q_0 = 2a$, we find that the size of the maximal interval of existence for this finite-time blow-up solution is exactly the period from Kepler's third law for a degenerate ellipse. This fact will become clear after regularising the Kepler problem at collision in the next chapter 4.

3.4 The circular restricted three-body problem

The main object of study in this work is the circular restricted three-body problem. Here, there are now three bodies M_1, M_2 and M_3 that attract each other by gravitational force. It is called restricted because we assume one body, M_3, to have no mass and thus it only gets attracted by M_1 and M_2 but does itself not influence their motion. We further assume that M_1 and M_2 move circularly in anti-clockwise direction around their common centre of mass at the origin. Normalising the sum of both masses and also

their distance to 1, we define the mass of M_2, which will usually be the smaller body, to be $\mu \in [0,1]$ and hence the mass of M_1 to be $1-\mu \in [0,1]$. Therefore, the trajectory of M_1 in inertial coordinates (Q,P) describes a circle of radius μ while M_2 moves around the origin at radius $1-\mu$, both at constant velocities and period 2π. The Hamiltonian of this system becomes

$$H_{\text{fix},\mu}(Q,P) = \frac{\|P\|^2}{2} - \frac{1-\mu}{\|Q-M_1\|} - \frac{\mu}{\|Q-M_2\|},$$

which is not autonomous for $\mu \in (0,1)$. For $\mu = 0$ and 1 we recover the Hamiltonian H_{fix} of the Kepler problem. In order to make the Hamiltonian autonomous for all μ, we apply proposition 2.18 with the auxiliary Hamiltonian $L(Q,P) = P_1Q_2 - P_2Q_1$ that generates the anti-clockwise rotation of the (Q_1,Q_2)-plane. We call these new coordinates

$$\begin{pmatrix} q_1 \\ q_2 \\ q_3 \end{pmatrix} = \begin{pmatrix} \cos(t) & \sin(t) & 0 \\ -\sin(t) & \cos(t) & 0 \\ 0 & 0 & 1 \end{pmatrix} \begin{pmatrix} Q_1 \\ Q_2 \\ Q_3 \end{pmatrix} \tag{3.13}$$

and the new transformed Hamiltonian

$$\begin{aligned} H_\mu(q,p) :&= L \diamond H_{\text{fix},\mu}(q,p) \\ &= \frac{\|p\|^2}{2} + p_1q_2 - p_2q_1 - \frac{1-\mu}{\|q-M_1\|} - \frac{\mu}{\|q-M_2\|} \\ &= \frac{1}{2}\left((p_1+q_2)^2 + (p_2-q_1)^2 + p_3^2\right) \underbrace{- \frac{1-\mu}{\|q-M_1\|} - \frac{\mu}{\|q-M_2\|} - \frac{q_1^2+q_2^2}{2}}_{=:V_\mu(q)} \end{aligned} \tag{3.14}$$

becomes autonomous since the positions of $M_1 = (-\mu,0,0)$ and $M_2 = (1-\mu,0,0)$ are now fixed along the q_1-axis. We call the remaining term V_μ the effective potential of our magnetic Hamiltonian with twist $A_q = q_2\,\mathrm{d}q_1 + q_1\,\mathrm{d}q_2$ as in definition 3.2. By Hamilton's equations of motion 2.20 we get the system of second order ODEs

$$\begin{aligned} \ddot{q}_1 &= 2\dot{q}_2 - \frac{\partial V_\mu}{\partial q_1} \\ \ddot{q}_2 &= -2\dot{q}_1 - \frac{\partial V_\mu}{\partial q_2} \\ \ddot{q}_3 &= -\frac{\partial V_\mu}{\partial q_3} \end{aligned} \tag{3.15}$$

that describes the Hamiltonian dynamics.

In the limit cases $\mu = 0$ and 1 we now get the so called *rotating Kepler problem*, or

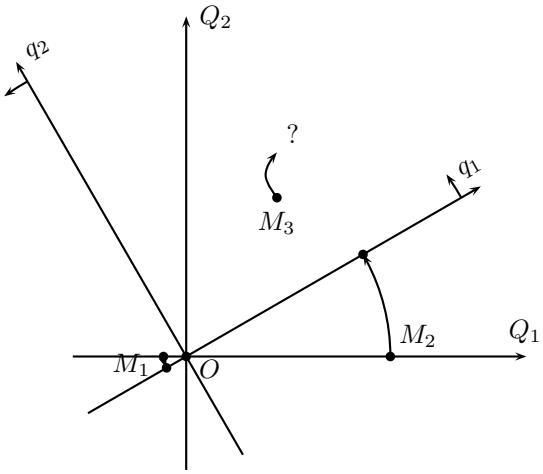

Figure 3.3: Fixed and rotating coordinates for the circular restricted three-body problem.

the Kepler problem in rotating coordinates (q, p), with its Hamiltonian

$$\begin{aligned} H_0(q,p) &= H_{\text{fix}}(q,p) + L(q,p) \\ &= \frac{\|p\|^2}{2} + q_1 p_2 - q_2 p_1 - \frac{1}{\|q\|} \\ &= \frac{1}{2}\left((p_1+q_2)^2 + (p_2-q_1)^2 + p_3^2\right) - \frac{1}{\|q\|} - \frac{q_1^2+q_2^2}{2} \end{aligned} \tag{3.16}$$

and differential equations of motion

$$\begin{aligned} \ddot{q}_1 &= 2\dot{q}_2 - \frac{q_1}{\|q\|^3} + q_1 \\ \ddot{q}_2 &= -2\dot{q}_1 - \frac{q_2}{\|q\|^3} + q_2 \\ \ddot{q}_3 &= -\frac{q_3}{\|q\|^3}. \end{aligned} \tag{3.17}$$

Solutions can be found by rotating Kepler solutions along with (3.13). Bounded solutions are now no longer necessarily periodic in the new coordinates (q, p) since by the time T of the old Kepler period the initial conditions at $(Q(0), P(0)) = (Q(T), P(T))$ have in general for $T \neq 2k\pi$ rotated to $(q(T), p(T)) \neq (q(0), p(0))$. The only orbits that remain periodic are those where the *mean motion* $2\pi/T = k/l$ of the Kepler orbit is rational, i. e. where the initial point $(q(0), p(0)) = (Q(0), P(0))$ comes back after k rotations of the Keplerian orbit and l rotations of the coordinates (q, p). All other bounded orbits are merely quasi-periodic, meaning the orbit comes back arbitrarily close to its initial position infinitely often, but never exactly. Such an orbit then densely fills the annulus $a(1-\epsilon) < \|q\| < a(1+\epsilon)$, where a is the semi-major axis and ϵ is the eccentricity of the Kepler ellipse.

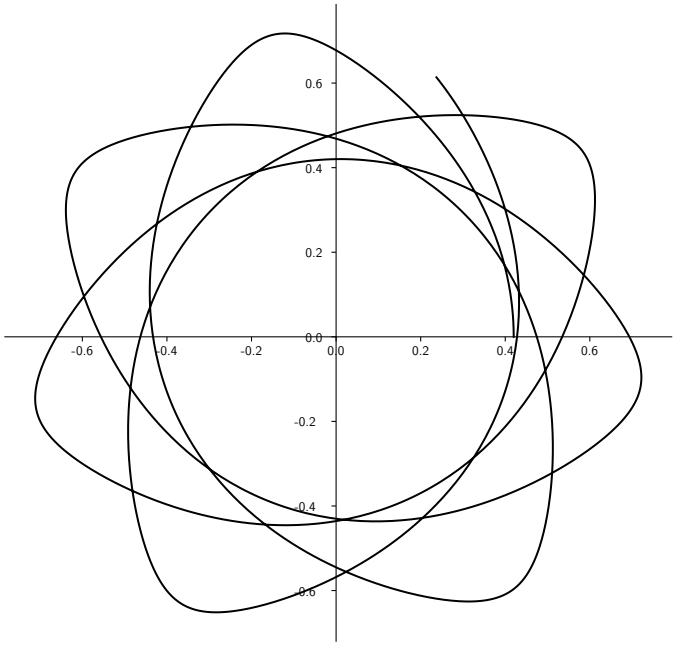

Figure 3.4: A bounded but nonperiodic rotating Kepler solution.

Both the circular restricted three-body problem (3.14) and the rotating Kepler problem(3.16) have been defined on $\mathbb{R}^3$ above. All constructions in this work will be done in the planar versions where we simply set $q_3 = p_3 = 0$. Planar orbits however, obviously also exist in the spatial setting, so we can use them to achieve results in the spatial case as well.

3.5 Hill's lunar problem

There is one more system from celestial mechanics that we will touch on briefly at a later point. Hill's lunar problem is designed as a limit case of the restricted three-body problem as $\mu \to 0$, but rather only in a neighbourhood of the vanishingly light primary M_2 than in the full view as the rotating Kepler problem. This limit is attained by shifting the origin to M_2, conformally scaling by $\nu = \mu^{1/3}$ and then simultaneously letting μ and ν tend to zero. The resulting Hamiltonian after Taylor approximation is

$$\begin{aligned} H(q,p) &= \frac{\|p\|^2}{2} + p_1 q_2 - p_2 q_1 - \frac{1}{\|q\|} - q_1^2 + \frac{q_2^2}{2} \\ &= \frac{1}{2}\left((p_1+q_2)^2 + (p_2-q_1)^2 + p_3^2\right) - \frac{1}{\|q\|} - \frac{3}{2}q_1^2. \end{aligned} \tag{3.18}$$

From a physical point of view the huge centrifugal and gravitational forces from the infinitely heavier primary M_1 cancel out at M_1 and in the limit there remains a tidal force $3q_1$ which makes the direction to the heavier primary indistinguishable. The

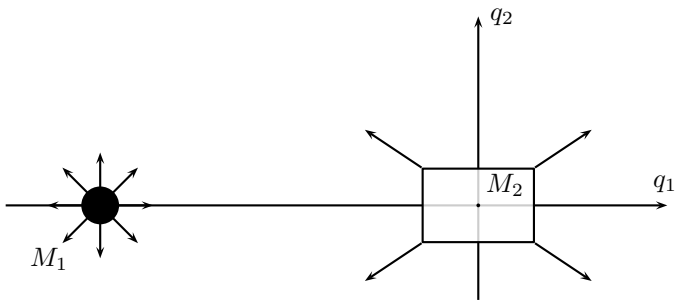

Figure 3.5: Setting of Hill's lunar problem.

original Coriolis and gravitational force from the vanishingly light primary M_2 remains in its neighbourhood. For more details on the derivation of the Hamiltonian and the dynamic of Hill's lunar problem see for example [MHO09], [Hil78] and [Hén69].

3.6 Periodic orbits and Hill's regions

We conclude this chapter by setting up the definitions to talk about periodic solutions of the Hamiltonian systems which were described above. Most of the notation in the first subsection are taken from [Hén97], where the focus is on families of periodic orbits. The definitions and some discussions of the Hill's regions which are done in the second subsection can also be found in [FvK18].

3.6.1 Periodic orbits and families

All the Hamiltonians (3.1), (3.3), (3.6), (3.14) and (3.18) above are autonomous, i. e. independent of time, and thus so are the differential equations (3.2), (3.5), (3.15) and (3.17) on the configuration space attained by Hamilton's equations of motion. Therefore, for every solution $Q(t)$ or $q(t)$ also the time-shifted function $s_*Q(t) := Q(s+t)$ or $s_*q(t) = q(s+t)$ is a solution.

Definition 3.6:
We call the class of all solutions that are equal up to time-shift an *orbit* or a *trajectory*.

Since the images of time-shifted solutions are all the same and since initial conditions in the phase space fully define a solution, we can define an orbit by the image of a solution in phase space. By specifying a point on the orbit for the initial time $t = 0$ or by declaring a time t_0 at any point on the orbit we can regain the specific solution.

Definition 3.7:
We call a solution to one of the dynamical systems a *periodic solution* if there exists a $T > 0$ such that $Q(t) = Q(T + t)$ or $q(t) = q(T + t)$ for all times t. The time T is called a *period* of the solution. For this discussion of families of orbits, we formally work

with tuples (Q, T) or (q, T), so the same solution with a different period gives in our language a different periodic solution. A *periodic orbit* is the orbit of a periodic solution together with the period T.

There are two types of periodic solutions: constant and nonconstant ones. For constant periodic solutions every positive time $T > 0$ is a period. Nonconstant periodic solutions have a *minimal period* $T_{\min} := \min\{T > 0 \text{ period}\}$ and every period T is a positive integer multiple of the minimal period $T_{\min}$.

Consider for the remainder of this subsection the planar circular restricted three-body problem, which is the main subject of our study. A nonconstant periodic solution is fully defined by initial conditions $q_1(0)$, $q_2(0)$, $p_1(0)$ and $p_2(0)$, and a period T, i. e. by five parameters. We have four equations in the equations of motion (3.15) and one relation in the Hamiltonian itself, so we are left with two degrees of freedom. One of them is the time-shift and then one more is left such that periodic orbits form one-parameter families.

Proposition 3.8 ([Win31]):
Periodic orbits form one-parameter families.

The period along this family can be chosen such that it is an analytic function of the family parameter as also shown by Wintner. If one simply chooses the minimal period for each orbit, the period can jump at orbits which are the multiple cover of a simpler orbit. To remove these singularities one assigns the same multiple of the minimal period to that particular orbit. This period is called the *period-in-family* T^*, which now varies smoothly along the family.

A family of periodic orbits behaves according to the principle of natural termination—see [Str34], [Str35], [Win31] and [Bir36]—where it either closes up on itself, called a *closed family*, or ends in *natural termination*, i. e. one of the following quantities grows without limit: the maximal distance from the origin, the Jacobi constant $C := -2H_\mu$ or the period T^*. Note, however, that a family can also reflect over itself to form an apparently nonnatural end, but it can not fork away from the original family at another point—see again [Win31] and [Hén97, chapter 2.5].

The family parameter is usually nontrivial, but we can mostly use the easily computable Jacobian energy C or, equivilantly, the Hamiltonian energy $c = -C/2$ as a substitute. In general, C is not strictly monotonic along families and we call the maximal interval of a family where C is strict *family segments*.

The reflection across the (q_1, q_3)-plane or, for the planar case, across the q_1-axis,

$$\rho\colon (q_1, q_2, q_3, p_1, p_2, p_3) \mapsto (q_1, -q_2, q_3, -p_1, p_2, p_3), \tag{3.19}$$

is an anti-symplectic involution, meaning $\rho^2 = \mathrm{id}$ and $\rho^*\omega_0 = -\omega_0$. It plays a special role in the discussion of periodic orbits, since the Hamiltonian H_μ, and also all the other Hamiltonians described earlier, are symmetric with respect to ρ. This means if $(q(t), p(t))$ is a solution to the equations of motion, then so is $\rho(q(-t), p(-t))$. We will call an orbit *symmetric* if it is invariant under this transformation. On the other hand,

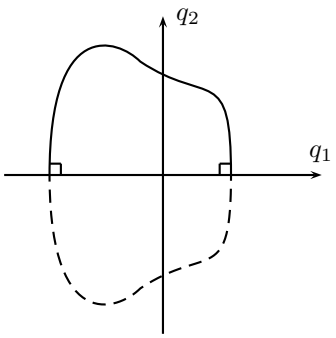

Figure 3.6: Finding symmetric periodic orbits using the reflection ρ.

the *symmetrical orbit* to a given orbit is obtained by applying the transformation. In other words: An orbit is symmetric if it is identical to its symmetrical orbit. Finding symmetric periodic orbits is a little easier, because one only needs to find half an orbit while making sure that it intersects the (q_1, q_3)-plane perpendicularly. The other half is then guaranteed by the reflection ρ.

3.6.2 Hill's regions and critical points

Since all Hamiltonians discussed here are autonomous and by the conservation of energy, proposition 2.15, a solution lies completely in an energy hypersurface $\Sigma_c \subset T^*\mathbb{R}^n \cong \mathbb{R}^{2n}$ for $n = 2$ and 3.

Definition 3.9:
Let $\pi_{\mathbb{R}^n} : T^*\mathbb{R}^n \to \mathbb{R}^n$ be the footpoint projection of the cotangent bundle. We call the projection $\mathfrak{H}_c := \pi_{\mathbb{R}^n}(\Sigma_c)$ of the energy level set Σ_c the *Hill's region* for the energy value $c \in \mathbb{R}$.

Remark 3.10:
For mechanical and magnetic Hamiltonians the Hills regions can be described as the sublevel set of that energy for the potential function

$$\mathfrak{H}_c = \{q \in \mathbb{R}^n \mid V(q) \leq c\}$$

since the remaining terms of the possibly twisted kinetic energy are always nonnegative.

The Hill's region is therefore the set of all possible locations in the configuration space for the given energy and the projection of a trajectory with energy c lies completely in $\mathfrak{H}_c$. Similarly as for the energy hypersurfaces, the topology of the Hill's regions can only change at critical points of the potential V. The shape of the Hill's regions can already offer some qualitative information about orbits of that energy. We will briefly discuss the shape of Hill's regions for our Hamiltonians and their implications.

For the free particle on $\mathbb{R}^n$ the effective potential is zero, so the Hill's regions is either everything for nonnegative energy or nothing for negative energy. There are no

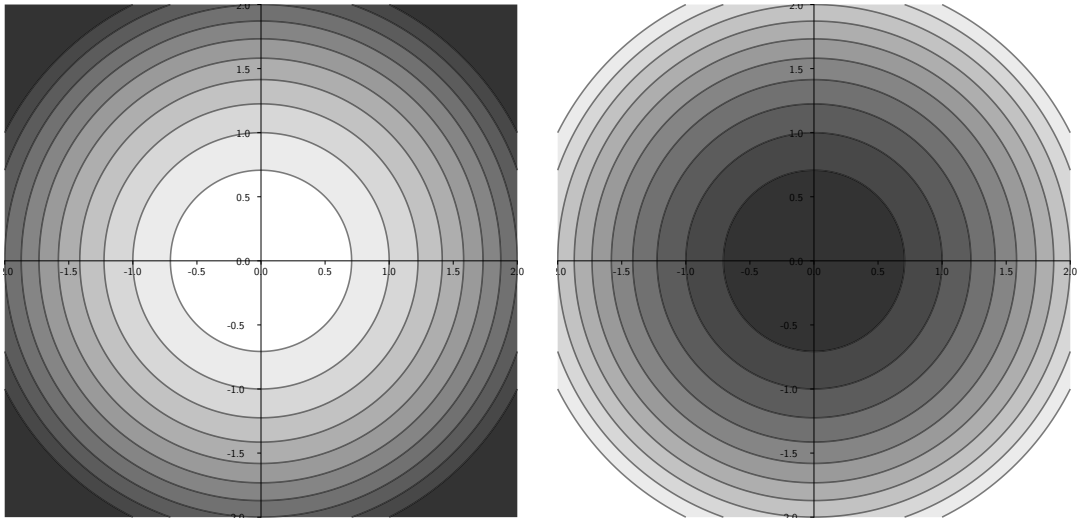

(a) $a = -4$ and $c = 0$ to 10 in steps of 1.

(b) $a = 4$ and $c = -10$ to 0 in steps of 1.

Figure 3.7: Hill's regions for a system of two uncoupled isotropic harmonic oscillators. Dark regions are the forbidden regions for the particular energy while the light regions represent the Hill's regions.

trajectories with negative kinetic energy, the only trajectory with zero kinetic energy is the constant solution at every point and for every positive speed there exists a geodesic with that speed in every direction which goes on infinitely.

The attractive harmonic oscillator has a nonnegative potential function $-\sum_k a_k q_k^2/2$ with $a_k < 0$, so the Hill's region is empty for negative energy and there are no orbits for $c < 0$. At $c = 0$ there is only the constant solution at the origin, which is the Hill's region here. For positive energy $c > 0$ the Hill's region is a closed elliptical disc with semi axes $\sqrt{-2c/a_k}$ and all orbits are bounded. The Hill's regions of the repulsive harmonic oscillator are in some sense the inverse of the attractive. For negative energies it is $\mathbb{R}^n$ minus an elliptical disc and for all other energies it is all of $\mathbb{R}^n$. In the case of zero energy the origin becomes a hyperbolic fixed point, where the unstable manifold is an n-dimensional linear subspace of $T^*\mathbb{R}^n \cong \mathbb{R}^{2n}$ which intersects the (q_k, p_k)-plane in the first and third quadrant with slope $\sqrt{a_k}$ and the stable manifold intersects the second and fourth quadrant with slope $-\sqrt{a_k}$.

In the Kepler problem we have the potential $-1/\|q\|$, so the Hill's region is a closed punctured ball with radius $-1/c$ for negative energy and all orbits are bounded, while for nonnegative energies all of $\mathbb{R}^n \setminus \{0\}$ can be reached.

The effective potential of the planar rotating Kepler problem is $-1/\|q\| - \|q\|/2$, which has a single critical value $-3/2$, the global maximum, attained at the unit circle. For $\|q\| \to 0$ or $\|q\| \to \infty$ the potential becomes infinitely small, so the Hill's regions are $\mathbb{R}^2 \setminus \{0\}$ minus an open annulus containing the unit circle for energies below $-3/2$, and all of $\mathbb{R}^2 \setminus \{0\}$ for all higher energies. At the critical energy value there exist

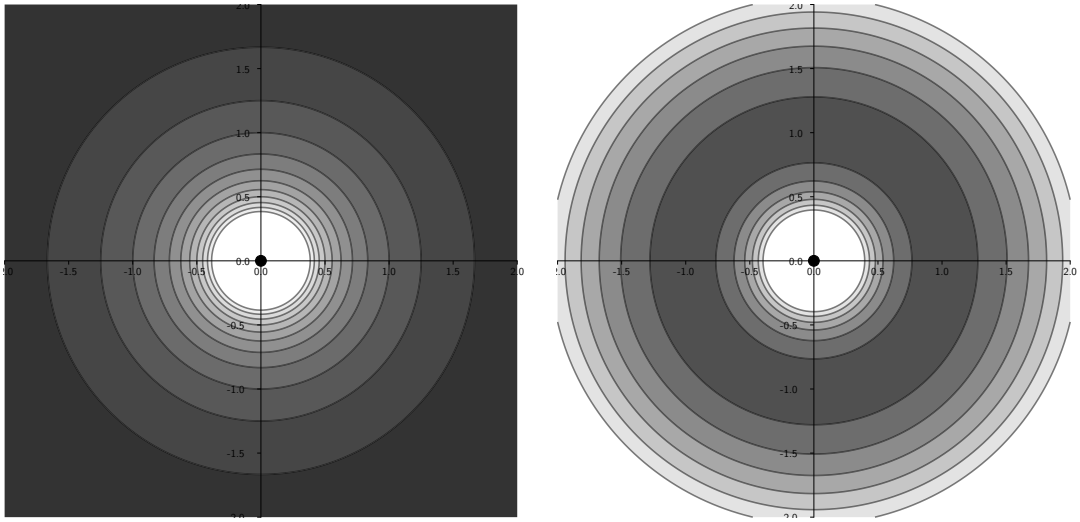

(a) Kepler Problem for energies $c = -2.6$ to -1.6 in steps of 0.2.

(b) Rotating Kepler Problem for energies $c = -2.6$ to -0.6 in steps of 0.2.

Figure 3.8: Hill's regions for the Kepler and rotating Kepler problem.

constant orbits at the unit circle, while below this value orbits are either in the bounded component of the Hill's region, and therefore themselves bounded, or in the unbounded component. In the spatial case the Hill's regions become all of $\mathbb{R}^3 \setminus \{0\}$ for energies above the critical value and $\mathbb{R}^3 \setminus \{0\}$ minus an open filled torus around the critical unit circle in the (q_1, q_2)-plane, staying always a single component.

In the restricted three-body problem with mass ratio $\mu \in (0, 1)$, the potential V_μ has five critical points, called the *Lagrange points*: The first Lagrange point L_1 lies on the q_1-axis between M_1 and M_2, L_2 lies on the far side of M_2 and L_3 lies on the far side of M_1, each on the q_1-axis. Both remaining critical points L_4 and L_5 lie symmetric to each other on an equilateral triangle in the (q_1, q_2)-plane where one side is the segment between M_1 and M_2. They are ordered in terms of energy by $H(L_1) < H(L_2) < H(L_3) < H(L_4) = H(L_5)$ for $\mu \in (0, 1/2)$. For $\mu = 1/2$ the energies at L_2 and L_3 coincide, while the order of the two reverses for $\mu > 1/2$. Global maxima of the effective potential are attained at L_4 and L_5 and the remaining Lagrange points are saddle points. The Hill's regions therefore evolve as follows: For small energies $c < H(L_1)$ the Hill's region is a small closed neighbourhood each of M_1 and M_2, which we denote by $\mathfrak{H}_c^1$ and $\mathfrak{H}_c^2$, and an unbounded component $\mathfrak{H}_c^u$ with large $\|q\|$. As the energy grows to $H(L_1) < c < H(L_2)$ the two bounded components join to a single bounded component $\mathfrak{H}_c^b$, while the unbounded component simply gets a little larger. When $H(L_2) < c < H(L_3)$, the bounded component merges with the unbounded component at the far side of M_2 leaving one horseshoe shaped hole containing L_3, L_4 and L_5. For $H(L_3) < c < H(L_4)$ a gap in the hole closes at L_3 at the far side of M_1 leaving two symmetric holes around each of L_4 and L_5. Finally, for $c > H(L_4)$ theses holes close and the Hill's region is all of $\mathbb{R}^n \setminus \{M_1, M_2\}$. For more details and computations see for

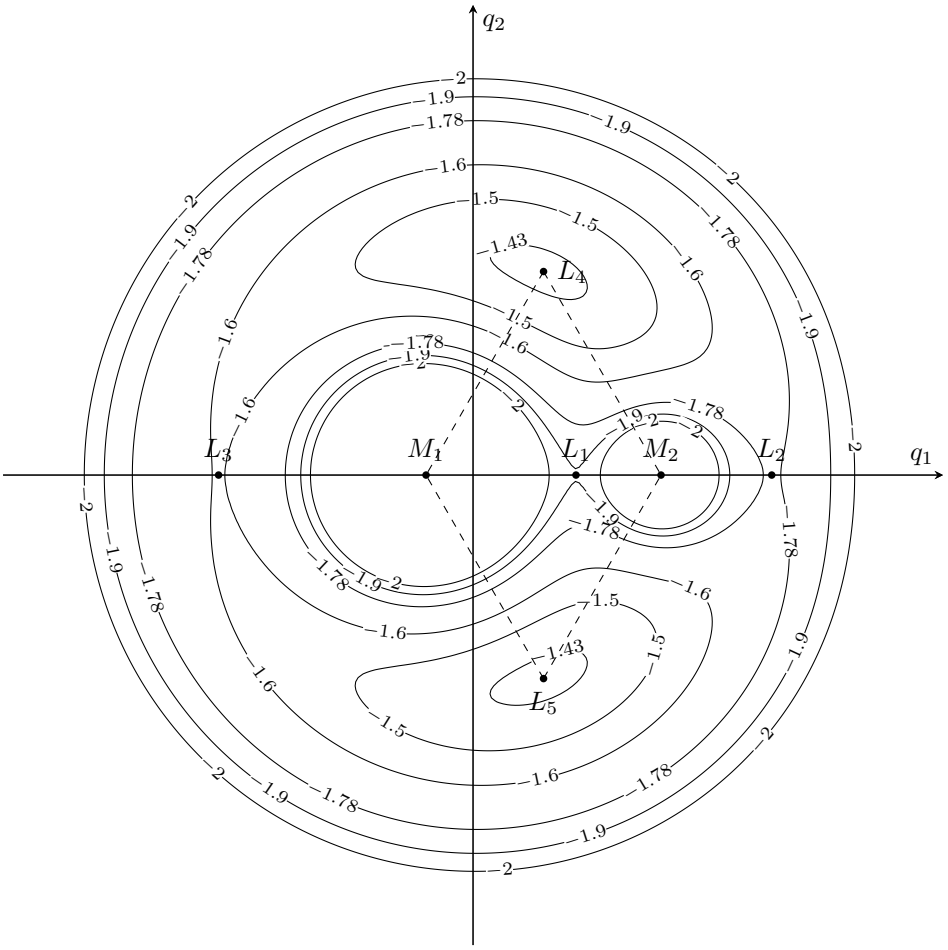

Figure 3.9: Hill's regions of the planar circular restricted three-body problem.

example [Sze67], [AM78], [MHO09] or [FvK18].

This concludes the chapter on Hamiltonian systems. The next step we want to take is to get rid of some of the singularities that the Kepler problem and the restricted three-body problem contain, namely binary collisions of the particle with one of the primaries.

Chapter 4

Regularisations

There are several ways to regularise two body collisions and we want to present two of them here: the Moser regularisation and the Levi-Civita regularisation. We will need each of them later on, while the Moser regularisation is more useful for topological arguments and the Levi-Civita regularisation for dynamical arguments. Both only regularise one primary, but here is also the Birkhoff regularisation, as described in [Bir14], which can regularise both singularities of the restricted three-body problem at the same time.

Before starting, we want to first explain what exactly we mean by a regularisation. Generally, one wishes to regularise a flow that does not exist for all time by extending it beyond its maximal interval of existence. Often there is also a change of parametrisation, i. e. a change of the time involved, so we use the notion of a Hamiltonian manifold from definition 2.17, that gives dynamics up to reparametrisation.

Definition 4.1:
A *regularisation* is an inclusion

$$\iota \colon \Sigma \hookrightarrow \overline{\Sigma}$$

of a Hamiltonian manifold (Σ, ω) into another Hamiltonian manifold $(\overline{\Sigma}, \overline{\omega})$ such that $\iota^* \overline{\omega} = \omega$.

This means that up to reparametrisation the flows coincide but the regularised manifold might be larger and the flow extends at some points. In our setting of a Hamiltonian flow on a symplectic manifold the Hamiltonian manifolds are given by energy level sets Σ_c and the Hamiltonian structure by the restriction $\omega|_{\Sigma_c}$ of the symplectic form. We want to extend the hypersurfaces to include the primaries, thus regularising collisions with the particle M_3.

4.1 Moser regularisation

The first regularisation we will look at is called the *Moser regularisation*, which was first described in [Mos70]. It basically consists of the switch map composed with the

stereographic projection to the round sphere. We will show the explicit computations for the Kepler problem with negative energy and explain how it can also be used to regularise the restricted three-body problem, both times following [FvK18].

Let $c < 0$ be a negative energy. We define a new Hamiltonian

$$\begin{aligned} K(q,p) &= \frac{1}{2}\left(\frac{\|q\|}{-2c}\left(H_{\text{fix}}\left(\frac{q}{\sqrt{-2c}}, \sqrt{-2c}p\right) - c\right) + \frac{1}{\sqrt{-2c}}\right)^2 \\ &= \frac{1}{2}\left(\frac{\|q\|}{-2c}\left(c\|p\|^2 - \frac{\sqrt{-2c}}{\|q\|} - c\right) + \frac{1}{\sqrt{-2c}}\right)^2 \\ &= \frac{1}{8}\left(\|p\|^2 + 1\right)^2 \|q\|^2, \end{aligned} \tag{4.1}$$

where we first composed the Kepler Hamiltonian (3.6) with a physical scaling pushed forward to an exact symplectomorphism on the cotangent bundle as in proposition 2.12. The hypersurface we are interested in is now

$$\Sigma_c = H_{\text{fix}}^{-1}(c) = K^{-1}\left(\frac{1}{-4c}\right).$$

On this level set the Hamiltonian vector fields of H_{fix} and K are parallel since

$$\begin{aligned} \mathrm{d}K\big|_{\Sigma_c}(q,p) &= \frac{1}{\sqrt{-2c}}\,\mathrm{d}\left(\frac{\|q\|}{-2c}\left(H_{\text{fix}}\left(\frac{q}{\sqrt{-2c}}, \sqrt{-2c}p\right) - c\right) + \frac{1}{\sqrt{-2c}}\right)\Big|_{\Sigma_c} \\ &= \frac{\|q\|}{\sqrt{(-2c)^3}}\,\mathrm{d}H_{\text{fix}}\big|_{\Sigma_c}\left(\frac{q}{\sqrt{-2c}}, \sqrt{-2c}p\right) \end{aligned}$$

and the Hamiltonian flows are just reparametrised depending on the distance to the origin $\|q\|$ and the energy c.

Next, we show that this is exactly the flow of the free particle on the round sphere in the map after stereographic projection and switching position and momentum. For this we first of all compute the metric in the chart of the stereographic projection: The metric coefficients of the stereographic projection

$$\begin{aligned} \Phi_{\mathcal{N}} \colon \mathbb{R}^n &\to S^n \setminus \{\mathcal{N}\} \subset \mathbb{R}^{n+1} \\ x = (x_1, \dots x_n) &\mapsto \left(\frac{2x_1}{\|x\|^2+1}, \dots \frac{2x_n}{\|x\|^2+1}, \frac{\|x\|^2-1}{\|x\|^2+1}\right) \end{aligned}$$

through the north pole $\mathcal{N} := (0, \dots, 0, 1) \in \mathbb{R}^{n+1}$ are

$$(g_{ij}(x))_{i,j} = \frac{4}{(\|x\|^2+1)^2}\begin{pmatrix} 1 & 0 \\ 0 & 1 \end{pmatrix}.$$

We invert the matrix $(g_{ij})_{i,j}$ to get

$$\left(g^{ij}(x)\right)_{i,j} = \frac{1}{4}(\|x\|^2+1)^2\begin{pmatrix} 1 & 0 \\ 0 & 1 \end{pmatrix}$$

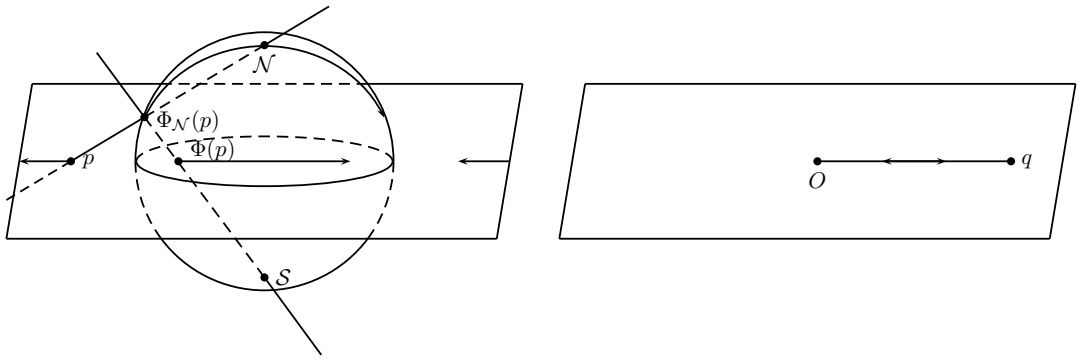

Figure 4.1: A collision orbit in the momentum p-plane regularised by stereographic projection and the corresponding position q-coordinates.

and hence the Hamiltonian of the free particle on the round sphere in the chart of stereographic projection through the north pole becomes

$$\begin{aligned} H_{\text{kin}}(q,p) &= \frac{1}{2}\|p\|_{g_q^*} \\ &= \frac{1}{2}\sum_{i,j=1}^{n} g^{ij}(q)p_i p_j \\ &= \frac{1}{8}(\|q\|^2+1)^2\|p\|^2. \end{aligned}$$

Going back to the transformed Hamiltonian K from (4.1), we can see now that after the switch map

$$\sigma\colon (q,p) \mapsto (-p,q)$$

from example 2.13 the flow of $K \circ \sigma$ on $\mathbb{R}^n$ is exactly the geodesic flow of the round sphere in the chart of the stereographic projection through the north pole.

The picture one should have in mind is the momentum p-plane as a chart of the sphere. As a collision orbit tends towards the point mass at the origin, its momentum tends towards infinity. Projected onto the sphere, the momentum of collision orbits corresponds to geodesics through the north pole and can obviously be continued past $\mathcal{N}$. A change of coordinates that regularises these collisions is for example the chart transition between the stereographic projection through the north pole and the stereographic projection through the south pole $\mathcal{S} := (0,\dots 0,-1) \in S^n \subset \mathbb{R}^{n+1}$, which is given by the map

$$\begin{aligned} \Phi := \Phi_{\mathcal{S}}^{-1} \circ \Phi_{\mathcal{N}}\colon \mathbb{R}^n \setminus \{0\} &\to \mathbb{R}^n \setminus \{0\} \\ p &\mapsto \frac{p}{\|p\|^2} \end{aligned} \tag{4.2}$$

in coordinates $p \in \mathbb{R}^n$.

For the restricted three-body problem we can use the same approach locally around each of the primaries M_1 and M_2. We will show that we can smoothly extend the Hamiltonian in the coordinates changed by the chart transition (4.2). Since we need to invert the Jacobian matrix in order to push forward the change of coordinates to the cotangent bundle, we will do the computations only for $n = 2$. As in the regularisation of the Kepler problem, this works for all dimensions $n \in \mathbb{N}$. For the planar case $n = 2$ see for example again [FvK18] or [AFvKP12] and for the spatial case $n = 3$ see for example [CJK20].

The Jacobian matrix of the chart transition is

$$\mathrm{d}\Phi(p) = \frac{1}{\|p\|^4} \begin{pmatrix} p_2^2 - p_1^2 & -2p_1p_2 \\ -2p_1p_2 & p_1^2 - p_2^2 \end{pmatrix} \tag{4.3}$$

and its inverse transpose is

$$((\mathrm{d}\Phi(p))^T)^{-1} = -\begin{pmatrix} p_1^2 - p_2^2 & 2p_1p_2 \\ 2p_1p_2 & p_2^2 - p_1^2 \end{pmatrix}.$$

By definition 2.11 and proposition 2.12 we get an exact symplectomorphism by

$$\begin{aligned} \mathrm{d}_*\Phi \colon T^*(\mathbb{R}^2 \setminus \{0\}) &\to T^*(\mathbb{R}^2 \setminus \{0\}) \\ (p, q) &\mapsto \left(\frac{p}{\|p\|^2}, -\begin{pmatrix} p_1^2 - p_2^2 & 2p_1p_2 \\ 2p_1p_2 & p_2^2 - p_1^2 \end{pmatrix} \begin{pmatrix} q_1 \\ q_2 \end{pmatrix} \right), \end{aligned} \tag{4.4}$$

where we already use p as the coordinate of the base and q as the coordinate of the fibre, as before. We will now push forward the Hamiltonian (3.14) of the restricted three-body problem along $\mathrm{d}_*\Phi$. This can be done quite easily because Φ is an involution. Therefore, also $\mathrm{d}_*\Phi$ is an involution and we can push forward by pulling back. First, however, we will need to centre the Hamiltonian at that primary where we want to regularise. We will chose M_2 but M_1 can be done the same way or by renaming and switching μ and $1 - \mu$. The shift of coordinates is given by

$$(q_1, q_2, p_1, p_2) \mapsto (q_1 + 1 - \mu, q_2, p_1, p_2 + 1 - \mu)$$

and the new Hamiltonian centred at M_2 becomes

$$\begin{aligned} H_{M_2,\mu}(q, p) &= H_\mu(q + (1 - \mu, 0), p + (0, 1 - \mu)) + \frac{(1 - \mu)^2}{2} \\ &= \frac{\|p\|^2}{2} + p_1q_2 - p_2q_1 - \frac{\mu}{\|q\|} - \frac{1 - \mu}{\|q + (1, 0)\|} - (1 - \mu)q_1, \end{aligned} \tag{4.5}$$

where the constant term was added to cancel out the remaining term from the angular momentum in shifted coordinates. We push forward each of the terms for kinetic energy

$$(\mathrm{d}_*\Phi)_* \left(\frac{\|p\|^2}{2} \right) = (\mathrm{d}_*\Phi)^* \left(\frac{\|p\|^2}{2} \right) = \frac{1}{2\|p\|^2},$$

gravitational potential with respect to M_2

$$\begin{aligned}(\mathrm{d}_*\Phi)_*\left(\frac{1}{\|q\|}\right) &= \frac{1}{\sqrt{(q_1(p_1^2-p_2^2)+2q_2p_1p_2)^2+(2q_1p_1p_2+q_2(p_2^2-p_1^2))^2}}\\ &= \frac{1}{\sqrt{q_1^2(p_1^4+2p_1^2p_2^2+p_2^4)+q_2^2\left(p_2^4+2p_1^2p_2^2+p_1^4\right)}}\\ &= \frac{1}{\|q\|\|p\|^2}\end{aligned}$$

and angular momentum

$$\begin{aligned}(\mathrm{d}_*\Phi)_*(p_1q_2-p_2q_1) &= \left(-2q_1p_1p_2-q_2\left(p_2^2-p_1^2\right)\right)\frac{p_1}{\|p\|^2}-\left(-q_1\left(p_1^2-p_2^2\right)-2q_2p_1p_2\right)\frac{p_2}{\|p\|^2}\\ &= \frac{p_1^2\left(-2q_1p_2+q_2p_1+q_1p_2\right)+p_2^2\left(-q_2p_1-q_1p_2+2q_2p_1\right)}{\|p\|^2}\\ &= p_1q_2-p_2q_1=L.\end{aligned}$$

For the remaining terms $W(q) := -(1-\mu)/\|q+(1,0)\|-(1-\mu)q_1$ we define

$$\begin{aligned}F^W\colon (d_*\Phi)\left(\left(\mathbb{R}^2\setminus\{0\}\times U\right)\cup\left(\{0\}\times\mathbb{R}^2\right)\right) &\to \mathbb{R}\\ (p,q) &\mapsto \begin{cases} W\left(\pi_q\left(\mathrm{d}_*\Phi(p,q)\right)\right) & \text{if } p\neq 0\\ W(0) & \text{if } p=0,\end{cases}\end{aligned}$$

where U is the set $\mathbb{R}^2\setminus\{(-1,0)\}$ on which W is defined and $\pi_q\colon (p,q)\mapsto q$ is the projection of $\mathbb{R}^2\setminus\{0\}\times U$ along p onto U with coordinates q. The map F^V is smooth since the q-coordinates of (4.4) converge to zero as $p\to 0$ and it is the pullback of W at all other points.

All in all, the Hamiltonian in the new coordinates is

$$(q,p)\mapsto \frac{1}{2\|p\|^2}-\frac{1}{\|p\|^2\|q\|}+L(q,p)+F^W(p,q)$$

for the restricted three-body problem and

$$(q,p)\mapsto \frac{1}{2\|p\|^2}-\frac{1}{\|p\|^2\|q\|}$$

for the Kepler problem. Let $c\in\mathbb{R}$ be any energy value of the transformed Hamiltonian in our new coordinates. Then we can extend the energy hypersurface Σ_c smoothly to the fibre over $p=0$. We call this extension the *regularised energy hypersurface* $\overline{\Sigma}_c$ and it intersects the fibre at $p=0$ in the map of the stereographic projection through the south pole in a circle with radius 2

$$\overline{\Sigma}_c\cup\{p=0\}=\left\{\frac{1}{2}=\frac{1}{\|q\|}\right\}.$$

One can see this by multiplying the equation

$$c = \frac{1}{2\|p\|^2} - \frac{1}{\|p\|^2\|q\|} + L(q,p) + F^W(q,p)$$

for the energy hypersurface Σ_c of the restricted three-body problem or the equation

$$c = \frac{1}{2\|p\|^2} - \frac{1}{\|p\|^2\|q\|}$$

for Σ_c of the Kepler problem by $\|p\|^2$ and taking the limit as $p \to 0$.

What we take away from these computations is that we can regularise the restricted three-body problem and the Kepler problem at collisions for all energies by applying the stereographic projection to the momentum coordinates p. We will use this later on to compute the topology of the energy hypersurfaces for energies above the highest critical value. Both the regularised energy hypersurface $\overline{\Sigma}_c$ of the Kepler problem for negative energies $c < 0$ as well as the bounded components $\overline{\Sigma}_c^1$ and $\overline{\Sigma}_c^2$ of the regularised energy hypersurface $\overline{\Sigma}_c$ of the restricted three-body problem for energies $c < H(L_1)$ below the lowest critical value are each diffeomorphic to the unit cotangent bundle S^*S^n of the n-sphere. So in the planar case we have $\overline{\Sigma}_c^1 \cong \overline{\Sigma}_c^2 \cong S^*S^2 \cong \mathbb{RP}^3$ and in the spatial case we have $\overline{\Sigma}_c^1 \cong \overline{\Sigma}_c^2 \cong S^*S^3 \cong S^2 \times S^3$. Between the first and the second critical value $H(L_1) < c < H(L_2)$ the bounded component $\overline{\Sigma}_c^b$ of the regularised energy hypersurface becomes diffeomorphic to the connected sum between two copies of S^*S^n.

4.2 Levi-Civita regularisation

The second regularisation we will use is the *Levi-Civita regularisation*, first introduced in [LC20]. Here, the squaring map in complex coordinates is used to get a regularised double cover of our original orbit. This obviously only works for dimension $n = 2$ but there is also a three-dimensional analogue in the Kustaanheimo-Stiefel regularisation from [KS65]. Since we have already regularised the spatial cases with the Moser regularisation and all constructions are planar, the Levi-Civita regularisation suffices for this work. The advantage of the Levi-Civita regularisation over the Moser regularisation is that one can get nice explicit formulae for the transformed orbit which even allows to check the shape of Kepler orbits as a bonus.

First of all, we will again focus on the Kepler problem and then regularise the restricted three-body problem. For the Kepler problem we follow [Fra17], but details can also be found in [FvK18] and very explicit formulae in a more dynamical point of view in [Cel06].

Consider the map

$$\begin{aligned} l\colon \mathbb{C} \setminus \{0\} &\to \mathbb{C} \setminus \{0\} \\ X &\mapsto X^2 = Q \end{aligned} \tag{4.6}$$

in complex coordinates $X \in \mathbb{C} \cong \mathbb{R}^2$. We push this forward as in proposition 2.12 to a local exact symplectomorphism

$$\mathrm{d}_* l\colon T^*(\mathbb{C} \setminus \{0\}) \to T^*(\mathbb{C} \setminus \{0\}) \tag{4.7}$$

on cotangent bundles by transposing and inverting the Jacobian

$$\mathrm{d}l(X_1, X_2) = \begin{pmatrix} 2X_1 & -2X_2 \\ 2X_2 & 2X_1 \end{pmatrix}$$

in real coordinates. The transformation of the momentum coordinates Y then becomes

$$\begin{aligned} \begin{pmatrix} Y_1 \\ Y_2 \end{pmatrix} &\mapsto \frac{1}{4\|X\|^2} \begin{pmatrix} 2X_1 & -2X_2 \\ 2X_2 & 2X_1 \end{pmatrix} \begin{pmatrix} Y_1 \\ Y_2 \end{pmatrix} \\ &= \frac{1}{2\|X\|^2} \begin{pmatrix} X_1Y_1 - X_2Y_2 \\ X_1Y_2 + X_2Y_1 \end{pmatrix} \end{aligned}$$

and we have the full change of coordinates

$$\begin{aligned} Q_1 &= X_1^2 - X_2^2 & P_1 &= \frac{X_1Y_1 - X_2Y_2}{2\|X\|^2} \\ Q_2 &= 2X_1X_2 & P_2 &= \frac{X_1Y_2 + X_2Y_1}{2\|X\|^2}, \end{aligned} \tag{4.8}$$

which can in complex notation be written as

$$\mathrm{d}_*l(X, Y) = \left(X^2, \frac{Y}{2\overline{X}} \right) = (Q, P).$$

We define for any Kepler energy $c \in \mathbb{R}$ the new regularised Hamiltonian by

$$\begin{aligned} K_c(X, Y) :&= 4\,|X|^2 \left((\mathrm{d}_*l)^*\, H_{\mathrm{fix}}(X, Y) - c \right) \\ &= 4\,|X|^2 \left(\frac{|Y|^2}{8\,|X|^2} - \frac{1}{|X|^2} - c \right) \\ &= \frac{1}{2}\,|Y|^2 - 4c\,|X|^2 - 4. \end{aligned}$$

The Hamiltonian vector fields are parallel again on $\Sigma_c = H_{\mathrm{fix}}^{-1}(c)$ by

$$\mathrm{d}K_c|_{\Sigma_c}(X, Y) = 4\,|X|^2\, \mathrm{d}H_{\mathrm{fix}}|_{\Sigma_c}(X, Y),$$

so we have the time transformation

$$\mathrm{d}t = 4\,|X|^2\, \mathrm{d}s \tag{4.9}$$

between the usual time t and the regularised time s. The relevant energy level set for the new Hamiltonian K_c is the preimage of zero

$$\Sigma_c = H_{\mathrm{fix}}^{-1}(c) = K_c^{-1}(0)$$

and we recognise in K_c the Hamiltonian for a system of two uncoupled isotropic harmonic oscillators with force $\ddot{q} = 8cq$. So for negative Kepler energy $c < 0$ we have an attractive

oscillator, for $c = 0$ we have the free particle and for $c > 0$ we have a repulsive oscillator, each with energy $H_{8c}(q, p) = 4$ of the Hamiltonian (3.3).

As we have seen in section 3.2, solutions to the harmonic oscillator with $a_k = 8c < 0$ for $k = 1, 2$ and positive energy are ellipses with centre at the origin and frequency

$$\varpi = \sqrt{-a_k} = \sqrt{-8H_{\text{fix}}}. \tag{4.10}$$

At $c = 0$ we get the free particle in the plane and solutions are geodesics, i. e. straight lines with constant velocity. For positive Kepler energies $c > 0$ we have a repulsive oscillator and solutions are hyperbolas with centre at the origin.

Obviously, we can continue all of the solutions of the harmonic oscillator through the origin and the image one should have in mind for the Levi-Civita regularisation is that of the orbit passing through the primary in regularised coordinates X and bouncing back after the double cover of the squaring map in original coordinates Q. The Levi-Civita-regularised energy hypersurface of negative energies becomes the level set $H_{8c}^{-1}(4) \cong S^3$ which is a double and universal cover of the Moser-regularised energy hypersurface $\overline{\Sigma}_c \cong \mathbb{RP}^3$.

With this knowledge about Levi-Civita-regularised Kepler orbits, we can quickly check the fact from section 3.3 that bounded Kepler solutions are ellipses with focus at the origin, and compute the shape of unbounded solutions as well:

Corollary 4.2:
Solutions to Kepler's problem for negative energies $c < 0$ are ellipses with focus at the origin, parabolas with focus at the origin for $c = 0$ and hyperbolas with focus at the origin for positive energies $c > 0$.

Proof: For the first part we simply square the solution (3.4) to an attractive isotropic harmonic oscillator to get

$$\begin{aligned} Q(s) = (X(s))^2 &= \left(Ae^{i\sqrt{-8c}s} + Be^{-i\sqrt{-8c}s}\right)^2 \\ &= A^2e^{2i\sqrt{-8c}s} + B^2e^{-2i\sqrt{-8c}s} + 2AB, \end{aligned}$$

which is an ellipse with centre in $2AB \in \mathbb{C}$. The property of being an ellipse or parabola or hyperbola with focus at the origin is invariant under rotation around 0 as well as under time-shift, so we can assume as in the proof of lemma 3.4 that $A, B \in \mathbb{R}$. We have seen there as well that the linear eccentricity of the ellipse can be computed by

$$\begin{aligned} \epsilon a &= \sqrt{(A^2 + B^2)^2 - (A^2 - B^2)^2} \\ &= \sqrt{4A^2B^2} = 2AB, \end{aligned}$$

which is exactly the distance, by which the ellipse is shifted.

At $c = 0$ we also rotate and time-shift the straight geodesic with constant speed $v \in \mathbb{R}$ such that it has the equation $X(s) = x_0 + ivs \in \mathbb{C}$ for some initial position

$X(0) = x_0 \in \mathbb{R}$. Then by squaring we have the Kepler solution $Q(s) = x_0^2 - s^2v^2 + 2ivs$ which is obviously a parabola with the equation

$$Q_1 = x_0^2 - \frac{1}{4x_0^2}Q_2^2.$$

The focus of this parabola lies at $x_0^2 + 1/(4\frac{1}{-4x_0^2}) = 0 \in \mathbb{C}$, as claimed.

Finally, for positive Kepler energies $c > 0$ we square the solution to a repulsive oscillator and get

$$\begin{aligned} Q(s) = (X(s))^2 &= \left(Ae^{\sqrt{8c}s} + Be^{-\sqrt{8c}s}\right)^2 \\ &= A^2e^{2\sqrt{8c}s} + B^2e^{-2\sqrt{8c}s} + 2AB. \end{aligned}$$

As in the proof of lemma 3.5, we can assume by rotation and time-shift that $A = \overline{B}$ to get the standard parametric form of a hyperbola

$$Q(s) = 2\mathrm{Re}\left(A^2\right)\cosh\left(2\sqrt{8c}s\right) + 2i\mathrm{Im}\left(A^2\right)\sinh\left(2\sqrt{-8c}s\right) + 2\left|A\right|^2$$

displaced by its focal distance $2\left|A\right|^2$.

One issue to note here is that by physical intuition we would expect the hyperbolic trajectory of the Kepler problem to go around its focus at the origin. This is not imminently clear from the equations yet because the focus at the origin could also be the second focus where that particular branch of the hyperbola does not go around. However, we can see that the intuition is true by plugging the initial conditions

$$X(0) = 2\mathrm{Re}(A) \qquad \text{and} \qquad X'(0) = 2i\sqrt{8c}\mathrm{Im}(A)$$

into the regularised Hamiltonian K_c and solve for the required energy zero:

$$\begin{aligned} & 0 = K_c(X(0), Y(0)) = \frac{\left(2\sqrt{8c}\mathrm{Im}(A)\right)^2}{2} - 4c\left(2\mathrm{Re}(A)\right)^2 - 4 \\ \iff \quad & \frac{1}{4c} = \mathrm{Im}(A)^2 - \mathrm{Re}(A)^2. \end{aligned}$$

So, for all positive Kepler energy c the imaginary part of A must be larger in absolute value than its real part, making the angle between the asymptotes

$$\{(x + iy) \in \mathbb{C} : \mathrm{Re}(A)y = \pm\mathrm{Im}(A)x\}$$

of the hyperbola between π and 3π. The squaring map doubles the angle between the asymptotes, while the initial position remains on the positive real axis, which now gives the shape one would expect. □

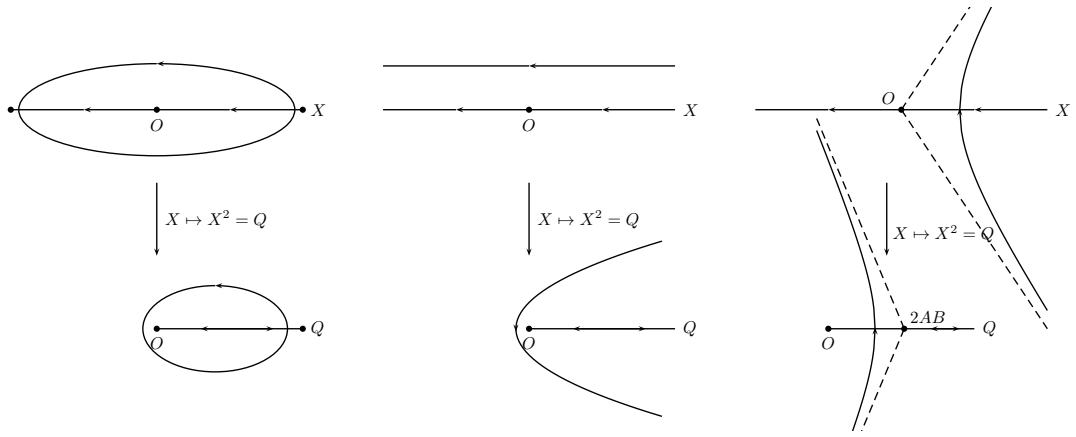

(a) $c < 0$ (b) $c = 0$ (c) $c > 0$

Figure 4.2: Levi-Civita-regularised Keper orbits in regularised position coordinates X and their images in usual position coordinates Q.

For later computations we want to just go back shortly to the ellipse in regularised coordinates X and make the connection to data from the Kepler ellipse: After rotation and time-shift as above the ellipse with initial conditions

$$\begin{aligned} X_1(0) &= \sqrt{Q_1(0)} & Y_1(0) &= 0 \\ X_2(0) &= 0 & Y_2(0) &= 2P_2(0)X_1(0) = 2\dot{Q}_2(0)\sqrt{Q_1(0)} \end{aligned}$$

has the equations

$$X_1(s) = \alpha\cos(\varpi s) \qquad X_2(s) = \beta\sin(\varpi s). \tag{4.11}$$

We can express the coefficients α and β using the semi-major axis a, the eccentricity ϵ and the direction of rotation ϵ', defined in (3.10), with the help of (3.8) and (3.6) by

$$\alpha = X_1(0) = \sqrt{a(1+\epsilon)} \tag{4.12}$$

$$\beta = \frac{Y_2(0)}{\varpi} = \frac{2\epsilon'\sqrt{2H_{\text{fix}} + 2\frac{1}{Q_1(0)}}\sqrt{Q_1(0)}}{\varpi} = \frac{2\epsilon'\sqrt{\frac{1-\epsilon}{a(1+\epsilon)}}\sqrt{a(1+\epsilon)}}{\frac{2}{\sqrt{a}}} = \epsilon'\sqrt{a(1-\epsilon)}. \tag{4.13}$$

This gives us all we need from the Levi-Civita regularisation of the Kepler problem. The next paragraphs will be about the regularisation of the restricted three-body problem where we will again focus on the lighter primary M_2. Additionally, we will consider the limit $\mu \to 0$ in this setting. A first use of this was in [Con63], while other references are [MN95] and [Che89].

We use the Hamiltonian (4.5) of the restricted three-body problem with M_2 shifted to the origin again. In complex notation $(\xi, \eta) \in T^*(\mathbb{C} \setminus \{0, -1\})$ this becomes

$$H_{2,\mu}(\xi,\eta) = \frac{|\eta|^2}{2} + \frac{i}{2}(\eta\overline{\xi} - \overline{\eta}\xi) - \frac{\mu}{|\xi|} - \frac{1-\mu}{|\xi+1|} - \frac{1-\mu}{2}(\xi + \overline{\xi}). \tag{4.14}$$

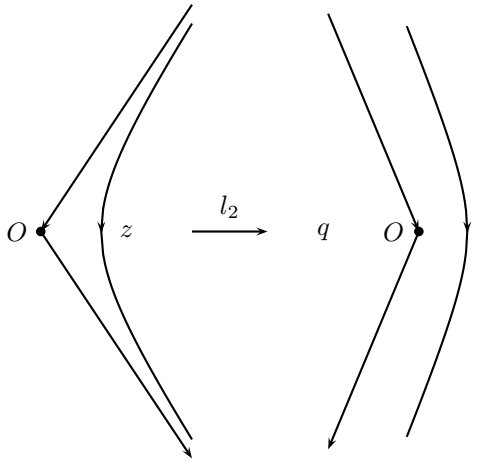

Figure 4.3: Solutions to this Hamiltonian system with $H = |w|^2/2 - |z|^2 + O_4(z,w)$ with energy μ get mapped by l_2 to solutions of the restricted three-body problem with mass ratio μ.

While we did the Moser regularisation at M_2 for all energies $c \in \mathbb{R}$, we are now mostly interested in the regularisation for energies above the highest critical value $H_\mu(L_5)$, which is where our constructed orbits will lie. We therefore define a new energy $h := c_2 + 1 - \mu$, where $c_2 := c + (1-\mu)^2/2$ is the energy of the Hamiltonian (4.14), which had an added term to cancel out remains from the shifted angular momentum. Assuming $h > 0$, we introduce the local conformal symplectomorphism

$$\begin{aligned} l_2 \colon T^*(\mathbb{C} \setminus \{0\}) &\to T^*(\mathbb{C} \setminus \{0\}) \\ (z,w) &\mapsto \left(\frac{z^2}{h}, \frac{\sqrt{h}w}{\overline{z}} \right) = (\xi, \eta), \end{aligned}$$

which is the Levi-Civita transformation from (4.7) with an extra conformal scaling by factor $2/\sqrt{h}$. We define the new Hamiltonian in regularised coordinates (z,w) by

$$\begin{aligned} K_{\mu,h}(z,w) :&= \frac{|z|^2}{h} \left(H_{2,\mu} \circ l_2(z,w) - h \right) \\ &= \frac{|z|^2}{h} \left(\frac{h\,|w|^2}{2\,|z|^2} + \frac{i}{2} \left(\frac{\sqrt{h}w\overline{z}^2}{\overline{z}h} - \frac{\sqrt{h}\overline{w}z^2}{zh} \right) - \frac{\mu h}{|z|^2} - \frac{(1-\mu)}{\left| \frac{z^2}{h} + 1 \right|} - h \right) \\ &= \frac{|w|^2}{2} + \frac{i\,|z|^2}{2\sqrt{h}^3} (w\overline{z} - \overline{w}z) - \mu - \frac{(1-\mu)\,|z|^2}{|z^2+h|} + \frac{(1-\mu)\,|z|^2 \left(z^2 + \overline{z}^2\right)}{2h^2} - |z|^2 \\ &= \frac{|w|^2}{2} - |z|^2 - \mu + O_4(z,w), \end{aligned} \tag{4.15}$$

where the last line is attained after Taylor expansion at zero. We are interested in the

energy hypersurface

$$\Sigma_c = H_{2,\mu}^{-1}(h) = K_{\mu,h}^{-1}(0),$$

where the Hamiltonian vector field are again parallel:

$$\mathrm{d}K_{\mu,h}\big|_{\Sigma_c} = \frac{|z|^2}{h}\,\mathrm{d}H_{\mu}\big|_{\Sigma_c}$$

Notice that as in the repulsive oscillator system there is a hyperbolic fixed point at zero for $\mu = 0$ in this energy hypersurface and solutions of the Hamiltonian system

$$K_{\mu,h}(z,w) + \mu = \frac{|w|^2}{2} - |z|^2 + O_4(z,w)$$

with energy μ get mapped by l_2 to solutions in the restricted three-body problem with mass ratio μ. The stable manifold corresponds to incoming collision orbits, that in the new regularised time s only asymptotically reach M_2, while the unstable manifolds corresponds to outgoing collision orbits. This will be useful later in the analysis of how collision orbits with M_2 at $\mu = 0$ change for infinitesimally small μ, or, in other words, what the limit of near collision orbits looks like as $\mu \to 0$.

Chapter 5

Energy hypersurfaces

The main goal of this chapter is to compute generators of the first de Rham cohomology, which is essential to us in view of remark 2.36 for the obstructions to contact forms. These generators are found by computing the fundamental group of the Moser-regularised energy hypersurface, then abelianising it to the first homology group, modding out torsion to get real coefficients and, finally, dualising to get generators of the first de Rham cohomology. We will write all groups that appear here multiplicatively unless they are inherently abelian, in which case we will write them additively. First of all, we will compute the planar case which will take most of this chapter and then comment on the spatial case.

Recall from chapter 3 the notation $\Sigma_c := H^{-1}(c)$ for the energy hypersurface of the Kepler problem or the restricted three-body problem. Denote by $\overline{\Sigma}_c$ the corresponding regularised energy hypersurface, where collisions have been added by Moser regularisation as described in section 4.1.

In the first step we compute the fundamental group of $\overline{\Sigma}_c$ using the well-known theorem of Seifert-van Kampen.

Theorem 5.1 (Seifert-van Kampen):
Let $X = U_1 \cup U_2$ be a topological space which can be decomposed as the union of two path-connected open subsets. Suppose that $U_3 := U_1 \cap U_2 \ni x_0$ is also path-connected and nonempty. Denote by the maps $v_k \colon \pi_1(U_1 \cap U_2, x_0) \to \pi_1(U_k, x_0)$ for $k = 1, 2$ and $u_k \colon \pi_1(U_k, x_0) \to \pi_1(U_1 \cup U_2, x_0)$ for $k = 1, 2, 3$ the homomorphisms on fundamental groups induced by the inclusions of subsets. Let G be a group and $p_i \colon \pi_1(U_k, x_0) \to G$ homomorphisms such that $p_3 = p_k \circ v_k$ for $k = 1$ and 2. Then there exists a unique homomorphism $p \colon \pi_1(X, x_0) \to G$ such that $p_k = p \circ u_k$ for all $k = 1, 2$ and 3. In particular, the fundamental group of X can be computed by

$$\pi_1(X, x_0) = \pi_1(U_1, x_0) *_{\pi_1(U_1 \cap U_2, x_0)} \pi_1(U_2, x_0),$$

where $*_{\pi_1(U_1 \cap U_2, x_0)}$ represents the free product amalgamated by $\pi_1(U_1 \cap U_2, x_0)$. I.e. we have the presentation

$$\pi_1(X, x_0) = \langle \zeta_1, \dots \zeta_k, \eta_1, \dots \eta_m \mid r_1, \dots r_l, s_1, \dots s_n, v_1(\xi_1) = v_2(\xi_1), \dots v_1(\xi_p) = v_2(\xi_p) \rangle \,,$$

where the fundamental groups of U_i are presented by $\pi_1(U_1, x_0) = \langle \zeta_1, \dots \zeta_k \mid r_1, \dots r_l \rangle$, $\pi_1(U_2, x_0) = \langle \eta_1, \dots \eta_m \mid s_1, \dots s_n \rangle$ *and* $\pi_1(U_1 \cap U_2, x_0) = \langle \xi_1, \dots \xi_p \mid t_1, \dots t_q \rangle$.

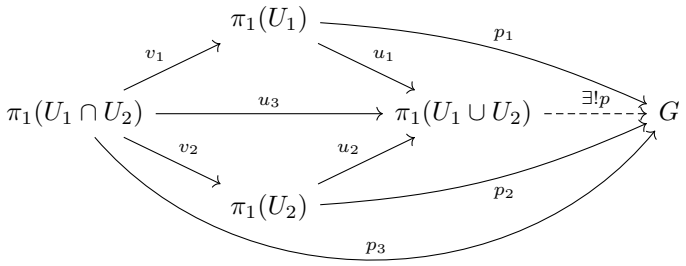

We will explicitly compute the fundamental group of the bounded component of the regularised energy hypersurface of the Kepler problem and then use the relations found there to compute the more complicated hypersurface of the restricted three-body problem above the highest critical value $H_\mu(L_5)$.

In the Moser regularisation from section 4.1 first the roles of P and Q are interchanged, such that the base points of the cotangent bundle now corresponded to the momentum of the particle and the fibre to its position. At every point in the base the intersection between the hypersurface and the fibre is then a circle of positions. The base as points of momentum is endowed with the metric of the stereographic projection of S^2 through the north pole $\mathcal{N}$, corresponding to infinite momentum at collision. The regularised energy hypersurface is thus the unit cotangent bundle $S^*(S^2) \cong \mathbb{RP}^3$ of the round 2-sphere. We choose as the second chart of S^2 the stereographic projection through the south pole $\mathcal{S}$, corresponding to zero momentum. The setting in terms of theorem 5.1 is then

$$\begin{aligned} U_1 &:= S^*(S^2 \setminus \{\mathcal{N}\}) \cong S(\mathbb{R}^2) \\ U_2 &:= S^*(S^2 \setminus \{\mathcal{S}\}) \cong S(\mathbb{R}^2) \text{ and} \\ U_3 &= S^*(S^2 \setminus \{\mathcal{S}, \mathcal{N}\}) \cong S(\mathbb{R}^2 \setminus \{0\}), \end{aligned}$$

where the trivialisations of U_1 and U_3 are given by the stereographic projection through the north pole and the trivialisation of U_2 by the stereographic projection through the south pole. Recall from (4.2) that the change of these variables is given in local coordinates $x \in \mathbb{R}^2$ by

$$\Phi(x_1, x_2) = \left(\frac{x_1}{x_1^2 + x_2^2}, \frac{x_2}{x_1^2 + x_2^2} \right)$$

and the Jaconian (4.3) is

$$\mathrm{D}\Phi(x_1, x_2) = \frac{1}{(x_1^2 + x_2^2)^2} \begin{pmatrix} x_2^2 - x_1^2 & -2x_1x_2 \\ -2x_1x_2 & x_1^2 - x_2^2 \end{pmatrix}.$$

As the base point for the fundamental groups we choose

$$x_0 := ((1,0),(1,0)) \in S(\mathbb{R}^2 \setminus \{0\}) \cong U_3 = U_1 \cap U_2,$$

i. e. the point with momentum $P = (1,0)$ and position $Q = (1,0)$. In the trivialisation of U_2 this point x_0 corresponds to $((1,0),(-1,0)) \in S(\mathbb{R}^2)$.

The fundamental groups of the subsets are

$$\begin{aligned}
\pi_1(U_1, x_0) &= \langle \zeta \rangle \cong \mathbb{Z} \\
\pi_1(U_2, x_0) &= \langle \eta \rangle \cong \mathbb{Z} \\
\pi_1(U_3, x_0) &= \langle \xi_1, \xi_2 \mid [\xi_1, \xi_2] \rangle \cong \mathbb{Z} \times \mathbb{Z},
\end{aligned}$$

where ζ and ξ_1 is each the class of homotopic loops based at x_0 and represented by

$$t \mapsto ((1,0),(\cos(2\pi t), \sin(2\pi t))),$$

i. e. a simple loop in the position fibre, η is also represented by a loop

$$t \mapsto ((1,0),(-\cos(2\pi t), \sin(2\pi t))),$$

in the fibre and ξ_2 is represented by a loop

$$t \mapsto ((\cos(2\pi t), \sin(2\pi t)),(1,0))$$

in the momentum base.

For theorem 5.1 we need to compute the images $v_i(\xi_j)$ for $i, j \in \{1,2\}$ of generators of $\pi_1(U_3, x_0)$ after the homomorphisms induced by the inclusions $U_1 \hookrightarrow U_3$ and $U_2 \hookrightarrow U_3$. Since we chose the same trivialisation for U_1 and U_3, the first two are simply $v_1(\xi_1) = \zeta$ and $v_1(\xi_2) = 1$ because ζ and ξ_1 are identically represented in the trivialisation and the representation of ξ_2 is contractible in U_1. For the second homomorphism v_2 we need to check the differential of the change of trivialisations, i. e. the Jacobian of the change of coordinates between the stereographic projection through the north and the south pole.

The representation of ξ_1 readily gets mapped onto the representation of η, so $v_2(\xi_1) = \eta$. The image of the representation of ξ_2 is again contractible in the base, but it twists the fibre twice in the opposite direction of η since

$$\begin{aligned}
\mathrm{D}\Phi(\cos(2\pi t), \sin(2\pi t)) \begin{pmatrix} 1 \\ 0 \end{pmatrix} &= \left(\sin^2(2\pi t) - \cos^2(2\pi t), -2\sin(2\pi t)\cos(2\pi t)\right) \\
&= \left(-\cos(4\pi t), -\sin(4\pi t)\right).
\end{aligned}$$

All in all we have

$$\begin{aligned}
v_1(\xi_1) &= \zeta, & v_1(\xi_2) &= 1, \\
v_2(\xi_1) &= \eta, & v_2(\xi_2) &= \eta^{-2}
\end{aligned}$$

and the fundamental group of $\overline{\Sigma}_c$ becomes

$$\pi_1(\overline{\Sigma}_c, x_0) = \langle \zeta, \eta \mid \zeta = \eta, \eta^{-2} \rangle = \langle \zeta \mid \zeta^2 \rangle \cong \mathbb{Z}_2.$$

Of course we would have known that earlier from the fact that $\overline{\Sigma}_c \cong S^*S^2 \cong \mathbb{RP}^3$, but now we can use the relations from above to compute the fundamental groups of more complicated regularised hypersurfaces.

The surface we are interested in is the energy level set of the restricted three-body problem above the highest critical value $H_\mu(L_5) < c$. Here, we need to regularise two singularities and we will therefore apply the theorem of Seifert-van Kampen twice. As the subsets we again choose the unregularised energy level set

$$U_1 := \Sigma_c \cong S^*(\mathbb{R}^2 \setminus \{M_1, M_2\}) \cong S(\mathbb{R}^2 \setminus \{M_1, M_2\}),$$

for the local regularising charts each a copy of the unit cotangent bundle of a small open 2-disc

$$U_2, U_3 := S^*(B_\varepsilon) \cong S(\mathbb{R}^2),$$

and the intersections become unit cotangent bundles of punctured 2-discs

$$U_4, U_5 := S^*(B_\varepsilon \setminus \{0\}) \cong S(\mathbb{R}^2 \setminus \{0\}).$$

Remember, however, that the trivialisation of Σ_c, where currently the position coordinates form the base, is changed in the first step of regularisation, such that the momentum becomes the base and the fibre is the position. The fundamental groups of these spaces are

$$\begin{aligned}
\pi_1(U_1) &= \langle r, w_1, w_2 \mid [r, w_1], [r, w_2] \rangle, \\
\pi_1(U_2) &= \langle \eta_2 \rangle, \\
\pi_1(U_3) &= \langle \eta_3 \rangle, \\
\pi_1(U_4) &= \langle \xi_1, \xi_2 \mid [\xi_1, \xi_2] \rangle \quad \text{and} \\
\pi_1(U_5) &= \langle \xi_3, \xi_4 \mid [\xi_3, \xi_4] \rangle,
\end{aligned}$$

where r is represented by the loop in momentum coordinates over a fixed position, w_1 is the winding in position around M_1 and w_2 is the winding in position around M_2, both commuting with r. The two η_2 and η_3 are defined, same as η above, as the loop in position coordinates, as well as ξ_1 and ξ_3, just as in ξ_1 from above, while ξ_2 and ξ_4 are a represented by a loop in momentum coordinates, as was ξ_2 from before. Denote the homomorphisms of fundamental groups induced by inclusions as

$$\begin{aligned}
&\upsilon_1 \colon \pi_1(U_4) \to \pi_1(U_1), && \upsilon_3 \colon \pi_1(U_5) \to \pi_1(U_1), \\
&\upsilon_2 \colon \pi_1(U_4) \to \pi_1(U_2), && \upsilon_4 \colon \pi_1(U_5) \to \pi_1(U_3).
\end{aligned}$$

We can now use the same relations as in the Kepler problem:

$$\begin{aligned}
\upsilon_1(\xi_1) &= w_1 & \upsilon_1(\xi_2) &= r \\
\upsilon_2(\xi_1) &= \eta_2 & \upsilon_2(\xi_2) &= \eta_2^{-2} \\
\upsilon_3(\xi_3) &= w_2 & \upsilon_3(\xi_4) &= r \\
\upsilon_4(\xi_3) &= \eta_3 & \upsilon_4(\xi_4) &= \eta_3^{-2}
\end{aligned}$$

The only difference is that the loop in momentum coordinates is no longer contractible in the original $\Sigma_c = U_1$. Putting together the generators and relations as in theorem 5.1, we get

$$\begin{aligned}\pi_1(\overline{\Sigma}_c) &= \langle r, w_1, w_2, \eta_2, \eta_3 \mid [r, w_1], [r, w_2], w_1 = \eta_2, r = \eta_2^{-2}, w_2 = \eta_3, r = \eta_3^{-2}\rangle \\ &= \langle r, w_1, w_2 \mid [r, w_1], [r, w_2], r = w_1^{-2}, r = w_2^{-2}\rangle \\ &= \langle w_1, w_2 \mid w_1^2 = w_2^2\rangle.\end{aligned} \tag{5.1}$$

In order to find the first de Rham cohomology, we first compute the abelianisation

$$\begin{aligned}H_1(\overline{\Sigma}_c, \mathbb{Z}) \cong \pi_1(\overline{\Sigma}_c)^{\mathrm{ab}} &= \langle w_1, w_2 \mid 2w_1 = 2w_2\rangle \\ &= \langle w_1, w_2, z \mid 2w_1 = 2w_2, z = w_2 - w_1\rangle \\ &= \langle w_1, z \mid 2z\rangle \\ &\cong \mathbb{Z} \times \mathbb{Z}_2,\end{aligned}$$

which is isomorphic to the first homology group with integer coefficients. By modding out torsion by the universal coefficient theorem we get the first homology with real coefficients

$$H_1(\overline{\Sigma}_c, \mathbb{R}) \cong \mathbb{R} \cong H^1_{\mathrm{dR}}(\overline{\Sigma}_c),$$

which is also isomorphic to the first de Rham cohomology by duality and de Rham's theorem. We compute the push forward of the inclusion $\iota\colon \Sigma_c \hookrightarrow \overline{\Sigma}_c$ on homology

$$\iota_*\colon H_1(\Sigma_c) \cong \mathbb{R}^3 \to H_1(\overline{\Sigma}_c) \cong \mathbb{R}.$$

The kernel of ι_* can be found from line (5.1) to be $\ker(\iota_*) = \langle r + 2w_1, r + 2w_2\rangle_{\mathbb{R}}$ and the coimage is then $\ker(\iota_*)^{\perp} = \langle 2r - w_1 - w_2\rangle_{\mathbb{R}}$. We abuse the notation from above of fundamental classes r, w_1 and w_2 to also denote generators of homology.

Dualising to cohomology, we see that the image of the pullback of ι on cohomology

$$\iota^*\colon H^1_{\mathrm{dR}}(\overline{\Sigma}_c) \cong \mathbb{R} \to H^1_{\mathrm{dR}}(\Sigma_c) \cong \mathbb{R}^3$$

is then $\mathrm{im}(\iota^*) = \langle 2\,\mathrm{d}\vartheta - \mathrm{d}\varphi_1 - \mathrm{d}\varphi_2\rangle$, where ϑ is the polar angle in momentum coordinates and φ_1 and φ_2 are polar angles in position coordinates centred at M_1 and M_2, respectively. So, we have found a generator of the first de Rham cohomology of the regularised energy hypersurface above the highest critical value, which we can compute easily for periodic non-collision orbits by twice the rotation number minus the two winding numbers around the primaries. We summarise the results from this chapter on the planar restricted three-body problem in the following lemma:

Lemma 5.2:
For the planar circular restricted three-body problem and energies c above the highest critical value $H_\mu(L_5)$ the first de Rham cohomology of the Moser-regularised energy hypersurface $\overline{\Sigma}_c$ is one-dimensional and has generator $[0] \neq [\beta_0] \in H^1_{\mathrm{dR}}(\overline{\Sigma}_c)$ which agrees with $2\,\mathrm{d}\vartheta - \mathrm{d}\varphi_1 - \mathrm{d}\varphi_2$ on the unregularised level set Σ_c.

If we use the same setup in the spatial case, we see that all sets

$$\begin{aligned} U_1 &= \Sigma_c \cong S(\mathbb{R}^2 \setminus \{M_1, M_2\}), \\ U_2, U_3 &= S^*(B_\varepsilon) \cong S(\mathbb{R}^2) \text{ and} \\ U_4, U_5 &= S^*(B_\varepsilon \setminus \{0\}) \cong S(\mathbb{R}^2 \setminus \{0\}) \end{aligned}$$

are simply connected. Consequently, by the theorem of Seifert-van Kampen 5.1 also the union $\overline{\Sigma}_c$ is simply connected. This means that in the spatial restricted three-body problem every closed orbit is contractible in the regularised as well as in the unregularised energy level set.

Chapter 6

Generating orbits

Next, we will describe the notion of generating orbits in our case for the restricted three-body problem. We will mainly introduce notation but also describe some results from other authors and highlight their relevance for the current work.

Generating orbits are limits of orbits of the restricted three-body problem. In our setting we will use the limit as $\mu \to 0$ but in general also other limits, for example letting the angular momentum tend to zero, might be possible. This chapter establishes terminology and results around these generating orbits, most of which is taken from [Hén97] which we follow closely throughout. Another extensive work on generating orbits is [Bru94], where more theory is explained and mainly rotating coordinates are used. In [Hén97] fixed coordinates are used to describe the generating orbits which makes it easier for us to use the geometry of Kepler ellipses and compute the action of generating orbits. We are only interested in periodic orbits here and, hence, we will only consider periodic generating orbits.

6.1 General definitions

Definition 6.1:
Let γ_μ be a periodic orbit of the restricted three-body problem with mass ratio $\mu > 0$. Then γ is called a *generating orbit* if there exists a sequence of orbits γ_μ such that $\gamma_\mu \to \gamma$ as $\mu \to 0$. Similarly, a *generating solution* is the limit of periodic solutions as $\mu \to 0$ and can be described as a generating orbit with an origin of time specified.

Remark 6.2:
In general, generating orbits are not orbits of the restricted three-body problem for $\mu = 0$, i. e. the rotating Kepler problem, and vice-versa. Furthermore, when we use the notion of a generating orbit, we usually mean this in Henon's terms, who mostly worked with numerical methods. For an analytical proof of the fact that there exist continued orbits in the restricted three-body problem we rely on section 6.5.

Similarly to proposition 3.8, we have

Proposition 6.3 (Proposition 2.9.1 in [Hén97]):
Generating orbits form one-parameter families.

This allows us to define a *family of generating orbits*. Note that families of generating orbits do not follow the natural termination principle as in 3.6.1 and there can be intersections between families. In contrast, a *generating family* is the limit as $\mu \to 0$ of a family of periodic orbits for $\mu > 0$. Generating families follow the natural termination principle again. The limit consists only of generating orbits but it will only follow a certain branch at an intersection of families of generating orbits. Generating orbits at these intersections belong to multiple families and are called *bifurcation orbits*. The study of how one can recover the generating family from starting at a single generating orbit, i. e. which turns one has to take at the intersections, is a main subject of [Hén97]. Similarly as in section 3.6.1, we can also subdivide the generating family into *family segments of generating orbits* by maximal intervals on which the Jacobi constant $C = -2H_0 = -2(H_{\text{fix}} + L)$ is strictly monotonic.

Next, we will classify *species* of generating orbits. This notion goes back to Poincaré in [Poi99] who called his predicted periodic orbits with near collisions in the general three-body problem "solutions périodiques de deuxième espèce". We will adopt Hénon's more general definition of orbit species:

Definition 6.4:
A generating orbit is of the *first species* if it is a Keplerian orbit, it is of the *second species* if at least one point coincides with M_2 and it is of the *third species* if it only consists of M_2.

This definition does not give mutually exclusive species. In fact, third species generating orbits are always also of both the first and the second species. There are second species orbits that are also of the first species but there are also orbits that are exclusively of the first or second species. However, this definition is in terms of Hénon's *principle of positive definition* where "a definition relating to orbits in a family should not be based on a negative property, such as an inequality". This principle gives families of generating orbits the same species at the cost of exclusivity of species.

In the remaining sections in this chapter we will discuss each of the species, further subdivide them and name the families according to [Hén97].

6.2 First species

First species orbits are periodic orbits of the rotating Kepler problem. We define in accordance with the principle of positive definition:

Definition 6.5:
A generating orbit of the first species is called of the *first kind* if it is a circular orbit and of the *second kind* if in fixed coordinates M_2 and M_3 each make an integral number of revolutions I and J around M_1.

Again, this definition is not exclusive and orbits belonging to both kinds are bifurcation orbits.

6.2.1 First kind

A circular Kepler solution is fully defined by a radius a, a direction of rotation ϵ'—defined by $+1$ for direct and -1 for retrograde orbits in fixed coordinates as in (3.10)—and an initial polar position angle ϕ_0 of M_3 at time $t = 0$.

There is a special case if $a = 1$ and $\epsilon' = +1$: Here, the angular velocity of the Kepler orbit in fixed coordinates is the same as M_2 and thus in rotating coordinates the orbit is stationary at ϕ_0. In order to qualify as a generating orbit, we need a converging sequence of orbits from the restricted three-body problem with positive mass ratios. This is done in [Sze67] and it turns out to be the case if and only if $\phi_0 = \pi$—corresponding to the Lagrange point L_3—$\phi_0 = \pm\pi/3$—corresponding to L_4 and L_5—or $\phi_0 = 0$—corresponding to L_1 and L_2. In the latter case the orbit coincides with M_2 for all times and is hence also of the third species.

In all other cases the orbit describes a full circle even in rotating coordinates and we can set $\phi_0 = 0$ by time-shift. The angular velocity—or mean motion—in fixed coordinates is constant at

$$n = \frac{\epsilon'}{\sqrt{a^3}} \tag{6.1}$$

and we get a parametrisation of the orbit in rotating coordinates by

$$q_1(t) = |n|^{-\frac{2}{3}} \cos\left((n-1)t\right), \qquad q_2(t) = |n|^{-\frac{2}{3}} \sin\left((n-1)t\right). \tag{6.2}$$

With this free parameter n we get three families: for $1 < n < \infty$ the family of *direct interior circular orbits* I_{di}, for $0 < n < 1$ the family of *direct exterior circular orbits* I_{de} and for $-\infty < n < 0$ the family of *retrograde circular orbits* I_{r}. These families are not connected and they are all open because as $n \to 0$ and as $n \to \pm\infty$ the energy

$$H_0 = -\frac{C}{2} = -\frac{1}{2}|n|^{\frac{2}{3}} - \frac{1}{n^{\frac{1}{3}}} \tag{6.3}$$

becomes unbounded, and as $n \to 1$ the period

$$\tau = \tau_{\min} = \tau^* = \frac{2\pi}{|n-1|} \tag{6.4}$$

becomes unbounded. In the retrograde family I_{r}, there is a special bifurcation orbit at $n = -1$, i. e. for $a = 1$ and $\epsilon' = -1$, as it is also a second species orbit. This particular one will reappear in section 7.4.2 as the first intersection of first species orbits with second species orbits in family h. All orbits with rational n are also second kind orbits and therefore bifurcation orbits of a multiple cover of that circular orbit.

6.2.2 Second kind

A general Kepler solution is fully defined by a semi-major axis a, an eccentricity ϵ, an angular position argument of pericentre ϕ, a time of passage at pericentre t_0 and a direction of motion ϵ'.

We replace ϵ and ϵ' by the *coeccentricity* $e := \epsilon'\sqrt{1-\epsilon^2}$, which has a range from -1 to 1 and rectilinear orbits have $e = 0$. We can go back by $\epsilon = \sqrt{1-e^2}$ and $\epsilon' = \operatorname{sgn}(e)$ and the Jacobi energy becomes

$$-2H_0 = C = \frac{1}{a} + 2\sqrt{a}e$$

Let I be the number of revolutions of M_2 and J of M_3 around M_1. We can choose I and J relatively prime to avoid multiple covers. The minimal period is then

$$\tau_{\min} = 2\pi I,$$

the mean motion in fixed coordinates is

$$|n| = \frac{J}{I}$$

and we can express the semi-major axis by

$$a = \left(\frac{I}{J}\right)^{\frac{2}{3}}. \tag{6.5}$$

Since I and J must vary continuously along a family and are integer valued, they must be constant and hence also the semi-major axis, the mean motion and also the period-in-family $\tau^* = \tau_{\min}$. The time t_0 of pericentre passage can be eliminated by time-shift and we are left with e and ϕ as parameters. The condition of being a generating orbit gives one relation, leaving one parameter for the family.

We will only be interested in symmetric periodic orbits here—symmetric with respect to (3.19)—and will leave out the case of asymmetric orbits. Symmetric orbits in rotating coordinates intersect the q_1-axis perpendicularly at two points: each at an apocentre or pericentre. Set the time $t = 0$ at one of the intersection points. At that time the fixed and the rotating coordinates coincide and the Kepler ellipse is at an apsis, so, the argument of pericentre ϕ is either 0 or π. Accordingly, we define

$$\epsilon'' := \begin{cases} +1 & \text{if } \phi = 0 \\ -1 & \text{if } \phi = \pi. \end{cases}$$

Define also a parameter ψ by $\cos\psi = e$, $\sin\psi = \epsilon''\epsilon$. This defines e, ϵ, and ϵ'', so for fixed semi-major axis a we have a closed one-parameter family of Keplerian ellipses. Their Jacobi energy is

$$C = 2\sqrt{a}\cos\psi + \frac{1}{a}.$$

We can show that we have in fixed coordinates

$$\begin{aligned} Q_1 &= a\left(s_0\cos E - \sin\psi\right), \\ Q_2 &= a s_0 \cos\psi \sin E \qquad \text{and} \\ t &= \sqrt{a^3}\left(E - s_0\sin\psi\sin E\right), \end{aligned}$$

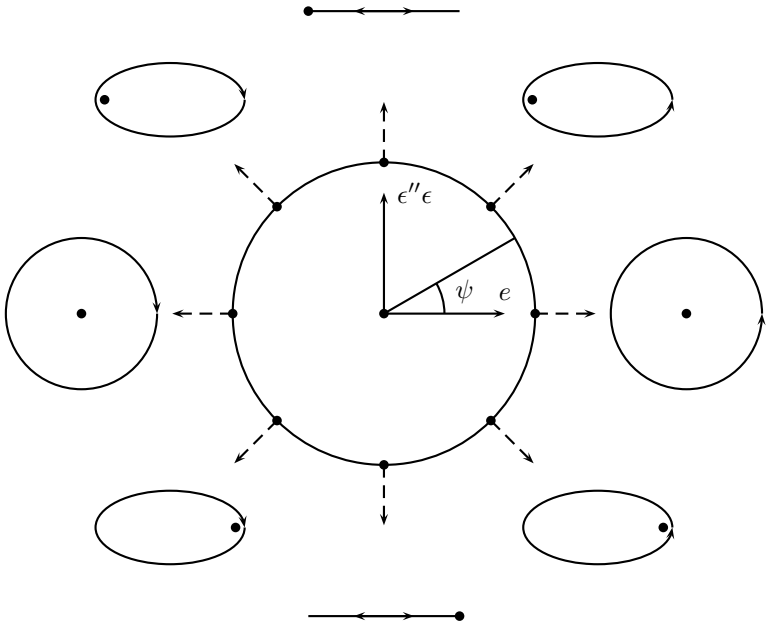

Figure 6.1: Closed family of first species second kind generating orbits with parameter ψ.

where $s_0 := \operatorname{sgn}(q_1(0))$ and E is the *eccentric anomaly*. The abscissa at $t = 0$ is at the point $x_0 := q_1(0) = Q_1(0) = a(s_0 - \sin\psi)$, while we get the other perpendicular intersection with the q_1-axis at $t = \tau_{\min}/2 = I\pi$, where $E = J\pi$, i. e. at

$$\begin{aligned} Q_1 &= a\left((-1)^J s_0 - \sin\psi\right), \text{ so} \\ x_1 := q_1 &= (-1)^{I+J} a\left(s_0 - (-1)^J \sin\psi\right). \end{aligned}$$

For $I + J$ odd x_0 and x_1 have opposite signs and so we can choose without loss of generality—by time-shift—that $x_1 < 0 < x_0$, i. e. $s_0 = 1$, and we have one closed family $E_{I,J}$.

For $I + J$ even both I and J need to be odd because they are mutually prime. So x_0 and x_1 have the same sign s_0 and there are two distinct families: $E^+_{I,J}$ for $s_0 = +1$ and $E^-_{I,J}$ for $s_0 = -1$. Both families are closed with reflections at $\psi = 0$ and $\psi = \pi$.

It is shown in [Are63] that almost all symmetric first species orbits of the second kind are in deed generating orbits in the sense of definition 6.1. Single orbits are excluded there because of technical reasons and because they collide with M_2 at some point. As mentioned in section 6.2.1, $E^+_{1,1}$ includes the third species orbit and $E^-_{1,1}$ includes the Lagrange point L_3.

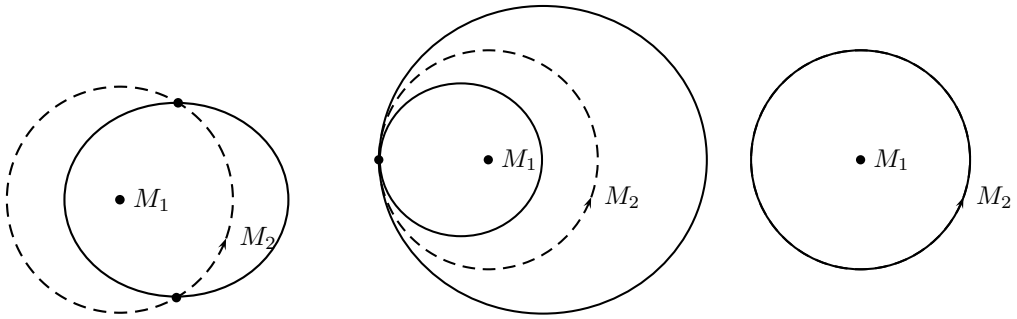

(a) Type 1: transverse intersection.

(b) Type 2: tangent to unit circle.

(c) Type 3 and 4: identical with unit circle in retrograde and direct direction.

Figure 6.2: Types of second species supporting ellipses.

6.3 Second species

According to definition 6.4 a second species orbit passes through M_2 at least once. We call this event a *collision*. A periodic second species generating orbit will collide infinitely many times, but there can also be multiple collisions during one minimal period. Abiding by the principle of positive definition, we declare a finite piece of a Keplerian orbit which begins and ends in collision an *arc*. Note that also an arc can include collisions, subdividing the arc into *basic arcs*. The angle at collision between basic arcs is called the *deflection angle* and a generating orbit of the second species is called *ordinary generating orbit* if all deflection angles are nonzero. Non-ordinary generating orbits are again bifurcation orbits.

The Kepler orbit belonging to the arc is called the *supporting Kepler orbit* or the *supporting Kepler ellipse*, if referring to the geometrical object. Each second species generating orbit consists of a sequence of arcs $U_1, U_2, \ldots U_k$, which is repeated periodically, and each arc is fully defined by its supporting Kepler solution and times t_j' and t_j'' of initial and final collision. The *duration* of an arc U_j is $\tau_j := t_j'' - t_j'$. We furthermore have:

Proposition 6.6 (proposition 4.1.2 in [Hén97]):
A generating orbit of the second species is fully defined by the duration and initial or final velocity of each arc.

Proposition 6.7 (proposition 4.1.1 in [Hén97]):
Arcs form one-parameter families.

The further study of second species orbits will from now on be confined to the study of arcs where we will continue to only state results and definitions which we will work with later.

Let r_1 be the pericentre distance and r_2 the apocentre distance of the supporting ellipse. For a collision to occur, we need $r_1 \leq 1 \leq r_2$. We will distinguish the following

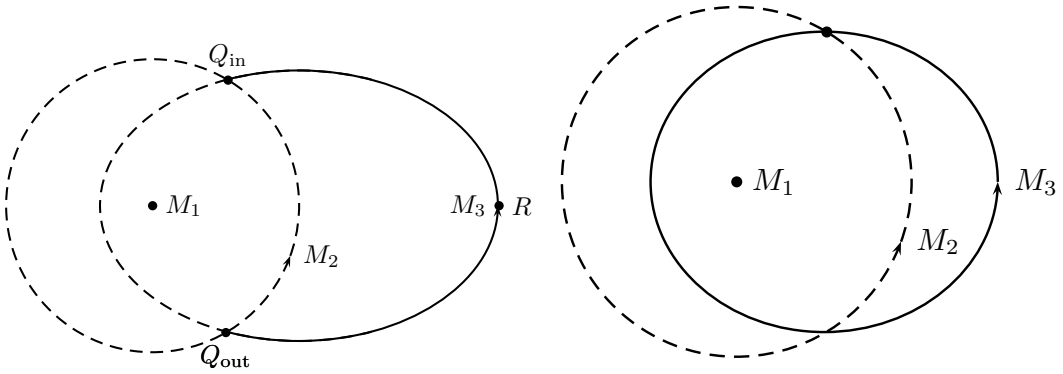

Figure 6.3: An outgoing S-arc and an ingoing T-arc.

cases: For $r_1 < 1 < r_2$ we have a non-circular supporting ellipse which intersects the unit circle in two distinct points transversally. The corresponding arcs will be called of *type 1*. For $r_1 = 1$ and $r_2 > 1$ or $r_1 < 1$ and $r_2 = 1$ the supporting Kepler ellipse is tangent to the unit circle and we will call the arcs of *type 2*. In the remaining case $r_1 = r_2 = 1$ the supporting Kepler ellipse is identical with the unit circle and we will call the corresponding arc of *type 3* if it is retrograde and of *type 4* if it is direct. Type 1 is the most interesting and comes in families while the other types are isolated.

6.3.1 Type 1

We will further subdivide type 1 arcs into *S-arcs* which in fixed coordinates begin and end at different points on the unit circle and *T-arcs* which begin and end at the same point. A type 1 arc will furthermore be called *ingoing* if at the initial collision its velocity vector points to the inside of the unit circle, and *outgoing* else. Both S-arcs and T-arcs can be ingoing and outgoing.

S-arcs

An S-arcs is symmetric with respect to the major axis of the supporting ellipse in fixed coordinates and intersects this axis $2J + 1$ times for $J \geq 0$. Let R be the central—i. e. the $J + 1^{\text{st}}$—intersection point. Then R lies either at the pericentre or apocentre and we call it the *midpoint*. Since both collision points lie at $(1, 0)$ in rotating coordinates, the midpoint R also lies on the q_1-axis and the arc is symmetric with respect to ρ from (3.19).

Second species arcs need to fulfil the timing condition, i. e. in fixed coordinates the elapsed time of M_3—on the arc from the first collision to the second—must be the same as the time of M_2 on the unit circle. Let the origin of time $t = 0$ be at the ingoing collision Q_{in} of the S-arc. Then M_2 passes through the outgoing intersection point Q_{out}

on the unit circle at times

$$t_2 = t_{20} + 2\pi\alpha,$$

where $\alpha \in \mathbb{Z}$ and t_{20} is the time of another passage of M_2 through Q_{out}. It is defined by

$$t_{20} := \begin{cases} \text{time of last passage of } M_2 \text{ through } Q_{\text{out}} \text{ before } t = 0 & \text{for direct orbits and} \\ \text{time of first passage of } M_2 \text{ through } Q_{\text{out}} \text{ after } t = 0 & \text{for retrograde orbits} \end{cases}$$

to assure continuity. In this convention we can convert from the number I of full revolutions of M_2 around M_1 in fixed coordinates:

$$\alpha = \begin{cases} -I & \text{for outgoing direct arcs} \\ I+1 & \text{for ingoing direct arcs} \\ -I-1 & \text{for outgoing retrograde arcs} \\ I & \text{for ingoing retrograde arcs} \end{cases} \tag{6.6}$$

Similarly, M_3 passes through Q_{out} at times

$$t_3 = t_{30} + 2\pi\sqrt{a^3}\beta,$$

where $\beta \in \mathbb{Z}$ and t_{40} is another passage. Again, to assure continuity, it is defined by

$$t_{30} := \begin{cases} \text{time of last passage of } M_2 \text{ through } Q_{\text{out}} \text{ before } t = 0 & \text{if } a < 1 \quad \text{and} \\ \text{time of first passage of } M_2 \text{ through } Q_{\text{out}} \text{ after } t = 0 & \text{if } a \geq 1, \end{cases}$$

where a is the semi-major axis of the supporting ellipse. We can convert again from the number J of full revolutions of M_3 around M_1 in fixed coordinates:

$$\beta = \begin{cases} -J & \text{for outgoing arcs with } a < 1 \\ J+1 & \text{for ingoing arcs with } a < 1 \\ -J-1 & \text{for outgoing arcs with } a \geq 1 \\ J & \text{for ingoing arcs with } a \geq 1 \end{cases} \tag{6.7}$$

The timing condition, i. e. the condition that M_3 collides with M_2 at Q_{out} for an arc with $t = 0$ at Q_{in}, is precisely $t_2 = t_3$, which is the case if and only if

$$\begin{aligned} & t_{20} + 2\pi\alpha = t_{30} + 2\pi\sqrt{a^3}\beta \\ \iff\ & t_{20} - t_{30} = 2\pi\left(\sqrt{a^3}\beta - \alpha\right) \\ \iff\ & Z = A\beta - \alpha. \end{aligned} \tag{6.8}$$

Here, $A = \sqrt{a^3}$ and $2\pi Z = t_{20} - t_{40}$ are the coordinates chosen by Hénon to plot the arc families. The analysis of arcs in these coordinates shows that there exists a family $S_{\alpha,\beta}$ of S-arcs for every

$$(\alpha = \beta = 0) \vee \left(\beta > 0, \alpha > 2^{-\frac{3}{2}}\beta\right) \vee \left(\beta < 0, \alpha < 2^{-\frac{3}{2}}\beta\right).$$

Moreover, almost all such α, β define a single family. Only for $\alpha = \beta < 0$ there is a separating discontinuity at $a = 1$.

T-arcs

T-arcs begin and end in the same point in fixed coordinates and are therefore full Kepler ellipses. Analogously to section 6.2.2, the semi-major axis of the supporting ellipse can be expressed by numbers I and J of rotation of M_2 and M_3 around M_1 by equation (6.5). Because we have

Proposition 6.8 (proposition 4.3.2 in [Hén97]):
An ordinary generating orbit of the second species can not contain two identical T-arcs of type 1 in succession.

the numbers I and J must again be relatively prime, i. e. no multiple covers are allowed. T-arcs are not symmetric and for every mutually prime I and J there exists a family $T^i_{I,J}$ of ingoing T-arcs and a family $T^e_{I,J}$ of outgoing T-arcs.

6.3.2 Other Types

Type 2 arcs, where the supporting ellipse is tangent to the unit circle, are similar to $T - arcs$. In general, the numbers of revolution need not be relatively prime and we can have a succession of m basic arcs, i. e. $I = mJ^*$ and $J = mJ^*$ for mutually prime I^* and J^*. If $a > 1$, the supporting ellipse is tangent at the pericentre and we have $a(1 - \epsilon) = 1$; if $a < 1$, the supporting ellipse is tangent at the apocentre and $a(1 + \epsilon) = 1$. Therefore, the eccentricity is always given by $\epsilon = |a - 1| / a$. A type 2 arc is hence fully defined by I^*, J^*, m and ϵ', and has period $\tau_{\min} = 2\pi m I^*$. Since all parameters are integers, there are only isolated type 2 arcs and they are all bifurcation orbits.

Type 3 arcs are a succession of m basic arcs, which each describe half a retrograde circle in fixed coordinates. They are isolated again and bifurcation orbits.

Type 4 arcs coincide with M_2 for all time and are therefore of the third species.

6.4 Third species

Third species orbits only consist of M_2. We can not study them by looking at Kepler orbits and we will therefore not consider them in this work. A model for third species orbits is Hill's lunar problem, which was introduced in section 3.5. Computing the action or even finding orbits in Hill's lunar problem is in its own right very hard to do analytically. For orbit families in Hill's lunar problem see for example the numerical work in [Hén69] and for the connection to generating orbits see [Hén97, chapter 5].

6.5 Continuation of second species generating orbits

In order to show analytically that the orbits described above are actually generating orbits we need to find converging sequences of orbits in the restricted three-body problem as $\mu \to 0$. Conversely, we then have for every generating orbit an arbitrarily close orbit in the restricted problem for some small enough mass ratio.

For first species orbits there are many works on the existence of such sequences, for example [Poi92], [Bir14] and [Hag70] for the first kind, [Are63] for symmetric, and [Bru94] for asymmetric second kind orbits. The remainder of his chapter is focused on second species generating orbits.

6.5.1 A more general result

The main theorem from [BM00] helps to show that many ordinary second species orbits are actually generating orbits. The setting is somewhat more general in that paper and we can also follow from the proof presented there that the action of the orbits in the restricted three-body problem converges to the action of the generating orbit. We will therefore first describe the notation which we adapt for our purposes and then explain in more detail the result and the relevance for the present work.

Let $\mathcal{Q}$ be a two- or three-dimensional smooth manifold and $\mathcal{P} = \{p_1, \dots p_n\} \subset \mathcal{Q}$ a finite subset. The set $\mathcal{Q} \setminus \mathcal{P}$ shall be the configuration space for the Lagrangian

$$\mathcal{L}_\mu(q, \dot{q}) = \mathcal{L}(q, \dot{q}) - \mu V(q)$$

or, in our setting, the Hamiltonian

$$H_\mu(q, p) = H_0(q, p) + \mu V(q),$$

where $H_0(q,p) = \frac{1}{2}\|p + A_q\|^2_{g_q^*} + W(q)$ is a magnetic Hamiltonian and V is another smooth potential with Newtonian singularities at every $p_i \in \mathcal{P}$. So, the Hamiltonian H_0 is defined on all of $T^*\mathcal{Q}$, while H_μ is defined on $T^*(\mathcal{Q} \setminus \mathcal{P})$. For the planar restricted three-body problem with small mass ratio μ we choose $\mathcal{Q} = \mathbb{R}^2 \setminus \{0\}$ and $\mathcal{P} = \{(1,0)\}$, i. e. we shift the coordinates such that the origin is always at the heavier primary M_1. The Hamiltonian then is of the form from above, with

$$\begin{aligned} A_q &= q_2 \,\mathrm{d}q_1 - q_1 \,\mathrm{d}q_2, \\ W(q) &= -\frac{1}{\|q\|} - \frac{\|q^2\|}{2} \qquad \text{and} \\ V(q) &= \frac{1}{\|q\|} - \frac{1}{\|q - (1,0)\|} - q_1. \end{aligned}$$

Fix an energy c such that the open Hill's region $\mathfrak{H}_c := \{q \in \mathcal{Q} \mid W(q) < c\}$ contains $\mathcal{P}$. Suppose we have a finite set K of nondegenerate collision orbits $\gamma_k \colon [0, \tau_k] \to \mathfrak{H}_c$ of the Hamiltonian system H_0 such that $\gamma_k(0) = p_{\alpha_k}$, $\gamma_k(\tau_k) = p_{\beta_k} \in \mathcal{P}$ and $\gamma(t) \in \mathfrak{H}_c \setminus \mathcal{P}$ for all other $t \in (0, \tau_k)$. A *chain* is a sequence $(\gamma_{k_i})_{i\in\mathbb{Z}}$ of orbits in K such that additionally $\gamma_{k_i}(\tau_{k_i}) = \gamma_{k_{i+1}}(0)$ and $\dot{\gamma}_{k_i}(\tau_{k_i}) \neq \dot{\gamma}_{k_{i+1}}(0)$, i. e. they are connected collision orbits with nonzero deflection angle. Let $\mathcal{W}_k$ be open neighbourhoods for each of the sets $\gamma_k([0, \tau_k])$ in $\mathcal{Q}$. An orbit $\gamma \colon \mathbb{R} \to \mathfrak{H}_c$ is said to *shadow* the chain $(\gamma_{k_i})_{i\in\mathbb{Z}}$ if there exists an increasing sequence $(t_i)_{i\in\mathbb{Z}}$ such that $\gamma([t_i, t_{i+1}]) \subset \mathcal{W}_{k_i}$.

The *nondegeneracy* of such orbits γ is defined as the Morse-nondegeneracy of the critical point $(u, \tau) \in W^{1,2}(p_\alpha, p_\beta) \times \mathbb{R}^+$ of the action functional $\mathcal{A}(\gamma)$, where $W^{1,2}(p_\alpha, p_\beta)$

is the space of all $W^{1,2}$-functions $u\colon [0,1] \to \mathcal{Q}$ with fixed endpoints $u(0) = p_\alpha$, $u(1) = p_\beta$ and $\gamma(t) = u(t/\tau)$. There are four other equivalent ways to define the nondegeneracy described in [BM00]. The only other one we will use here is the following: Denote by $q(\lambda, t)$ the general solution of Hamilton's second order differential equations of motion in the configuration space with parameter λ and by $h(\lambda)$ the Hamiltonian energy. Then the collision orbit is nondegenerate if the system

$$q(\lambda, 0) = p_\alpha, \quad q(\lambda, \tau) = p_\beta, \quad h(\lambda) = c \tag{6.9}$$

has full rank $2 \dim \mathcal{Q} + 1$.

Theorem 6.9 (theorem 1.1 from [BM00]):
There exists $\mu_0 > 0$ such that for all $\mu \in (0, \mu_0]$ and any chain $(\gamma_{k_i})_{i\in\mathbb{Z}}$ the following holds:

- *There exists a trajectory $\gamma\colon \mathbb{R} \to \mathfrak{H}_c$ of energy c for the system H_μ shadowing the chain $(\gamma_{k_i})_{i\in\mathbb{Z}}$ and it is unique up to a time-shift if the neighbourhoods $\mathcal{W}_k$ are chosen small enough.*

- *The orbit γ converges to the chain of collision orbits as $\mu \to 0$: There exists an increasing sequence $(t_i)_{i\in\mathbb{Z}}$ such that*

  $$\max_{t_i \le t \le t_{i+1}} \operatorname{dist}(\gamma(t), \gamma_{k_i}([0, \tau_{k_i}])) \le \mu C_1,$$

  where the constant $C_1 > 0$ depends only on the set K of collision orbits.

- *If we additionally have $\dot\gamma_{k_i}(\tau_{k_i}) \neq -\dot\gamma_{k_{i+1}}(0)$, the orbit γ avoids collision by a distance of order μ: there exists a constant $C_2 \in (0, C_1)$, depending only on K, such that*

  $$\mu C_2 \le \min_{t_{i-1} \le t \le t_{i+1}} \operatorname{dist}(\gamma(t), p_{\alpha_{k_i}}).$$

Below, we will sketch the proof of theorem 6.9 as shown in the paper, describe the important steps and then apply it to our situation in the next section.

The key points are a careful analysis of the Levi-Civita regularisation in a small neighbourhood of the lighter primary M_2 as μ tends to zero and using the nondegeneracy condition of the chain orbits as a critical point of the action functional. We computed in section (4.2) that the Levi-Civita-regularised Hamiltonian system (4.15) in rotating coordinates centred at M_2 has a hyperbolic fixed point at the origin for $\mu = 0$. Furthermore, it takes trajectories of energy μ to trajectories of the system with Hamiltonian H_μ on the energy level $H_\mu = c$. This has also been done in [MN95] and [Che89] for the hyperbolic case with positive energy and in [Con63] for the elliptical case with negative energy h. The key aspects here are that while the transformation does not preserve the time, it does preserve the action.

From here on, the stable and unstable manifolds of this hyperbolic fixed point are analysed and new coordinates for the flow on the stable and unstable manifolds yield

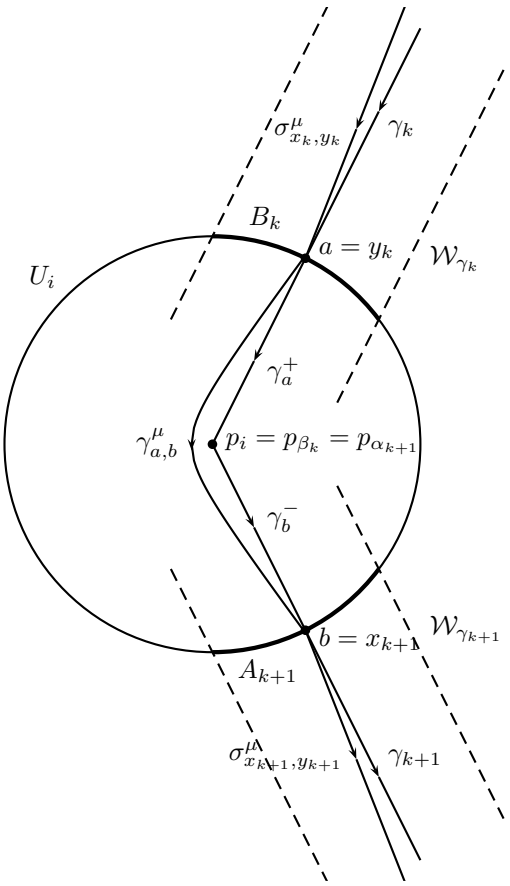

Figure 6.4: Notation in the neighbourhood of collision.

the trajectories in regularised coordinates, their action and energy and uniform bounds. Using the monotonicity of time in these small neighbourhoods, the connecting trajectories for small mass ratios in regularised coordinates with their formulae for elapsed time, action and uniform bounds is achieved. The squaring map and reparametrisation is applied to find the trajectories with the required properties.

Let a and b be points in a small neighbourhood U_i of p_i and $\gamma_a^+ \colon [0, \tau^+(a)] \to U_i$ and $\gamma_b^- \colon [\tau^-(b), 0] \to U_i$ the respective unique trajectories of the system H_0 connecting a to p_i and p_i to b, while $S^+(a)$ and $S^-(b)$ are their actions. The set

$$X_i := \left\{(a,b) \in (\partial U_i)^2 : \|u^+(a) - u^-(b)\| \geq \delta\right\}$$

is the set where the tangent vectors $u^+(a) := \dot{\gamma}_a^+(\tau^+(a))$ and $u^-(b) := \dot{\gamma}_b^-(\tau^-(b))$ at p_i differ by at least af fixed $\delta > 0$. On the other hand, let

$$Y_i := \left\{(a,b) \in X_i : \|u^+(a) + u^-(b)\| \geq \delta\right\}$$

be the set where the velocity vectors are additionally not too close to being opposite. Then the auxiliary lemma is

Lemma 6.10 (lemma 4.1 in [BM00]):
There exists $\mu_0 > 0$ such that the following statements hold:

- *For $\mu \in (0, \mu_0]$ and $(a, b) \in X_i$ there exists a unique trajectory $\gamma = \gamma^\mu_{a,b} \colon [0, \tau] \to U_i$ of energy c for the system H_μ connecting a to b, i. e. $\gamma^\mu_{a,b}(0) = a$ and $\gamma^\mu_{a,b}(\tau) = b$.*
- *$\tau = \tau(a, b, \mu)$ is a C^2 function on $X_i \times (0, \mu_0]$ and $\tau(a, b, \mu) \to \tau^+(a) + \tau^-(b)$ uniformly as $\mu \to 0$.*
- *$\gamma^\mu_{a,b}|_{[0,\tau^+(a)]} \to \gamma^+_a$ and $\gamma^\mu_{a,b}(\,\cdot\, + \tau)|_{[\tau^-(b),0]} \to \gamma^-_b$ uniformly as $\mu \to 0$. More precisely, there exists a constant $C_1 > 0$ depending only on δ such that*

$$\max_{0 \le t \le \tau^+(a)} \operatorname{dist}(\gamma^\mu_{a,b}(t), \gamma^+_a(t)) \le C_1 \mu$$
$$\max_{\tau + \tau^-(b) \le t \le \tau} \operatorname{dist}(\gamma^\mu_{a,b}(t), \gamma^+_b(t - \tau)) \le C_1 \mu$$

- *The action of the trajectory γ is a C^2 function on $X_i \times (0, \mu_0]$ and*

$$\mathcal{A}(\gamma) = S(a, b, \mu) = S^+(a) + S^-(b) + \mu s(a, b, \mu)$$

  where s is uniformly C^2 bounded on X_i as $\mu \to 0$.
- *If additionally $(a, b) \in Y_i$, then the trajectory $\gamma^\mu_{a,b}$ does not pass too close to p_i:*

$$\min_{0 \le t \le \tau} \operatorname{dist}\left(\gamma^\mu_{a,b}(t), p_i\right) \ge C_2 \mu \quad \text{for some } C_2 > 0.$$

With the help of this lemma one can glue together trajectories at collision under the given conditions of nonidentical tangent vectors and nondegeneracy of trajectories as critical points:

Lemma 6.11 (lemma 5.1 in [BM00]):
The function $g_k(u, v) = f_0(u, v) + S^-_{\alpha_k}(u) + S^-_{\beta_k}(v)$ on $A_k \times B_k$ has a nondegenerate critical point at $z_k = (x_k, y_k)$.

Here x_k and y_k are the intersections of ∂U_{α_k} and ∂U_{β_k} with the trajectory γ_k in the chain, connecting p_{α_k} with p_{β_k}. The sets A_k and B_k are the intersections of $\mathcal{W}_k$ with ∂U_{α_k} and ∂U_{β_k} and $f_\mu(u, v)$ is the action of the unique trajectory $\sigma = \sigma^\mu_{u,v}$ of energy c in the system H_μ connecting $u \in A_k$ to $v \in B_k$.

Critical points of this formal action functional are now piecewise smooth trajectories as the concatenation of arcs $\sigma_{u,v}$ with connecting trajectories $\gamma_{a,b}$. Furthermore, by differentiating the action in the general case $\mu \ge 0$ one gets that a vanishing derivative implies that there are no jumps in the tangential momentum component and the trajectory is smooth everywhere. Uniformly bounded action, the second derivative matrix of g being uniformly invertible and the implicit function theorem give the result from theorem 6.9. Using lemma 6.11, we can also add to the theorem that the action of the shadowing orbit stays close to the action of the chain. This concludes the more general discussion on continuing generating orbits with collisions.

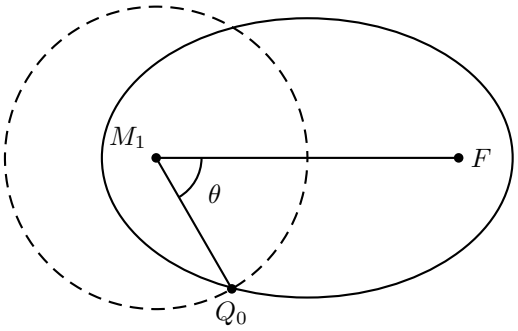

Figure 6.5: Parametrisation of second species ellipses.

6.5.2 Application to the restricted three-body problem

We now want to apply this theorem 6.9 to the restricted three-body problem and find orbits for positive mass ratios $\mu > 0$ shadowing chains of collision orbits, i. e. second species generating orbits. In the same paper [BM00] a partial result is already shown:

Lemma 6.12 (lemma 3.2 in [BM00]):
For $c \in (-3/2, \sqrt{2})$ the collision orbit at $\mu = 0$ in the rotating frame corresponding to a whole number I of revolutions of an ellipse with rational frequency $I/J \in A_c$ in the allowed set of frequencies A_c for energy c starting and ending at a collision with M_2 is nondegenerate.

In the language of generating orbits this means that every ordinary generating orbit composed of T-arcs is indeed a generating orbit. We would like to use generating orbits composed of S-arcs and we will therefore have to prove accordingly:

Lemma 6.13:
For $c \in (-3/2, \sqrt{2})$ a non-rectilinear ordinary S-arc collision orbit starting and ending in M_2 with semi-major axis $a > 1$ of the supporting ellipse is nondegenerate.

Proof: This proof is very similar to the proof of lemma 6.12 in [BM00] but a lot harder to actually compute the estimates. Enforcing the first equation of (6.9), we have $\dim \mathcal{Q} = 2$ free parameters left for λ. We parametrize the supporting ellipse through our initial point of collision Q_0 by the position of the second focus $F \in \mathbb{R}^2$ using two variables: the polar angle θ between Q_0 and F and the semi-major axis

$$\begin{aligned} a &= \frac{1}{2}(1 + \operatorname{dist}(Q_0, F)) \\ &= \frac{1}{2}(1 + \sqrt{1 + \operatorname{dist}(M_1, F)^2 - 2\cos(\theta)\operatorname{dist}(M_1, F)}). \end{aligned}$$

This is a good parameter if $\operatorname{dist}(M_1, F) \neq \cos\theta$ or, equivalently, if $\operatorname{dist}(Q_0, F) \neq \sin\theta$, so we restrict to $\operatorname{dist}(Q_0, F) > 1$, i. e. if and only if $a > 1$. We will see later on that this

does effectively not restrict S-arcs in the direct sense of rotation $\epsilon' = +1$, which are the only ones we need in the main proof.

The second condition of (6.9) is satisfied nondegenerately since the supporting ellipse intersects the unit circle transversely and both M_2 and M_3 have nonzero velocities. Fixing the endpoint also fixes the angle θ, so the remaining free parameter is a.

We are left to show that the derivative of the energy by a is nonzero. Dependent on a and θ we compute the eccentricity and the energy, as will be also done in section 7.4.2 later on:

$$\epsilon = \frac{\cos\theta + \sqrt{4a^2 - 4a + \cos^2\theta}}{2a}$$
$$H_0 = -\frac{1}{2a} - \epsilon' \sqrt{1 - \cos\theta \frac{\cos\theta + \sqrt{4a^2 - 4a + \cos^2\theta}}{2a}}$$

We exclude the case of rectilinear orbits with $\theta = 0$ due to the root being zero and the sign of ϵ' changing here. For numbers of revolution $J > 0$ there would also occur a collision with M_3 and M_1 in that case which one would have to deal with additionally.

For all other orbits with $\theta \in (0, \pi)$ and $a > 1$ we differentiate H_0 by a to get

$$\frac{\partial H_0}{\partial a} = \frac{1}{2a^2} + \epsilon' \frac{\cos\theta \frac{\frac{4a^2-2a}{\sqrt{4a^2-4a+\cos^2\theta}} - \cos\theta - \sqrt{4a^2-4a+\cos^2\theta}}{2a^2}}{2\sqrt{1 - \cos\theta \frac{\cos\theta + \sqrt{4a^2-4a+\cos^2\theta}}{2a}}}.$$

This vanishes if and only if

$$\begin{aligned} 2\sqrt{1 - \cos\theta \frac{\cos\theta + \sqrt{4a^2 - 4a + \cos^2\theta}}{2a}} = \\ = -\epsilon' \cos\theta \left(\frac{4a^2 - 2a}{\sqrt{4a^2 - 4a + \cos^2\theta}} - \cos\theta - \sqrt{4a^2 - 4a + \cos^2\theta} \right) \\ = \frac{-2\epsilon' a \cos\theta}{\sqrt{4a^2 - 4a + \cos^2\theta}} \underbrace{\left(1 - \cos\theta \frac{\cos\theta + \sqrt{4a^2 - 4a + \cos^2\theta}}{2a} \right)}_{=a(1-\epsilon^2)>0}. \end{aligned}$$

Based on this equation, we can distinguish four cases: Case 1 is $\epsilon' = +1$ and $\cos\theta \geq 0$, case 2 is $\epsilon' = +1$ and $\cos\theta < 0$, case 3 is $\epsilon' = -1$ and $\cos\theta > 0$, and case 4 is $\epsilon' = -1$ and $\cos\theta \leq 0$.

In cases 1 and 4 the right-hand side becomes nonpositive and the nondegeneracy is obvious since the left-hand side is always positive for $\epsilon \neq 1$. For the remaining cases we will have to work a little bit harder. In the following computations we will denote the left-hand side by $u = u(a, \theta)$ and the right-hand side by $v = v(a, \theta)$.

In case 2 the sign of $\cos\theta$ is negative, so we can estimate the left-hand side by $u > 2$. To show that the right-hand side v is smaller, we insert the boundary value $a = 1$ to get

$$v(1, \theta) = \frac{-2\cos\theta}{|\cos\theta|} \left(1 - \cos\theta \left(\cos\theta + |\cos\theta|\right)\right) = 2$$

and then see that the derivate $\partial v/\partial a$ is negative by

$$\frac{\partial v}{\partial a} =$$
$$-\cos\theta\left(\frac{(8a-2)\sqrt{4a^2-4a+\cos^2\theta}-(4a^2-2a)\frac{8a-4}{2\sqrt{4a^2-4a+\cos^2\theta}}}{4a^2-4a+\cos^2\theta}-\frac{8a-4}{2\sqrt{4a^2-4a+\cos^2\theta}}\right)$$
$$=-\cos\theta\frac{4a\cos^2\theta-4a}{(4a^2-4a+\cos^2\theta)^{\frac{3}{2}}}<0.$$

In the last remaining case 3 we have $\cos\theta>0$ and $\epsilon'=-1$, so we can estimate the root in the left-hand side from below to get

$$u(a,\theta)>2\left(1-\cos\theta\frac{\cos\theta+\sqrt{4a^2-4a+\cos^2\theta}}{2a}\right).$$

Therefore, $u>v$ reduces to

$$\begin{aligned} 2&>\frac{2a\cos\theta}{\sqrt{4a^2-4a+\cos^2\theta}} &&\iff\\ 4a^2-4a+\cos^2\theta&>a^2\cos^2\theta &&\iff\\ (a-1)(a(4-\cos^2\theta)-\cos^2\theta)&>0 \end{aligned}$$

which is obviously true due to $a>1$. □

Briefly summarizing this section with focus on the information relevant for the main proof in chapter 8, we can state the following:

Corollary 6.14:
Let γ be an ordinary second species generating orbit with action $\mathcal{A}(\gamma)$ composed of S-arcs and T-arcs with energy $c\in(-3/2,\sqrt{2})$ where all supporting ellipses are non-rectilinear and S-arcs have semi-major axes $a>1$. Then there exists an $\varepsilon>0$ and $\mu_0>0$ such that for all $\mu\in(0,\mu_0]$ there exists a unique periodic orbit γ_μ with energy c in the restricted three-body problem with mass ratio μ shadowing γ with action $|\mathcal{A}(\gamma_\mu)-\mathcal{A}(\gamma)|<\varepsilon$.

Backed by this result, we will in the next chapter compute the action of generating orbits in order to construct orbits with negative action in the restricted three-body problem with positive mass ratio $\mu\in(0,1)$.

Chapter 7

Action of generating orbits

In this chapter we compute the action of first and second species generating orbits for the restricted three-body problem. The first two sections will focus on general formulae for the action of the two species, while the third section will provide a helpful method to compute the elapsed time of second species arcs. Finally, in the last section we construct sequences of second species generating orbits that have special properties with respect to their action and energy. First of all however, we will recall the formula for the action from definition 2.34 and convert to fixed coordinates (Q, P) in order to subsequently use the geometry of Kepler orbits.

Let $\gamma\colon S^1 \to \Sigma_c$ be a nonconstant periodic orbit of the planar restricted three-body problem with period $\tau > 0$ and energy $H_\mu = c$. In rotating coordinates (3.13) we have the action

$$\begin{aligned}\mathcal{A}(\gamma) :&= \int_{S^1} \gamma^*\lambda \\ &= \int_0^\tau p_1(t)\frac{\mathrm{d}q_1(t)}{\mathrm{d}t} + p_2(t)\frac{\mathrm{d}q_2(t)}{\mathrm{d}t}\,\mathrm{d}t \\ &= \int_0^\tau p_1(t)\,(p_1(t) + q_2(t)) + p_2(t)\,(p_2(t) - q_1(t))\,\mathrm{d}t \\ &= \int_0^\tau \|p(t)\|^2 + L(t)\,\mathrm{d}t,\end{aligned} \tag{7.1}$$

where $L(t)$ is the angular momentum $p_1(t)q_2(t) - p_2(t)q_1(t)$. Using fixed coordinates (Q, P) allows us to use all our knowledge about Kepler orbits for our generating orbits. Since both $\|p\|^2$ and $L(t)$ are invariant under the rotation that defines the transformation between fixed and rotating coordinates, the action can simply be written as

$$\mathcal{A}(\gamma) = \int_0^\tau \|P(t)\|^2 + L(t)\,\mathrm{d}t.$$

Solving the Kepler Hamiltonian (3.6) for $\|P\|^2$ and inserting, we are left with

$$\mathcal{A}(\gamma) = \int_0^\tau 2H_{\mathrm{fix}}(t) + L(t) + \frac{2}{\|Q(t)\|}\,\mathrm{d}t. \tag{7.2}$$

While for general orbits of the restricted three-body problem the Kepler energy H_{fix}, angular momentum L and distance to the origin $\|Q\|$ all depend on time, at least H_{fix} and L are integrals of motion for the limit case $\mu = 0$. Since generating orbits are merely rotating Kepler ellipses or sequences of Keplerian arcs, we can now quite easily compute their action. To further get rid of the term $2/\|Q\|$, we apply the change of variables (4.9) to the regularised time of the Levi-Civita transformation. Ultimately, we get that the action of a generating orbit γ which consists of only one Keplerian arc can be computed by

$$\begin{aligned} \mathcal{A}(\gamma) &= \tau(2H_{\text{fix}} + L) + \int_0^\sigma \frac{2}{\|X\|^2} 4X^2 \,\mathrm{d}s \\ &= \tau(2H_{\text{fix}} + L) + 8\sigma, \end{aligned} \tag{7.3}$$

where $\sigma = s(\tau)$ is the duration of the arc in Levi-Civita-regularised time. For generating orbits composed of multiple arcs both H_{fix} and L can change between arcs while the relevant energy $H_0 = H_{\text{fix}} + L$ must remain the same. The total action can simply be computed by adding up the actions of all arcs.

7.1 First species

We first compute the action for generating orbits of the fist species, i. e. when the orbit is just a full rotating Kepler orbit. One has to keep in mind, however, that the notion of periodicity remains that from the rotating setting.

7.1.1 First kind

For the fist kind—circular orbits—the computation is quite easy. One only has to compute the period, which in general differs from the Kepler period.

For circular orbits, additionally to the conserved quantities H_{fix} and L, also the radius $\|Q\|$ is conserved. This means that the integrand of (7.2) itself is a conserved quantity and integration is merely a multiplication with the period:

$$\mathcal{A}(\gamma) = \tau \left(2H_{\text{fix}} + L + \frac{2}{\|Q\|} \right) \tag{7.4}$$

Using the computation $n := 2\pi\epsilon'/T = \epsilon'/\sqrt{a^3}$ from (6.1) in fixed coordinates, the mean motion is decreased by the rotation of the coordinate axes to give an angular velocity of $n - 1 = \epsilon'/\sqrt{a^3} - 1$. The period of circular orbits in the rotating frame is hence

$$\tau = \left| \frac{2\pi}{\frac{\epsilon'}{\sqrt{a^3}} - 1} \right| = \frac{2\pi}{\left| \frac{1}{\sqrt{a^3}} - \epsilon' \right|}. \tag{7.5}$$

Using equations (3.8) and (3.9) for the Kepler energy and angular momentum from the data of the ellipse, we get the action of circular orbits in rotating coordinates as a

function of the semi-major axis a and direction of rotation ϵ':

$$\begin{aligned}\mathcal{A}(\gamma) &= \frac{2\pi}{\left|\frac{1}{\sqrt{a^3}} - \epsilon'\right|}\left(2\left(-\frac{1}{2a}\right) - \epsilon'\sqrt{a} + \frac{2}{a}\right) \\ &= \frac{2\pi}{\left|\frac{1}{\sqrt{a^3}} - \epsilon'\right|}\left(\frac{1}{a} - \epsilon'\sqrt{a}\right)\end{aligned} \tag{7.6}$$

The exceptional case, where the period (7.5) is undefined, is when $n = 1$, i. e. $a = 1$ and $\epsilon' = +1$. In this case solutions are stationary in rotating coordinates and lie on the unit circle with the free parameter ϕ_0.

In general, the action of first kind generating orbits is positive if $\epsilon' = -1$, i. e. for all retrograde circular orbits I_r. Direct orbits exist for energies $H_0 = -1/(2a) - \epsilon'\sqrt{a} < -3/2$ and have negative action for radii $a > 1$—direct exterior circular orbits I_{de}—and positive action for $a < 1$—direct interior circular orbits I_{di}—with the action converging towards -2π and $+2\pi$ at the singularity, respectively. These orbits of negative action are not that interesting for us, because they only exist in the unbounded component of the Hill's region for energies below the first critical energy.

7.1.2 Second kind

First species orbits of the second kind are defined by mutually prime numbers of revolution I of M_2 and J of M_3 around M_1 in fixed coordinates. By Kepler's third law (3.7) the period is

$$\tau = 2\pi I = JT = 2\pi\sqrt{a^3}J,$$

and, hence, the semi-major axis a can be expressed as

$$a = \sqrt[3]{\frac{I^2}{J^2}}.$$

By the frequency (4.10) of the regularised ellipse, we know that the period of a full Kepler orbit in Levi-Civita regularised time is $S := s(T) = \pi/\varpi = \pi/\sqrt{-8H_{\text{fix}}}$. The action from (7.3) then becomes

$$\begin{aligned}\mathcal{A} &= JT(2H_{\text{fix}} + L) + 8JS \\ &= 2\pi\sqrt{a^3}J\left(2\left(-\frac{1}{2a}\right) - \epsilon'\sqrt{a(1-\epsilon^2)}\right) + \frac{8\pi J}{\sqrt{-8\left(-\frac{1}{2a}\right)}} \\ &= 2\pi J\left(\sqrt{a} - \epsilon' a^2\sqrt{1-\epsilon^2}\right) \\ &= 2\pi\left(\sqrt[3]{IJ^2} - \epsilon'\sqrt[3]{\frac{I^4}{J}}\sqrt{1-\epsilon^2}\right)\end{aligned} \tag{7.7}$$

and we see that while there are many combinations of I, J and ϵ that produce negative action, line (7.7) shows that the semi-major axis a must be greater than 1 on order for the action to become negative. So, in the bounded component $\mathfrak{H}_c^b$ of the Hill's region no generating orbit of the first species can produce negative action.

7.2 Second species

A periodic second species generating orbit is a periodic sequence of basic Keplerian arcs joined at collision with M_2. So in order to compute its action we need to compute the action of theses arcs and add them up. Keplerian arcs are divided into four types as in section 6.3: Type 1 intersects the unit circle in two distinct points, type 2 is tangent to the unit circle at one point and types 3 and 4 are identical to the unit circle in retrograde and direct direction, respectively. Type 1 is subdivided into S-arcs and T-arcs, where in S-arcs the collisions occur in two distinct points on the unit circle, while T-arcs begin and end in collision on the same point on the unit circle in fixed coordinates. T-arcs can be computed as in the last section, since both M_2 and M_3 revolve an integer number of times during one arc. The same holds for arcs of type 2.

For S-arcs we shift time and rotate, such that at $t = 0$ the orbit is at it's apocentre or pericentre and on the positive abscissa. We are going to compute the first intersection time of the regularised orbit with the unit circle in order to find the regularised period of the generating orbit. Setting the apocentre on the positive abscissa here corresponds to outgoing S-arcs, while the pericentre yields ingoing S-arcs. Remember that type 1 arcs require the pericentre to be closer than 1 and the apocentre to be farther away than 1 in order to get two distinct intersection points of the Kepler ellipse with the unit circle. The parametrisation of the regularised orbit can then be given from (4.11), (4.12) and (4.13) by

$$X_1(s) = \alpha \cos(\varpi s) \quad \text{and} \quad X_2(s) = \beta \sin(\varpi s),$$

where $\alpha = \sqrt{Q_1(0)}$ and $\beta = 2\dot{Q}_2(0)\sqrt{Q_1(0)}/\varpi$. The regularised orbit first intersects the unit circle at time $\sigma_0/2 > 0$ when

$$1 = X_1\left(\frac{\sigma_0}{2}\right)^2 + X_2\left(\frac{\sigma_0}{2}\right)^2.$$

Note that σ_0 is not necessarily the actual regularised period σ, since an S-arc can first wind around M_1 at the origin J times before colliding with M_2 again. The actual regularised period will then be $\sigma = JS + \sigma_0$. Obviously, the Levi-Civita transformation (4.6) preservers the unit circle, so an intersection with the unit circle in regularised coordinates corresponds to an intersection in usual coordinates. Inserting the parametrisation in regularised coordinates, one gets

$$\begin{aligned}
1 &= \alpha^2 \cos^2\left(\varpi\frac{\sigma_0}{2}\right) + \beta^2 \sin^2\left(\varpi\frac{\sigma_0}{2}\right) \\
&= \alpha^2 \cos^2\left(\varpi\frac{\sigma_0}{2}\right) + \beta^2 \sin^2\left(\varpi\frac{\sigma_0}{2}\right) + \beta^2 \cos^2\left(\varpi\frac{\sigma_0}{2}\right) - \beta^2 \cos^2\left(\varpi\frac{\sigma_0}{2}\right) \\
&= \beta^2 + \cos^2\left(\varpi\frac{\sigma_0}{2}\right)(\alpha^2 - \beta^2) \\
\iff \quad \cos^2\left(\varpi\frac{\sigma_0}{2}\right) &= \frac{1-\beta^2}{\alpha^2-\beta^2} \\
\iff \quad \sigma_0 &= \frac{2}{\varpi}\arccos\left(\sqrt{\frac{1-\beta^2}{\alpha^2-\beta^2}}\right).
\end{aligned}$$

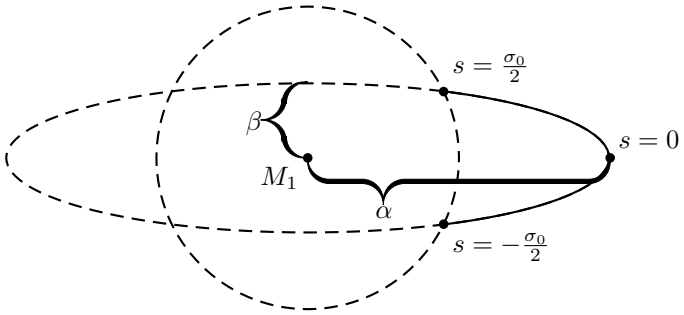

Figure 7.1: First intersection time of Levi-Civita-regularised Kepler ellipses with the unit circle.

Equivalences hold because $\varpi\sigma_0/2 \in (0, pi)$ and $\beta^2 = \alpha^2 \iff \alpha = 1 \wedge \beta = \pm 1$. Both these latter cases do not admit an S-arc, but are rather of types 3 and 4, respectively. Using the formulae (4.10) for the angular frequency, (4.12) for α, and (4.13) for β in terms of the Kepler ellipse data, we get

$$\begin{aligned}
\sigma_0 &= \frac{2}{\sqrt{-8H_{\text{fix}}}} \arccos\left(\sqrt{\frac{1-\beta^2}{\alpha^2-\beta^2}}\right) \\
&= \frac{2}{\sqrt{-8\left(-\frac{1}{2a}\right)}} \arccos\left(\sqrt{\frac{1-a(1-\epsilon)}{a(1+\epsilon)-a(1-\epsilon)}}\right) \\
&= \sqrt{a} \arccos\left(\sqrt{\frac{1-a(1-\epsilon)}{2a\epsilon}}\right). \qquad (7.8)
\end{aligned}$$

Inserting this into the formula (7.3) for the action, we get

$$\begin{aligned}
\mathcal{A} &= (JT+\tau_0)(2H+L) + 8(JS+\sigma_0) \\
&= (2\pi\sqrt{a}J+\tau_0)\left(2\left(-\frac{1}{2a}\right) - \epsilon'\sqrt{a(1-\epsilon^2)}\right) + 8\left(J\frac{\pi}{\varpi} + \sqrt{a}\arccos\left(\sqrt{\frac{1-a(1-\epsilon)}{2a\epsilon}}\right)\right) \\
&= (2\pi\sqrt{a}J+\tau_0)\left(-\frac{1}{a} - \epsilon'\sqrt{a(1-\epsilon^2)}\right) + 8\sqrt{a}\left(\frac{\pi J}{2} + \arccos\left(\sqrt{\frac{1-a(1-\epsilon)}{2a\epsilon}}\right)\right), \qquad (7.9)
\end{aligned}$$

where $\tau_0 = t(\sigma_0)$ is two times the first intersection time with the unit circle in normal time. This quantity has to be computed separately, which is done in the subsequent section.

The action of type 2 arcs is identical to the previous case of first species generating orbits of the second kind, since they are complete integer revolutions of Keplerian ellipses. Type 3 is half a circular retrograde Kepler orbit with radius $a = 1$ and identical with

the circular retrograde generating orbit of family I_r with radius 1 and action $\mathcal{A} = 2\pi$. Type 4 on the other hand is in rotating coordinates the constant solution identical with M_2 at all times and therefore a third species generating orbit, which can not be computed using the Kepler problem.

7.3 Lambert's Theorem

A great tool that especially enables us to compute the elapsed time of Keplerian arcs of the second species is Lambert's theorem from [Lam61]. Its history, modern proofs and many remarks about it can be found in [Alb19] and [AU20]. We will state the main theorems and definitions needed for this work, while adapting the notation slightly. Objects of study for Lambert's theorem are Keplerian arcs beginning in point A at time t_A and ending in point B at time t_B in fixed coordinates.

Theorem 7.1 (Lambert, Theorem 1 in [Alb19]):
Consider Keplerian arcs around the origin O of $\mathbb{R}^d$. If we change continuously such an arc while keeping constant the distance $\|B - A\|$ between both ends, the sum of the radii $\|A\| + \|B\|$ and the energy H_{fix}, then the elapsed time $\tau_0 = t_B - t_A$ is also constant.

Theorem 7.2 (Lambert, Theorem 2 in [Alb19]):
Starting from any given Keplerian arc, we can arrive at some rectilinear arc by a continuous change which keeps constant the three quantities $\|B - A\|$, $\|A\| + \|B\|$ and H_{fix}.

Definition 7.3 (see Definition 5 in [Alb19]):
A Keplerian arc around O is called *simple* if its elapsed time is less than or equal to the period of its supporting ellipse. It is said to be *indirect*, or I_O, if its convex hull contains O; *direct*, or D_O, if its convex hull does not contain O; *indirect with respect to the second focus F*, or I_F, if its convex hull contains F; *direct with respect to F*, or D_F, if its convex hull does not contain F.

In order to avoid confusion between terminologies we will only use the notation of I_O, D_O, I_F and D_F. The important feature of these types is that they are preserved during the *Lambert cycle*, which is the continuous change of Keplerian arcs as in theorem 7.1:

Proposition 7.4 (Proposition 5 in [Alb19]):
If a Keplerian arc in a Lambert cycle is I_O or D_O and I_F or D_F, then all the Keplerian arcs of the cycle are I_O or D_O and I_F or D_F, respectively.

In our case of second species generating orbits we have as parameters the semi-major axis a, the eccentricity ϵ and the polar angle θ of the intersection with the unit circle. They are interrelated by the equation for the polar distance

$$r(\theta) = \frac{a(1 - \epsilon^2)}{1 - \epsilon \cos \theta} \tag{7.10}$$

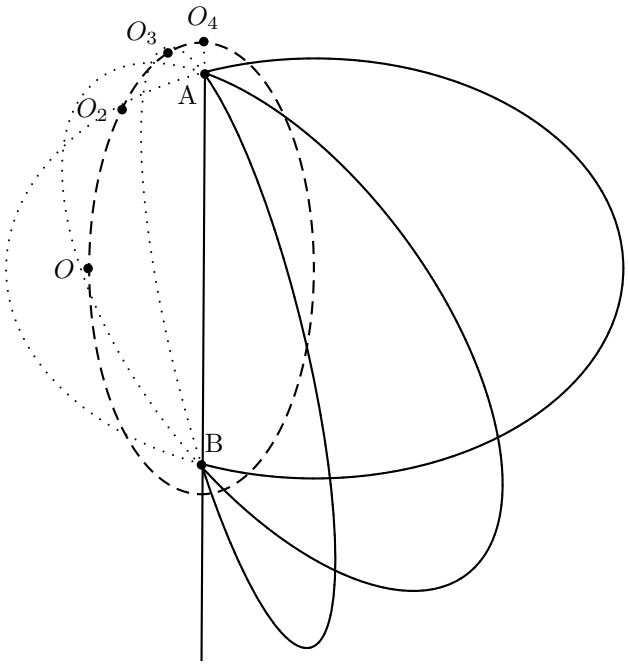

Figure 7.2: Lambert cycle of Keplerian arcs where the origin moves along a second ellipse with foci A and B.

of an ellipse with one focus in the origin, so we have

$$\cos\theta = \frac{1 - a(1-\epsilon^2)}{\epsilon}.$$

The elapsed time can then be computed with the help of theorem 7.1 and 7.2 by the elapsed time of a rectilinear arc. Since the energy $H_{\text{fix}} = -1/(2a)$ remains constant, the semi-major axis remains constant during the continuous change and, consequently, the supporting rectilinear orbit has length $2a$. We can follow the shape of the supporting ellipse during the continuous change by shifting the focus of the ellipse along a second ellipse with foci A and B going through the origin. The semi-major axis of this second ellipse is 1 in our case, since A and B lie on the unit circle, and therefore the elapsed time can be computed by using the free-fall time (3.12) from height $2a$ to A and to B.

By Proposition 7.4, depending on whether the original arc was I_O or D_O and I_F or D_F, the new rectilinear arc will also be I_O or D_O and I_F or D_F, respectively. The original arc is

$$\left\{\begin{matrix} I_O & \text{if } \theta \geq \dfrac{\pi}{2} \\ D_O & \text{if } \theta < \dfrac{\pi}{2} \end{matrix}\right\} \qquad \text{and} \qquad \left\{\begin{matrix} I_F & \text{if } 2a\epsilon \geq \cos\theta \\ D_F & \text{if } 2a\epsilon < \cos\theta \end{matrix}\right\},$$

and we can state the following conclusion:

Lemma 7.5:
The elapsed time of an outgoing second species generating arc is

$$\tau = 2\pi J\sqrt{a^3} + \begin{cases} t_{2a}(1+\sin\theta) + t_{2a}(0) + (t_{2a}(0) - t_{2a}(1-\sin\theta)) & \text{if } \cos\theta \leq 0 \\ t_{2a}(1+\sin\theta) + t_{2a}(1-\sin\theta) & \text{if } 0 < \cos\theta \leq 2a\epsilon \\ t_{2a}(1+\sin\theta) - t_{2a}(1-\sin\theta) & \text{if } 2a\epsilon < \cos\theta. \end{cases}$$

Remark 7.6:
There is no case I_O and D_F. If we rotate the arc such that the apoapsis—which has to be farther away than 1—lies on the Q_1-axis, then the second focus lies between the apoapsis and the origin on the Q_1-axis. Hence, if an outgoing arc is I_O, it is necessarily also I_F. The times of ingoing second species arcs are simply $2\pi\sqrt{a^3} = 2t_{2a}(0)$ minus the outgoing time.

The orbits which we will construct in the next section will only be outgoing second species generating orbits without M_3 winding around M_1, i. e. with $J = 0$. This restriction makes sense particularly in view of (7.2), where for negative angular momentum the only positive contribution to the action comes from the the term $1/\|Q\|$ which we try to keep as small as possible in order to get negative action. In this situation the following statement helps us to exclude orbits without winding of M_2 around M_1.

Theorem 7.7 (Theorem 7.2 from [AU20]):
In the Euclidean plane or space consider three distinct points O, A, B such that O is not on the segment AB. There is a unique D_O Keplerian arc around O and a unique simple I_O Keplerian arc around O going from A to B in a given positive elapsed time. In the exceptional case $O \in]A, B[$ there exist exactly two distinct I_O Keplerian arcs which are reflections of each-other.

Corollary 7.8:
There exist no S-arcs with $I = J = 0$ and $\epsilon' = +1$ which are not identical to M_2 at all times.

Proof: An S-arc requires a Keplerian arc with two distinct ends A and B on the unit circle. The timing condition for $I = J = 0$ requires that the elapsed time of the arc is exactly the elapsed time of M_2 between A and B. Since both M_2 and M_3 move in the same direct direction around M_1, the arc of M_3 is D_O and I_O if and only if the arc of M_2 is D_O and I_O, respectively. Uniqueness in theorem 7.7 give us that both arcs are the same and hence M_3 coincides with M_2 for all time. □

7.4 Sequences of generating orbits

We will now describe some sequences of generating orbits and also show where they are found in terms of Hénon's notation for generating families. Using our formulae from the

previous sections of this chapter, we can find generating orbits with negative action that have additional properties. In our case we want to control the energy and show that these orbits exist for all energies between $-\sqrt{2}$ and 0. All generating orbits described here will be of the second species, but not all orbits in this section will actually have negative action. They are then rather included here either because they are instructive and arise in Hénon's classification of families or because they are at the beginning of a sequence where the action tends towards negative values but is not necessarily negative throughout the entire sequence.

The main formula we will use to compute the action is equation (7.9), which is quite powerful but still requires the elapsed time of the Kepler arc between collisions with M_2. Since the Kepler arc corresponding to the generating orbit is usually not a full Kepler ellipse, we will use Lemma 7.5 for the remaining cases. To further simplify things, we will always set $J = 0$, i. e. the arc of M_3 does not wind around M_1 in fixed coordinates. The reason for this is equation (7.2), where the only term contributing positively to the action is $1/\|Q\|$ and we intend to keep this term small by not letting the orbit come unnecessarily close to M_1. Also, our generating orbits here will only consist of a single outgoing S-arc which is repeated infinitely to give a periodic generating orbit.

Another issue in order to analytically describe second species generating orbits is the timing condition

$$\tau = \begin{cases} 2\pi I + 2\theta & \text{for direct and rectilinear orbits} \\ 2\pi(I+1) - 2\theta & \text{for retrograde orbits,} \end{cases} \tag{7.11}$$

i. e. the requirement that M_3 collides again with M_2 after starting at collision and following the arc. This problem is avoided in this chapter by leaving a free parameter which will be the semi-major axis a of the supporting Kepler ellipse. We will then show that $\tau - 2\epsilon'\theta$ tends smoothly towards infinity as $a \to \infty$. This means that for all large enough numbers of revolution I of M_2 around M_1 in fixed coordinates there will be an a that solves the timing condition for that particular I. A one-parameter family with a as the free parameter will in this way give a sequence of second species generating orbits with an orbit for each large enough integer $I \geq 1$. Other parameters of the supporting Keplerian orbit which will be used in this section are the eccentricity ϵ, the semi-minor axis b, the polar angle of intersection with the unit circle θ and the direction of rotation ϵ'.

7.4.1 Fixed semi-minor axis

The first sequence we want to present is one where the energy converges towards zero and the action against negative infinity. This can be achieved by fixing the semi-minor axis b. The relation between b, a and ϵ is $b = a\sqrt{1-\epsilon^2}$, i. e.

$$\epsilon = \sqrt{1 - \frac{b^2}{a^2}}. \tag{7.12}$$

Inserting this into the Kepler energy (3.8) and the angular momentum (3.9), the rotating Kepler energy (3.16) becomes

$$H_0 = -\frac{1}{2a} - \epsilon' \frac{b}{\sqrt{a}} \tag{7.13}$$

which strictly monotonically tends towards zero from below as $a \to \infty$ and $\epsilon' = +1$ for any fixed b. We choose the easiest nonzero $b = 1$ for the sequence.

In order to define an outgoing arc not part of the unit circle, we need the maximal focal distance

$$a(1+\epsilon) = a + \sqrt{a^2 - 1} > 1, \qquad \text{i. e.} \qquad a > 1.$$

For the elapsed time of the arc we use Lemma 7.5, for which we need $\sin\theta$. Also, we need to check if the arcs are I_O and I_F, or D_O and I_F, or D_O and D_F. We can compute $\cos\theta$ from the equation for focal distances of ellipses (7.10):

$$\cos\theta = \frac{1 - a(1-\epsilon^2)}{\epsilon} = \frac{1 - \frac{1}{a}}{\sqrt{1 - \frac{1}{a^2}}} = \sqrt{\frac{a-1}{a+1}}$$

Since $a > 1$, we have

$$0 < \cos\theta = \sqrt{\frac{a-1}{a+1}} < 2\sqrt{(a-1)(a+1)} = 2a\epsilon,$$

i. e. all arcs in this sequence are D_O and I_F, and we can compute

$$\begin{aligned} \tau &= t_{2a}(1 - \sin\theta) + t_{2a}(1 + \sin\theta) \\ &= 2\sqrt{a^3} \left(\sqrt{\frac{1-\sin\theta}{2a}\left(1 - \frac{1-\sin\theta}{2a}\right)} + \sqrt{\frac{1+\sin\theta}{2a}\left(1 - \frac{1+\sin\theta}{2a}\right)} \right. \\ &\qquad \left. + \arccos\left(\sqrt{\frac{1-\sin\theta}{2a}}\right) + \arccos\left(\sqrt{\frac{1+\sin\theta}{2a}}\right) \right), \end{aligned} \tag{7.14}$$

where

$$\sin\theta = \sqrt{1 - \cos^2\theta} = \sqrt{1 - \frac{a-1}{a+1}} = \sqrt{\frac{2}{a+1}}. \tag{7.15}$$

Obviously, the elapsed time tends towards infinity as $a \to \infty$. In particular for $\epsilon' = +1$ the time $\tau - 2\theta$ becomes zero for the limit case $a = 1$ and depends smoothly on a. So there exists for every $I \geq 1$ an $a > 1$ solving the timing condition (7.11) and we get a sequence of second species generating orbits.

The regularised time from (7.8) becomes

$$\begin{aligned}\sigma &= \sqrt{a}\arccos\left(\sqrt{\frac{1-a(1-\epsilon)}{2a\epsilon}}\right)\\ &= \sqrt{a}\arccos\left(\sqrt{\frac{1-a\left(1-\sqrt{1-\frac{1}{a^2}}\right)}{2\sqrt{a^2-1}}}\right)\\ &= \sqrt{a}\arccos\left(\sqrt{\frac{1}{2}-\frac{1}{2}\sqrt{\frac{a-1}{a+1}}}\right) \qquad (7.16)\end{aligned}$$

and by inserting (7.12), (7.14) and (7.16) into (7.3), we get the action of these generating orbits:

$$\begin{aligned}\mathcal{A} = 2\sqrt{a^3}\left(-\frac{1}{a}-\epsilon'\frac{1}{\sqrt{a}}\right)&\left(\sqrt{\frac{1-\sqrt{\frac{2}{a+1}}}{2a}\left(1-\frac{1-\sqrt{\frac{2}{a+1}}}{2a}\right)}\right.\\ &+\sqrt{\frac{1+\sqrt{\frac{2}{a+1}}}{2a}\left(1-\frac{1+\sqrt{\frac{2}{a+1}}}{2a}\right)}+\arccos\left(\sqrt{\frac{1-\sqrt{\frac{2}{a+1}}}{2a}}\right)+\arccos\left(\sqrt{\frac{1+\sqrt{\frac{2}{a+1}}}{2a}}\right)\Bigg)\\ &+8\sqrt{a}\arccos\left(\sqrt{\frac{1}{2}-\frac{1}{2}\sqrt{\frac{a-1}{a+1}}}\right)\end{aligned}$$

This tends towards negative infinity as a goes towards infinity.

Summarising so far, we can state

Lemma 7.9:
There exists a sequence of second species generating orbits consisting of non-rectilinear S-arcs with semi-major axis $a > 1$, action tending towards negative infinity and energy H_0 strictly monotonically converging towards zero from below.

7.4.2 Fixed polar intersection angle with the unit circle

For more general sequences we fix the angle of intersection θ with the unit circle. We will look at all $\theta \in [0, \pi]$ but we will also highlight some special cases that arise. Let from now on $a > 1$. The eccentricity is computed by solving the equation (7.10) of the

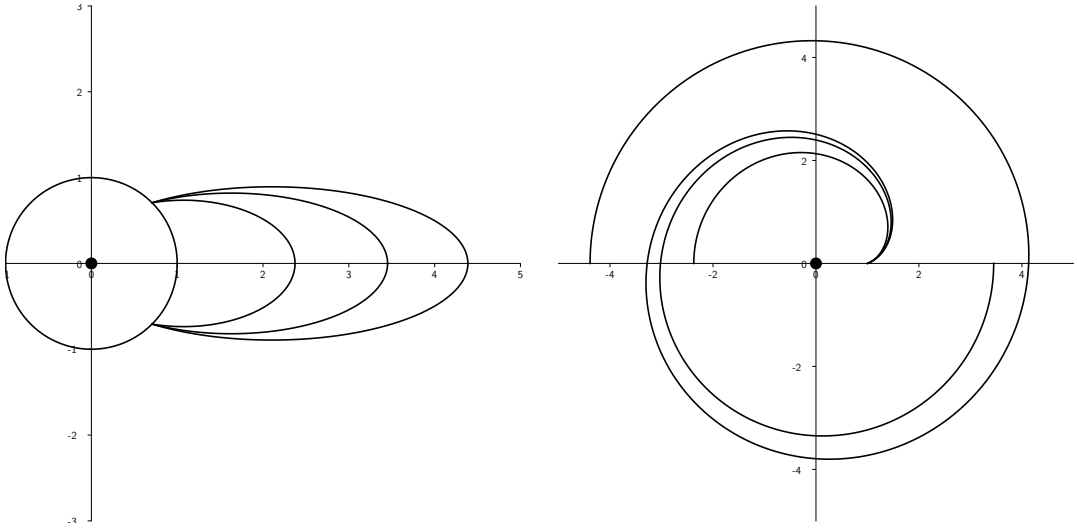

(a) In fixed coordinates. (b) Half orbits in rotating coordinates.

Figure 7.3: Second species arcs with fixed $\theta = \pi/4$ and $I = 1, 2$.

focal distance of ellipses for ϵ:

$$\begin{aligned} & 1 = \frac{a(1-\epsilon^2)}{1-\epsilon\cos\theta} \\ \iff \quad & a\epsilon^2 - \epsilon\cos\theta - a + 1 = 0 \\ \iff \quad & \epsilon = \frac{\cos\theta \pm \sqrt{\cos^2\theta + 4a(a-1)}}{2a} \qquad (7.17) \\ \overset{\epsilon\geq 0}{\iff} \quad & \epsilon = \frac{\cos\theta + \sqrt{\cos^2\theta + 4a(a-1)}}{2a} \qquad (7.18) \end{aligned}$$

Remark 7.10:
There exist ellipses intersecting the unit circle at polar angle $\theta \in [0, \pi/2]$ also for semi-major axes $a \leq 1$. However, a is no longer a monotone parameter there. Now both signs of (7.17) return nonnegative eccentricity. The actually smallest semi-major axis is attained at the largest root of the discriminant $\cos^2\theta + 4a(a-1)$. A better parameter for small a would for example be the eccentricity ϵ—see also proposition 2.5 in [AU20]—but we will stick to the semi-major axis as our parameter because computations of the energy and action are easier. Another advantage of setting $a > 1$ is that

$$2a\epsilon = \cos\theta + \sqrt{\cos^2\theta + 4a(a-1)} > \cos\theta, \qquad (7.19)$$

i. e. all arcs are I_F.

The energy becomes

$$\begin{aligned}
H_0 &= -\frac{1}{2a} - \epsilon'\sqrt{a(1-\epsilon^2)} \\
&= -\frac{1}{2a} - \epsilon'\sqrt{a\left(1 - \frac{\left(\cos\theta + \sqrt{\cos^2\theta + 4a(a-1)}\right)^2}{4a^2}\right)} \\
&= -\frac{1}{2a} - \epsilon'\sqrt{\frac{4a^2 - \cos^2\theta - 2\cos\theta\sqrt{\cos^2\theta + 4a(a-1)} - \cos^2\theta - 4a(a-1)}{4a}} \\
&= -\frac{1}{2a} - \epsilon'\sqrt{1 - \cos\theta\frac{\cos\theta + \sqrt{4a^2 - 4a + \cos^2\theta}}{2a}} \quad \overset{a\to\infty}{\longrightarrow} \quad -\epsilon'\sqrt{1-\cos\theta} \qquad (7.20)
\end{aligned}$$

and tends towards values between $-\sqrt{2}$ and $\sqrt{2}$ depending on θ and ϵ'. It was also computed in lemma 6.13 that the derivative $\partial H_0/\partial a$ never vanishes, so the energy strictly increases for $\epsilon' = +1$ and strictly decreases for $\epsilon' = -1$ along a.

In the first case $\theta < \pi/2$ all arcs are D_O and I_F, and we compute the elapsed time from lemma 7.5 to be

$$\begin{aligned}
\tau &= t_{2a}(1+\sin\theta) + t_{2a}(1-\sin\theta) \\
&= 2\sqrt{a^3}\left(\sqrt{\frac{1-\sin\theta}{2a}\left(1 - \frac{1-\sin\theta}{2a}\right)} + \sqrt{\frac{1+\sin\theta}{2a}\left(1 - \frac{1+\sin\theta}{2a}\right)}\right. \qquad (7.21) \\
&\qquad \left. + \arccos\left(\sqrt{\frac{1-\sin\theta}{2a}}\right) + \arccos\left(\sqrt{\frac{1+\sin\theta}{2a}}\right)\right).
\end{aligned}$$

In the second case $\theta \geq \pi/2$ all arcs are I_O and I_F, and we use the first case in lemma 7.5, so

$$\begin{aligned}
\tau &= t_{2a}(1+\sin\theta) + t_{2a}(0) + (t_{2a}(0) - t_{2a}(1-\sin\theta)) \\
&= 2\sqrt{a^3}\left(\sqrt{\frac{1+\sin\theta}{2a}\left(1 - \frac{1+\sin\theta}{2a}\right)} + \arccos\left(\sqrt{\frac{1+\sin\theta}{2a}}\right) + \frac{\pi}{2}\right. \\
&\qquad \left. + \left(\frac{\pi}{2} - \sqrt{\frac{1-\sin\theta}{2a}\left(1 - \frac{1-\sin\theta}{2a}\right)} - \arccos\left(\sqrt{\frac{1-\sin\theta}{2a}}\right)\right)\right).
\end{aligned}$$

It is obvious in both cases that for fixed θ the elapsed time τ increases strictly and tends towards infinity as $a \to \infty$ because τ is only the sum of free-fall times to the same points from increased heights $2a$. This means the timing condition (7.11) has a unique solution for every large enough $I \geq 1$. Note that corollary 7.8 states that there is no nontrivial solution for $I = 0$. We also see that the assumption $a > 1$ is no restriction, since for $a = 1$ and $\theta > 0$ we get

$$\tau < 2t_2(0) = 2\pi < 2\pi + 2\theta.$$

Hence, the timing condition for $\epsilon' = +1$, $I = 1$ and any fixed $\theta > 0$, is always satisfied for an $a > 1$. The case $\theta = 0$ will later be treated separately.

The regularised time is

$$\begin{aligned}\sigma &= \sqrt{a}\arccos\left(\sqrt{\frac{1-a(1-\epsilon)}{2a\epsilon}}\right)\\ &= \sqrt{a}\arccos\left(\sqrt{\frac{\frac{2-2a+\cos\theta+\sqrt{\cos^2\theta+4a(a-1)}}{2}}{\cos\theta+\sqrt{\cos^2\theta+4a(a-1)}}}\right)\\ &= \sqrt{a}\arccos\left(\sqrt{\frac{1}{2}-\frac{a-1}{\cos\theta+\sqrt{\cos^2\theta+4a(a-1)}}}\right)\end{aligned}$$

and the action from (7.9) becomes

$$\begin{aligned}\mathcal{A} = \tau&\left(-\frac{1}{a}-\epsilon'\sqrt{1-\cos\theta\frac{\cos\theta+\sqrt{4a^2-4a+\cos^2\theta}}{2a}}\right)\\ &+8\sqrt{a}\arccos\left(\sqrt{\frac{1}{2}-\frac{a-1}{\cos\theta+\sqrt{\cos^2\theta+4a(a-1)}}}\right).\end{aligned}\tag{7.22}$$

The important feature is that the action tends towards negative infinity for every fixed and positive θ as $a \to \infty$ and $\epsilon' = +1$ since the angular momentum tends towards $\sqrt{1-\cos\theta}$. This holds in both cases $\theta < \pi/2$ and $\theta \geq \pi/2$ since $\sqrt{a^3}$ multiplied by bounded terms outweighs the only positive term of $\sqrt{a}$ times something bounded.

In the limit case $\theta = 0$, however, the angular momentum vanishes completely and we get

$$\begin{aligned}H_0 &= -\frac{1}{2a}\\ \tau &= 2\sqrt{a^3}\left(2\sqrt{\frac{1}{2a}\left(1-\frac{1}{2a}\right)}+2\arccos\left(\sqrt{\frac{1}{2a}}\right)\right)\\ \sigma &= \sqrt{a}\arccos\left(\sqrt{\frac{1}{2a}}\right)\end{aligned}$$

and hence

$$\begin{aligned}\mathcal{A} &= -\frac{4}{a}\sqrt{a^3}\left(\sqrt{\frac{1}{2a}\left(1-\frac{1}{2a}\right)}+\arccos\left(\sqrt{\frac{1}{2a}}\right)\right)+8\sqrt{a}\arccos\left(\sqrt{\frac{1}{2a}}\right)\\ &= 4\sqrt{a}\arccos\left(\sqrt{\frac{1}{2a}}\right)-2\sqrt{2-\frac{1}{a}}.\end{aligned}$$

The action here no longer tends towards negative values and is in fact always nonnegative. In fixed coordinates M_3 would fall freely towards M_1—where we would have to regularise—and then bounce back to the place it started. In our setting of an outgoing generating orbit of the second species with $J = 0$, however, M_3 would not make it that far since it would first collide with M_2 moving on the unit circle.

Two more special cases will be mentioned here: the case $\theta = \pi/2$ and $\theta = \pi$. For $\theta = \pi$ the arcs are full Kepler ellipses, i. e. second species of type 2. We get

$$\begin{aligned} H &= -\frac{1}{2a} - \epsilon' \sqrt{2 - \frac{1}{a}} \\ \tau &= 2\pi\sqrt{a^3} \\ \sigma &= \frac{\pi\sqrt{a}}{2} \end{aligned}$$

and

$$\begin{aligned} \mathcal{A} &= 2\pi\sqrt{a^3}\left(-\frac{1}{a} - \epsilon'\sqrt{2 - \frac{1}{a}}\right) + 8\frac{\pi\sqrt{a}}{2} \\ &= 2\pi\sqrt{a} - 2\pi\epsilon' a\sqrt{2a-1}. \end{aligned}$$

This action obviously has the same sign as $-\epsilon'$ for all $a > 1$. Since these generating orbits are both first and second species orbits, they are naturally bifurcation orbits. In the continuation to the restricted three-body problem the intersection of the corresponding families splits into two separate families here.

In the remaining special case we fix $\theta = \pi/2$. The data simplifies to

$$\begin{aligned} H_0 &= -\frac{1}{2a} - \epsilon', \\ \tau &= 2\sqrt{a^3}\left(\sqrt{\frac{1}{a}\left(1 - \frac{1}{a}\right)} + \arccos\left(\sqrt{\frac{1}{a}}\right) + \frac{\pi}{2}\right) \\ &= \pi\sqrt{a^3} + 2\sqrt{a(a-1)} + 2\sqrt{a^3}\arccos\left(\sqrt{\frac{1}{a}}\right), \\ \sigma &= \sqrt{a}\arccos\left(\sqrt{\frac{1}{2} - \frac{a-1}{\sqrt{4a(a-1)}}}\right) \\ &= \sqrt{a}\arccos\left(\sqrt{\frac{1}{2} - \frac{1}{2}\sqrt{\frac{a-1}{a}}}\right) \end{aligned}$$

and

$$\mathcal{A} = \left(\pi\sqrt{a^3} + 2\sqrt{a(a-1)} + 2\sqrt{a^3}\arccos\left(\sqrt{\frac{1}{a}}\right)\right)\left(-\frac{1}{a} - \epsilon'\right) + 8\sqrt{a}\arccos\left(\sqrt{\frac{1}{2} - \frac{1}{2}\sqrt{\frac{a-1}{a}}}\right).$$

What happens here is that in fixed coordinates the angular velocity (3.11) of M_3 exactly matches that of M_2 at the point of collision:

$$\frac{\mathrm{d}\varphi}{\mathrm{d}t} = \frac{\sqrt{a\,(1-\epsilon^2)}}{r^2} = \sqrt{a\left(1 - \frac{4a(a-1)}{4a^2}\right)} = 1 \tag{7.23}$$

Theorem 6.9 can no longer exclude a collision in the perturbation to the restricted three-body problem because the ingoing and outgoing vectors in rotating coordinates are parallel. So, at this point a new loop forms around M_2. More explicitly, in the restricted three-body problem, orbits coming from generating orbits with $\theta < \pi/2$ will wind $I-1$ times around both M_1 and M_2 and then pass in between M_1 and M_2, while orbits coming from generating orbits with $\theta > \pi/2$ will wind $I-1$ times around M_1 and then wind once around M_2 before starting over. This transition from $\theta = \pi$ and $\epsilon' = -1$ to $\theta = \pi$ and $\epsilon' = +1$ via $\theta = 0$ happens in the $\{S_{-\alpha-1}\}$ segments in families f and h as described in [Hén97]. For generating orbits with $I = 1$ and corresponding continued orbits in the restricted three-body problem for small mass ratios as θ crosses $\pi/2$ see also figure 8.2 in the next chapter.

Generating family f—see figure 7.4a—comes from the simple direct orbits in Hill's lunar problem and transitions into family $E^+_{1,1}$ of first species generating orbits at the critical point with energy $H_0 = -3/2$ and abscissa $q_1(0) = 1$ for negative $\dot{q}_2(0)$. It follows $E^+_{1,1}$ with growing energy, undergoes collision with M_1 at $H_0 = -1/2$ and $q_1(0) = 2$, and picks up a loop around M_1 there. The generating family arrives at $H_0 = 1/2$ and $q_1(0) = 1$ as a double cover of the retrograde circular orbit, which is also a second species orbit with $\theta = \pi$ and $\epsilon' = -1$. From there it follows the branch of second species generating orbits $S_{-2,-1}$, transitioning to $\theta = \pi$ and $\epsilon' = +1$ and picking up a loop at $\theta = \pi/2$ and $\epsilon' = +1$ as described above. The last orbit at $\theta = \pi$ is again a first species orbit in the family E^+_{31} and this cycle continues indefinitely between $E^+_{2k-1,1}$ and $S_{-2k,-1}$ for all $k > 0$.

Family h comes from the retrograde circular orbits I_r and then at $a = 1$ goes into the branch $S_{-1,-1}$ at $\theta = \pi/2$ and $\epsilon' = -1$. Then it goes along, while taking up a loop, to $\theta = \pi$ and $\epsilon' = +1$ as described above. There, it takes the branch of first species family E_{21}, which takes up another loop at collision with M_1, and carries on until the inner loop collides with M_2 again. From there on it resumes a similar pattern as family f and alternates between $S_{-2k-1,-1}$ and $E_{2k,1}$ for all $k > 0$.

The summary of the information from this chapter which is important for the proof of the main theorem is

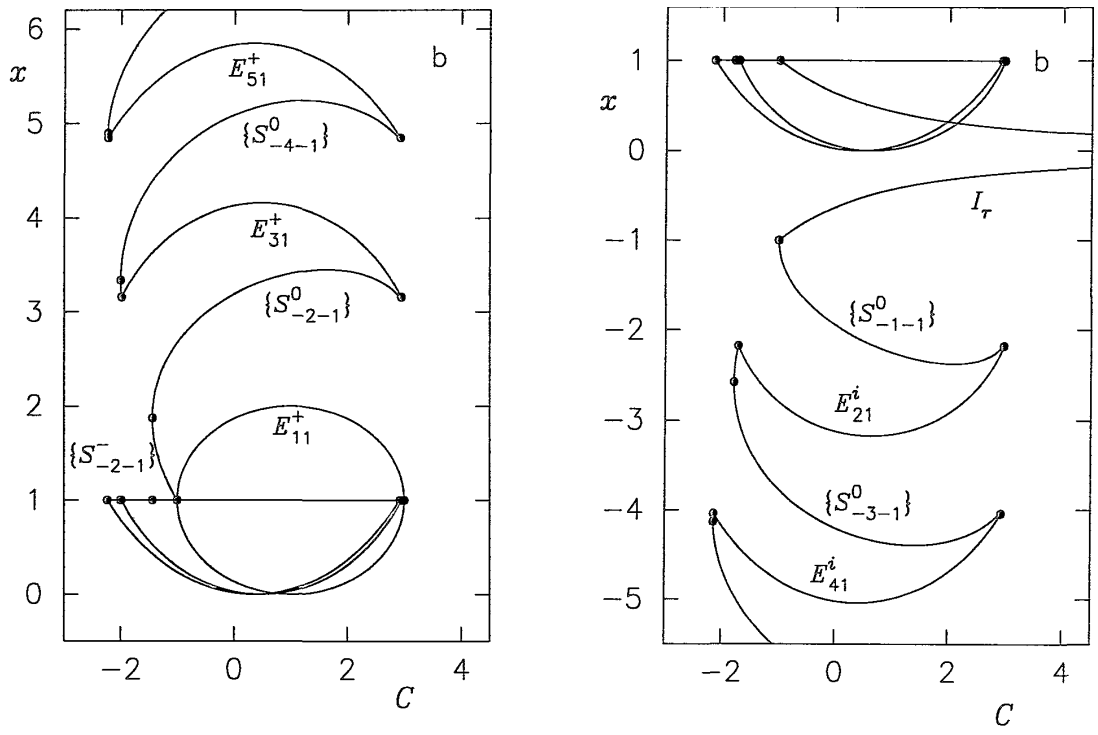

(a) Family f (b) Family h

Figure 7.4: Two symmetric families of generating orbits as shown in [Hén97].

Lemma 7.11:
For every $c \in [-\sqrt{2}, 0]$ there exists a sequence of second species generating orbits consisting of S-arcs with action tending towards negative infinity and energy converging strictly from below to c.

Chapter 8

Proof of main theorem

We are now ready to put everything together and show up the consequences of these orbits for the existence of contact structures in the restricted three-body problem. For this we first of all want to improve lemma 7.11. In fact, we can get sequences of orbits with negative action tending towards negative infinity with constant energy at any value between 0 and $-\sqrt{2}$. We can also choose these sequences such that all orbits are ordinary and nondegenerate. This is particularly helpful since the statement of theorem 6.9 finds orbits close to the generating orbit with the exact same energy under these circumstances.

Lemma 8.1:
For every $c \in [-\sqrt{2}, 0)$ there exists a sequence of ordinary nondegenerate generating orbits of the second species with energy c and negative action tending to $-\infty$.

Proof: As we have seen in the preceding chapter 7, there exists for every polar intersection angle $\theta \in [0, \pi]$ with the unit circle and every number of rotation $I \geq 1$ a unique second species arc. For $\epsilon' = +1$ these arcs have energy converging strictly monotonically to $-\sqrt{1 - \cos\theta}$ from below and their action tends to $-\infty$ if $\theta > 0$ as $I \to \infty$. Since the elapsed time τ and the energy $H_0 = c$ of the arcs depend smoothly on θ, we get for every $I \geq 1$ a smooth curve

$$c_I \colon [0, \pi] \to \mathbb{R}$$

mapping θ to the energy of the unique direct arc where the timing condition (7.11) is satisfied for I and θ. The sequences for all fixed θ are strictly increasing in c along a, so we have $c_{I_1} < c_{I_2}$ for all $I_1 < I_2$ and the curves c_I converge to $-\sqrt{1 - \cos\theta}$ as $I \to \infty$.

Let $c_0 \in [-\sqrt{2}, 0)$. We restrict the curves c_I to $[\arccos(1 - c_0^2)/2, \pi] \subset (0, \pi]$. Here, for all sequences of arcs with fixed θ, the action tends towards $-\infty$ as $a \to \infty$. So we can find for every $\theta \in [\arccos(1 - c_0^2)/2, \pi]$ an $N_\theta > 0$ such that the action of the arc with polar intersection angle θ and semi-major axis $a > N_\theta$ is negative. Assign this real number N_θ to every θ by the smooth function

$$\begin{aligned} N \colon [\arccos(1 - c_0^2)/2, \pi] &\to \mathbb{R} \\ \theta &\mapsto N_\theta. \end{aligned}$$

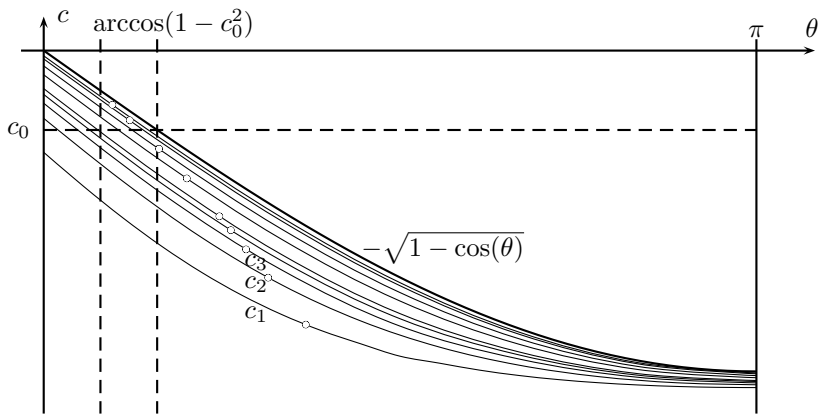

Figure 8.1: The curves c_I mapping a simple direct arc of polar intersection angle θ to its energy.

Then N attains its maximum $\hat{N}$ at some point and for all $\theta \in [\arccos(1-c_0^2)/2, \pi]$ and $a > \hat{N}$ the corresponding arcs have negative action.

To find the smallest I where every point on the curve c_I is attained for an arc with semi-major axis $a > \hat{N}$, we look at solutions of the timing condition for all real $I_\theta \in (1, \infty)$. Again we assign this value to every arc with semi-major axis $a = \hat{N}$ and $\theta \in [\arccos(1-c_0^2)/2, \pi]$ by the smooth function

$$\begin{aligned} I\colon [\arccos(1-c_0^2)/2, \pi] &\to (1, \infty) \subset \mathbb{R} \\ \theta &\mapsto I_\theta. \end{aligned}$$

This, again, attains its maximum $\hat{I} \in (0, \infty)$ at some point. So for all integers $I > \hat{I}$ we have full curves $c_I\colon [\arccos(1-c_0^2)/2, \pi] \to (-\infty, 0)$ corresponding to arcs with semi-major axis $a > \hat{N}$, i. e. with negative action. Finally,

$$\Big\{(\theta, c_I(\theta)) \mid I > \hat{I}, \theta \in [\arccos(1-c_0^2)/2, \pi)\Big\} \cap \big\{(\theta, c_0) \mid \theta \in [\arccos(1-c_0^2)/2, \pi)\big\}$$

is a sequence of points on the graphs $\bigcup_I \Gamma(c_I)$ converging to $(\arccos(1-c_0^2), c_0)$. There are no degenerate or non-ordinary orbits in these sequences anymore since $\theta \neq 0, \pi$. Furthermore, the only orbits with parallel velocities at collision in these sequences are where the arcs intersect the unit circle with angle $\theta = \pi/2$. We can simply exclude these, since this affects at most one single element in the sequence. Hence, we have found a sequence of ordinary nondegenerate second species generating orbits with energy c_0 and negative action.

By doing the same process again for an arbitrarily small action we can show that the action of orbits in this sequence indeed tends towards $-\infty$. □

In a next step we will check the integral of the first de Rham generator β_0—which was computed in 5.2—along the continued orbits that we get from the sequences of

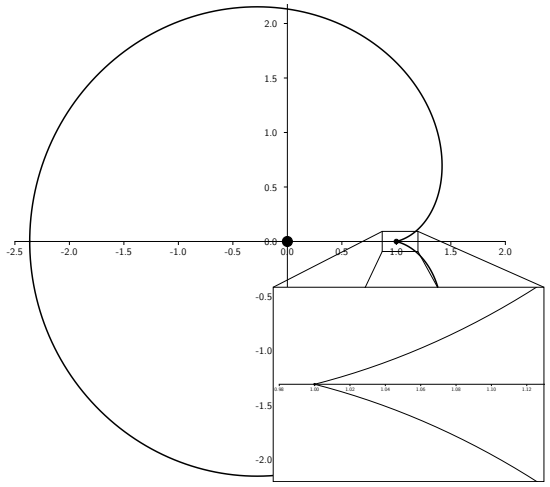

(a) Generating orbit for $\theta = \pi/3$

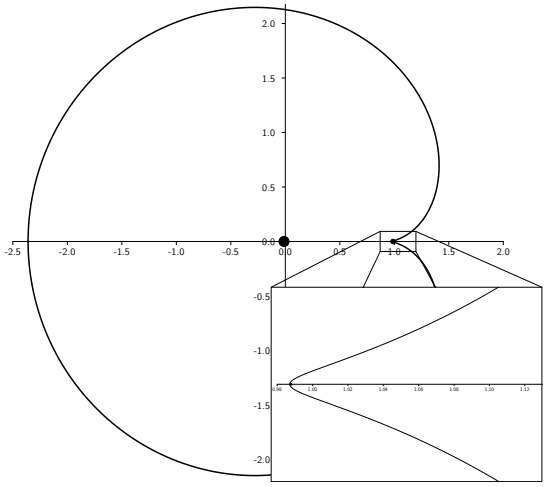

(b) Continued orbit for $\theta = \pi/3$

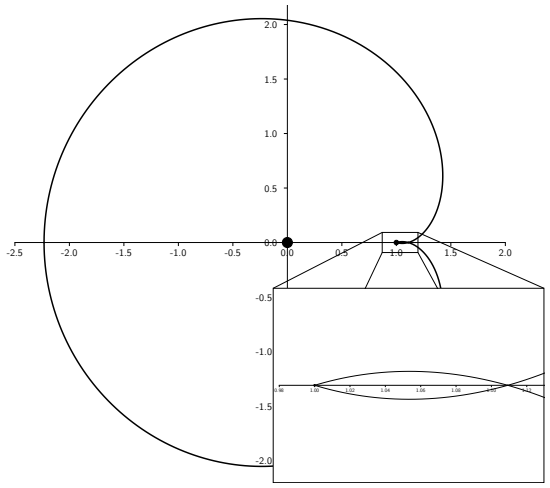

(c) Generating orbit for $\theta = 2\pi/3$

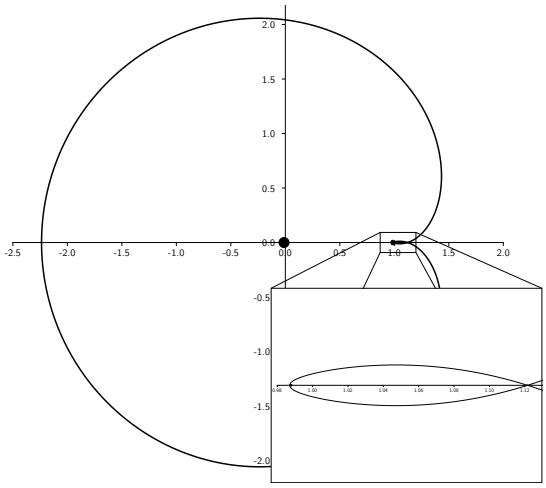

(d) Continued orbit for $\theta = 2\pi/3$

Figure 8.2: Generating orbits as θ crosses $\pi/2$ and their continuations at the same energy level in the restricted three-body problem with earth-moon mass ratio $\mu = 0.01214$.

generating orbits. We need this for the planar case in view of remark 2.36 to construct an obstruction to contact forms using noncontractible orbits.

Lemma 8.2:
Let γ be an orbit in one of the sequences from lemma 8.1 and γ_μ a continuation to the restricted three-body problem with mass ratio μ by theorem 6.9. Then the integral over the first de Rham generator β_0 of $\overline{\Sigma} \cong \overline{\Sigma}_{\mu,c}$ along γ_μ is

$$\int_S^1 \gamma_\mu^* \beta_0 = -1.$$

Proof: As in the proof of 8.1, the initial and final velocities of the generating arc at collision are non-parallel in rotating coordinates and by theorem 6.9 the continued orbit γ_μ does not collide with M_2. We can compute the integral over $\beta_0|_{\Sigma_{\mu,c}} = 2\,\mathrm{d}\vartheta - \mathrm{d}\varphi_1 - \mathrm{d}\varphi_2$ by two times the rotation number minus the two winding numbers around M_1 and M_2.

In the case $\theta \in (0, \pi/2)$ the angle between the initial and final velocities of the generating arc at collision is between 0 and π in rotating coordinates. The continuation uses hyperbolic solutions on the Levi-Civita regularisation close to M_2 and all arcs are outgoing. So the continued orbit passes between M_1 and M_2 on a trajectory that looks like a hyperbola close to M_2. Recall the integer numbers of rotation I and J of M_2 and M_3 around M_1. In all of our sequences we have $J = 0$ while $I \geq 1$. This gives us the rotation number $-I$, the winding number $-I$ around M_1 and the winding number $-I+1$ around M_2. Overall, this gives

$$\int_{S^1} \gamma_\mu^* \beta_0 = -2I + I + I - 1 = -1.$$

In the case $\theta \in (\pi/2, \pi)$ the angle between initial and final velocity at collision is in between π and 2π, and the angular velocity dropping below one—see(7.23)—forming an additional loop around M_2 in the continuation. Therefore, the rotation number becomes $-I-1$, the winding numbers $-I$ around M_1 and $-I-1$ around M_2. All in all we get the same integral

$$\int_{S^1} \gamma_\mu^* \beta_0 = 2(-I-1) + I + I + 1 = -1,$$

as claimed. □

Before we can finally prove the main theorem, we first need to discuss exactly what Hamiltonian structures and primitives we are dealing with:
Let $\overline{\Sigma}_{\mu,c}$ be the Moser-regularised energy hypersurface of the restricted three-body problem with mass ratio $\mu \in (0,1)$ for an energy $c > H_\mu(L_5)$ above the highest critical value. By the Moser regularisation, the Hamiltonian structure ω on $\Sigma_{\mu,c}$ extends to collisions and we get the Hamiltonian manifold $(\overline{\Sigma}_{\mu,c}, \overline{\omega})$. The Liouville 1-form $\lambda = p\,\mathrm{d}q$, on the other hand, does not extend. We do, however, have a local primitive $\tilde{\lambda}$ of $\overline{\omega}$ in a neighbourhood U of collision at each primary because the fibre is Lagrangian and so ω vanishes on the intersection of the regularised hypersurface with the fibre over $p = \infty$. On the intersection $V := \Sigma_{\mu,c} \cap U$ both $\lambda|_V$ and $\tilde{\lambda}|_V$ are primitives of $\overline{\omega}|_V = \omega|_V$, so $\mathrm{d}(\lambda|_V - \tilde{\lambda}|_V) = 0$. The subset $V \subset \overline{\Sigma}_{\mu,c}$ is diffeomorphic to $S^*(\mathbb{R}^n \setminus \{0\})$, which has trivial fundamental group for $n = 3$. So in this case the first de Rham cohomology of V is trivial and the closed 1-form $\lambda|_V - \tilde{\lambda}|_V$ has a primitive $f \in C^\infty(V)$. Let $g \in C^\infty(V)$ be a smooth cut-off function which is identically zero on $\Sigma_{\mu,c}$ and identically one in a small neighbourhood of $p = \infty$ in U. Define

$$\overline{\lambda} := \begin{cases} \lambda & \text{in } \Sigma_{\mu,c} \setminus V \\ \lambda - \mathrm{d}(gf) & \text{in } V \\ \tilde{\lambda} & \text{in } U \setminus V \end{cases}$$

as a smooth extension of $\lambda|_{\Sigma_{\mu,c}\setminus V}$ onto $\overline{\Sigma}_{\mu,c}$. For $n=2$, V does have a large fundamental group, but we can simply define $\overline{\lambda}$ as the restriction of the three-dimensional construction. The minimal distance to collision for all second species orbits with non-parallel velocity vectors at collision gives us enough space for our small neighbourhood U. In that way the local change of primitive does not change the action of the orbit.

Using this notation, we can now explicitly state the main theorem which will be divided into the planar case $n=2$ and the spatial case $n=3$:

Theorem 8.3:
In the planar case we have:
For every $c \in [-\sqrt{2}, 0)$ and $r_0 \in \mathbb{R}$ there exists a $\mu_0 > 0$ such that for every $\mu \in (0, \mu_0]$ the Hamiltonian manifold $(\overline{\Sigma}_{\mu,c}, \overline{\omega})$ of the planar circular restricted three-body problem with mass ratio μ does not admit an $\overline{\omega}$-compatible contact form α such that $[\alpha - \overline{\lambda}] = [r\beta_0] \in H^1_{\mathrm{dR}}(\overline{\Sigma}_{\mu,c})$ for any coefficient $r \geq r_0$.
For the spatial case:
For every $c \in [-\sqrt{2}, 0)$ there exists a $\mu_0 > 0$ such that for every $\mu \in (0, \mu_0]$ the Hamiltonian manifold $(\Sigma_{\mu,c}, \omega)$ of the circular restricted three-body problem with mass ratio μ does not admit an ω-compatible contact form α.

Proof: We begin with the planar case: Let $c_0 \in [-\sqrt{2}, 0)$ and $r_0 \in \mathbb{R}$ be arbitrary. Then lemma 8.1 from above gives us an ordinary non-degenerate generating orbit γ_0 with energy c and action $\mathcal{A}(\gamma_0) < r_0 - \varepsilon$ for any $\varepsilon > 0$. By theorem 6.9 there exists a $\mu_0 > 0$ such that for all $\mu \in (0, \mu_0]$ there an orbit orbit γ_μ in the restricted three-body problem with mass ratio μ that has energy c and action $\mathcal{A}(\gamma_\mu) \in (\mathcal{A}(\gamma_0) - \varepsilon, \mathcal{A}(\gamma_\mu) + \varepsilon)$, i. e. $\mathcal{A}(\gamma_\mu) < r_0$. We have furthermore seen in lemma 8.2 that the continued orbits from lemma 8.1 in the restricted three-body problem all have $\int \gamma_\mu^* \beta_0 = -1$.

Assume by contradiction that we have an $\overline{\omega}$-compatible contact form $\alpha \in \Omega^1(\overline{\Sigma}_{\mu,c})$ such that $[\alpha - \overline{\lambda}] = [r\beta_0] \in H^1_{\mathrm{dR}}(\overline{\Sigma})$ for an $r \geq r_0$. Then we can write $\alpha = \overline{\lambda} + r\beta_0 + \mathrm{d}f$ and integrate

$$\int_{S^1} \gamma_\mu^* \alpha = \int_{S^1} \gamma_\mu^* (\overline{\lambda} + r\beta_0 + \mathrm{d}f) = \int_{S^1} \gamma_\mu^* \lambda + r \int_{S^1} \gamma_\mu^* \beta_0 = \mathcal{A}(\gamma_\mu) - r \leq \mathcal{A}(\gamma_\mu) - r_0 < 0.$$

This contradicts fact (2.2), stating that the integral over a compatible contact form along a Hamiltonian solution needs to be positive.

In the spatial case all constructed orbits are contractible since already $\Sigma_{\mu,c}$ has trivial fundamental group. Therefore, we can use equation (2.3) to directly get the claimed statement. □

This concludes the main part of this work and in the remaining chapters we will fist look at some numerical computations on these orbits and then discuss what questions arise and what future research could be suggested on this topic.

Chapter 9

Numerical results

After the analytical results from the previous chapter we want to add some numerical computations to visualise the continuations for actual mass ratios. There will be two sections which both focus on direct orbits from sequences of section 7.4.2. In the first section we will fix the number of rotation I of M_2 around M_1 at 1 and vary θ, i. e. we will look at the first orbit in these sequences. For the second section we will fix a θ and look at the first several orbits in this sequence.

The data for generating orbits was obtained by numerically solving the timing condition (7.11) for the semi-major axis a and then computing the energy H_0 and the action $\mathcal{A}$ from equations (7.20) and (7.22). The remaining parameter q_0 represents the apoapsis distance from the origin, which is the initial position of the orbit. Continued orbits for small mass ratios were found by using the symmetry (3.19) and shooting perpendicularly from the q_1-axis while searching for perpendicular intersections when returning. The programming for finding these orbits was done in python using standard libraries for solving ODEs and integration. The results are numerical evidence of how far the described generating orbits might be followed and do not represent numerical or computer assisted proofs.

9.1 First orbit in sequence with varying intersection angle

Table 9.1 shows the data for generating orbits for $I = 1$ and varying θ from 0 to π. We use degrees instead of radians to describe the angle θ which will be incremented in 10 degree steps. From (7.22) we know that the action of generating orbits in the sequences with fixed $\theta \in (0, \pi]$ tends to $-\infty$ as $I \to \infty$. However, not all sequences always have negative action, as one can see in the case where θ is at 10 degrees. In the boundary case $\theta = 0$ the action of orbits in the sequence does not tend to negative values and is instead always positive. Figure 9.1 shows every third of these generating orbits in fixed coordinates Q and in rotating coordinates q. We note the special cases $\theta = \pi$ where the deflection angle is zero, i. e. the generating orbit is non-ordinary, and $\theta = \pi/2$ where the deflection angle is $-\pi$ and even the continued orbit might collide with M_2.

Table 9.2 shows the initial positions of these orbits when continued to the astronomical

mass ratios $\mu \approx 0.000953$ of the Sun-Jupiter system, $\mu \approx 0.012143$ of the Earth-Moon system and $\mu \approx 0.108511$ of the Pluto-Charon system. These mass ratios were chosen for the relevance in our solar system: The Sun-Jupiter system has the largest mass ratio of all the planets in relation to the sun and governs many phenomena like the occurrence of asteroids. Obviously, the Earth-Moon system is of major importance to us and plays a large part in near-Earth satellites and lunar space missions. Pluto and Charon have the largest mass ratio of a binary system in our solar system and serves as the largest mass ratio we will have to deal with in our current reach. Table 9.3 adds some larger non-astronomical values as well. In all the continuations the same energy value is held as the generating orbit in accordance with theorem 6.9.

We can see that smaller values of θ seem to continue up to higher mass ratios as opposed to larger values of θ. Here, after some point no orbit could be found nearby and the corresponding entries are marked with an "x". This makes good sense since the limit orbits at $\theta = \pi$ are bifurcation orbits and here two intersecting families of generating orbits split in the continuation and move away from the original bifurcation orbit.

Also the action of continued orbits seems to always be slightly larger than that of the generating orbit. On the other hand, even the first generating orbits in most of theses sequences yield negative action, especially for large values of θ. The smallest energy where one gets a generating orbit with negative action is already very close to the critical value $-3/2$. Although these are only isolated orbits, one might now expect that there is an obstruction for the restricted three-body problem to be of contact type for all energies between 0 and the highest critical value $H_\mu(L_5)$.

9.2 Sequence at 10 degrees intersection angle

We now take a closer look at the first sequence from 9.1 where the intersection angle θ is nonzero. This was the only one where the action of the first orbit is nonnegative. So, we are firstly interested in how quickly the action becomes negative, but also if we can still continue the generating orbit to the large mass ratio of $\mu = 0.5$ as the sequence goes on.

These generating orbits are computed in table 9.4 and we see that the action becomes negative at the 10^{th} orbit in the sequence. Furthermore, we can see the energy slowly converging to $-\sqrt{1-\cos(\pi/18)} \approx -0.123256$ while the semi-major axis grows. Tables 9.5 and 9.6 show again the continued orbits to the same mass ratios as before. Here, we notice that also the higher orbits in the sequence so far all continue all the way up to $\mu = 0.5$ and eventually even the action becomes negative for this large mass ratio. This evidence suggests that the restricted three-body problem might not be of contact type in between the highest critical value and zero for any mass ratio $\mu \in (0, 1)$. Note, as mentioned in section 7.4.2, that all orbits with even I belong to the same family f and all orbits with odd I belong to family h in Hénon's notation. This is visualised in figure 9.2 where the generating and continued orbits of this sequence are depicted for the first three $I = 1, 2, 3$.

θ	a	q_0	H_0	$\mathcal{A}$
0	1.114891	2.229783	-0.448474	1.434641
10	1.151460	2.289513	-0.597508	0.472433
20	1.191803	2.331984	-0.737353	-0.479144
30	1.234738	2.358649	-0.865060	-1.392612
40	1.278895	2.371414	-0.978834	-2.246054
50	1.322831	2.372473	-1.077948	-3.024066
60	1.365152	2.364145	-1.162569	-3.717803
70	1.404646	2.348721	-1.233529	-4.324279
80	1.440377	2.328356	-1.292090	-4.845201
90	1.471746	2.304988	-1.339732	-5.285607
100	1.498494	2.280307	-1.377985	-5.652556
110	1.520668	2.255753	-1.408307	-5.954007
120	1.538560	2.232546	-1.432015	-6.197965
130	1.552639	2.211726	-1.450243	-6.391878
140	1.563480	2.194211	-1.463929	-6.542246
150	1.571719	2.180859	-1.473821	-6.654366
160	1.578013	2.172531	-1.480481	-6.732160
170	1.583022	2.170155	-1.484294	-6.777997
180	1.587401	2.174802	-1.485467	-6.792454

Table 9.1: Generating orbits for $I = 1$ and θ in degrees.

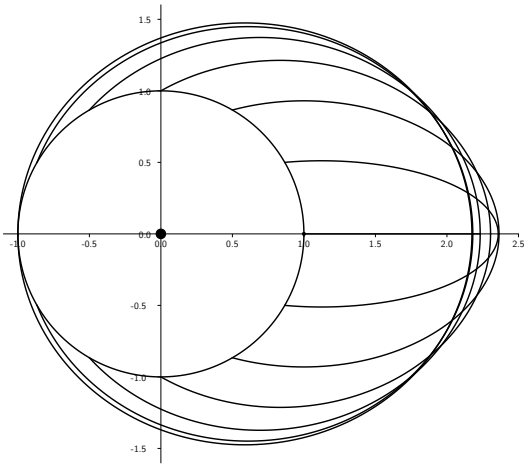

(a) In fixed coordinates Q.

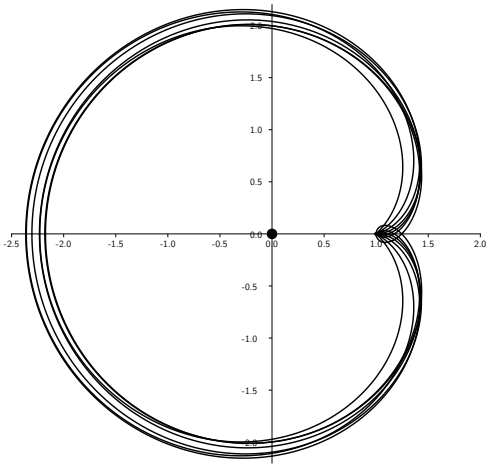

(b) In rotating coordinates q.

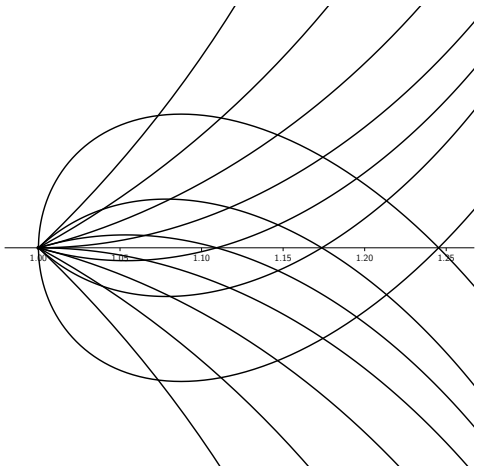

(c) Close-up view of the neighbourhood of M_2 in rotating coordinates.

Figure 9.1: Generating orbits for $I = 1$ and varying θ from 0 to π in steps of 10 degrees.

	Sun-Jupiter		Earth-Moon		Pluto-Charon	
θ	q_0	$\mathcal{A}$	q_0	$\mathcal{A}$	q_0	$\mathcal{A}$
0	2.229061	1.446733	2.220504	1.546640	2.142401	2.136580
10	2.288901	0.485253	2.281639	0.590492	2.216384	1.209834
20	2.331460	-0.465552	2.325234	-0.355078	2.269946	0.288979
30	2.358198	-1.378186	2.352824	-1.262459	2.305515	-0.597382
40	2.371026	-2.230715	2.366375	-2.109609	2.325631	-1.426317
50	2.372143	-3.007720	2.368130	-2.881020	2.332950	-2.181565
60	2.363871	-3.700338	2.360452	-3.567767	2.330171	-2.853621
70	2.348508	-4.305571	2.345684	-4.166823	2.319969	-3.439064
80	2.328214	-4.825112	2.326039	-4.679890	2.305002	-3.939387
90	2.304939	-5.263994	2.303542	-5.112050	2.288258	-4.359638
100	2.280390	-5.629270	2.280016	-5.470452	2.281012	-4.707251
110	2.256040	-5.928906	2.257156	-5.763208	x	x
120	2.233168	-6.170932	2.236858	-5.998577	x	x
130	2.212958	-6.362855	x	x	x	x
140	2.196764	-6.511324	x	x	x	x
150	2.190318	-6.622143	x	x	x	x
160	x	x	x	x	x	x
170	x	x	x	x	x	x
180	x	x	x	x	x	x

Table 9.2: Continued orbits for $I = 1$ and θ in degrees for astronomical mass ratios.

	$\mu = 0.2$		$\mu = 0.5$	
θ	q_0	$\mathcal{A}$	q_0	$\mathcal{A}$
0	2.059605	2.593750	x	x
10	2.150085	1.693790	1.816536	3.069224
20	2.215887	0.792632	1.992154	2.275666
30	2.261108	-0.079578	2.113013	1.462972
40	2.289277	-0.898644	x	x
50	2.303809	-1.647264	x	x
60	2.308293	-2.315120	x	x
70	2.307463	-2.898274	x	x
80	x	x	x	x
90	x	x	x	x
100	x	x	x	x
110	x	x	x	x
120	x	x	x	x
130	x	x	x	x
140	x	x	x	x
150	x	x	x	x
160	x	x	x	x
170	x	x	x	x
180	x	x	x	x

Table 9.3: Contiunued orbits for $I = 1$ and θ in degrees for non-astronomical mass ratios.

I	a	q_0	H_0	$\mathcal{A}$
1	1.151461	2.289514	-0.597508	0.472433
2	1.703950	3.397169	-0.439704	0.971722
3	2.180544	4.351247	-0.369431	1.179810
4	2.610411	5.211440	-0.328406	1.217261
5	3.007662	6.006225	-0.301045	1.142278
6	3.380347	6.751789	-0.281280	0.986919
7	3.733587	7.458411	-0.266220	0.770813
8	4.070887	8.133123	-0.254297	0.506915
9	4.394782	8.781000	-0.244582	0.204272
10	4.707173	9.405855	-0.236486	-0.130527
11	5.009538	10.010645	-0.229617	-0.492519
12	5.303051	10.597720	-0.223702	-0.877859
13	5.588663	11.168989	-0.218546	-1.283506
14	5.867162	11.726026	-0.214003	-1.707004
15	6.139207	12.270150	-0.209966	-2.146341
16	6.405358	12.802481	-0.206349	-2.599845
17	6.666093	13.323979	-0.203088	-3.066108
18	6.921829	13.835474	-0.200128	-3.543935
19	7.172927	14.337693	-0.197428	-4.032299
20	7.419707	14.831273	-0.194953	-4.530312

Table 9.4: Generating orbits for fixed $\theta = \pi/18$.

	Sun-Jupiter		Earth-Moon		Pluto-Charon	
I	q_0	$\mathcal{A}$	q_0	$\mathcal{A}$	q_0	$\mathcal{A}$
1	2.288901	0.485253	2.281639	0.590492	2.216384	1.209834
2	3.396803	0.984282	3.392470	1.089921	3.353351	1.733091
3	4.350951	1.192265	4.347446	1.297962	4.315925	1.949195
4	5.211184	1.229658	5.208155	1.335366	5.180883	1.990792
5	6.005993	1.154636	6.003252	1.260344	5.978585	1.918388
6	6.751575	0.999251	6.749047	1.104955	6.726282	1.764807
7	7.458211	0.783125	7.455838	0.888823	7.434486	1.550010
8	8.132933	0.519211	8.130687	0.624905	8.110475	1.287122
9	8.780818	0.216555	8.778675	0.322245	8.759385	0.985285
10	9.405681	-0.118255	9.403624	-0.012570	9.385118	0.651146
11	10.010477	-0.480255	10.008494	-0.374574	9.990653	0.289708
12	10.597558	-0.865603	10.595640	-0.759926	10.578382	-0.095163
13	11.168832	-1.271256	11.166970	-1.165583	11.150223	-0.500404
14	11.725873	-1.694760	11.724061	-1.589089	11.707773	-0.923547
15	12.270001	-2.134103	12.268235	-2.028434	12.252356	-1.362572
16	12.802335	-2.587611	12.800611	-2.481946	12.785104	-1.815798
17	13.323836	-3.053878	13.322149	-2.948216	13.306981	-2.281813
18	13.835334	-3.531709	13.833682	-3.426048	13.818826	-2.759415
19	14.337556	-4.020076	14.335935	-3.914418	14.321365	-3.247575
20	14.831139	-4.518092	14.829547	-4.412436	14.815244	-3.745402

Table 9.5: Continued orbits for fixed $\theta = \pi/18$ for astronomical mass ratios.

	$\mu = 0.2$		$\mu = 0.5$	
I	q_0	$\mathcal{A}$	q_0	$\mathcal{A}$
1	2.150085	1.693790	1.816536	3.069224
2	3.313535	2.246562	3.137846	3.758241
3	4.283998	2.472591	4.146060	4.022613
4	5.153181	2.519383	5.033830	4.088841
5	5.953545	2.450237	5.846074	4.031746
6	6.703154	2.298919	6.603994	3.888747
7	7.412800	2.085796	7.319979	3.681770
8	8.089940	1.824206	8.002119	3.424935
9	8.739790	1.523409	8.656086	3.127945
10	9.366317	1.190125	9.286061	2.797789
11	9.972531	0.829403	9.895240	2.439691
12	10.560854	0.445144	10.486136	2.057670
13	11.133216	0.040432	11.060773	1.654893
14	11.691232	-0.382250	11.620811	1.233905
15	12.236233	-0.820866	12.167634	0.796784
16	12.769361	-1.273728	12.702410	0.345255
17	13.291585	-1.739416	13.226138	-0.119236
18	13.803747	-2.216723	13.739680	-0.595463
19	14.306580	-2.704616	14.243785	-1.082372
20	14.800730	-3.202198	14.739113	-1.579057

Table 9.6: Continued orbits for fixed $\theta = \pi/18$ for nonastronomical mass ratios.

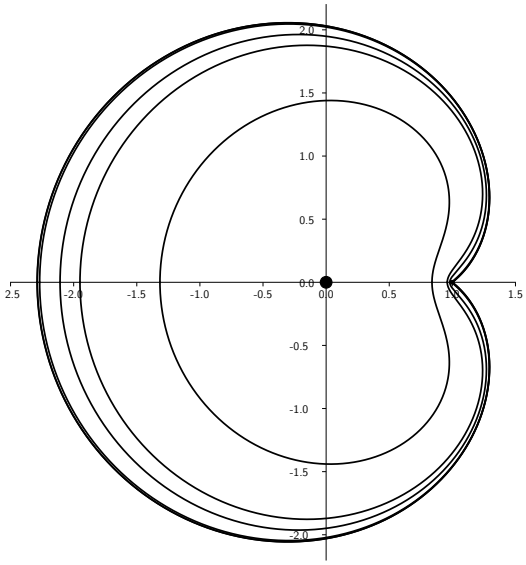

(a) $I = 1$

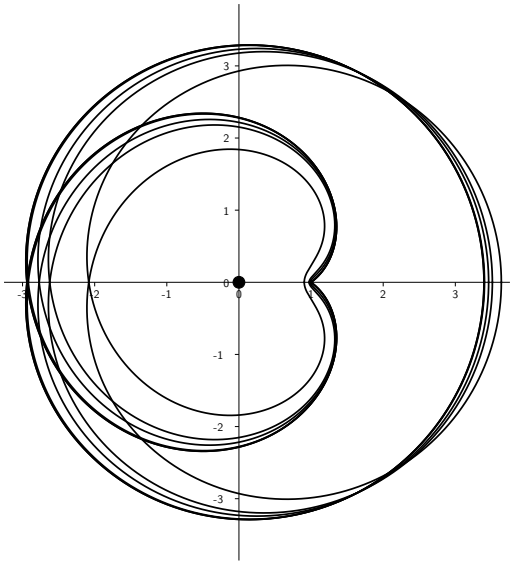

(b) $I = 2$

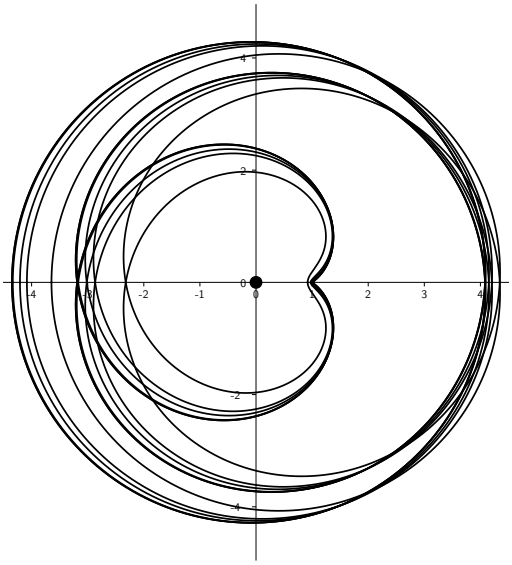

(c) $I = 3$

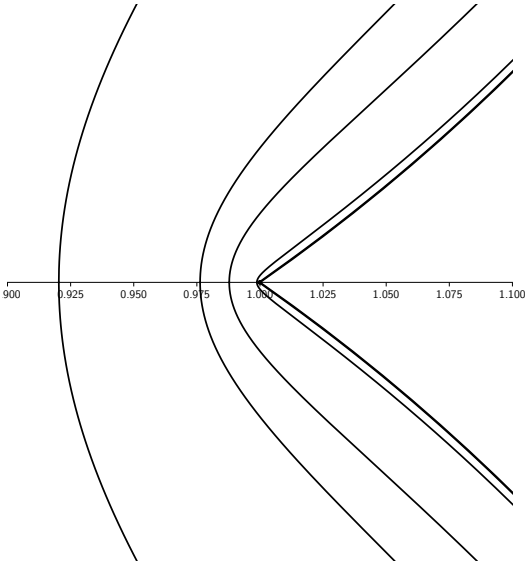

(d) Close-up view of the neighbourhood of M_2.

Figure 9.2: Generating orbit and continued orbits for $\theta = \pi/18$.

Chapter 10

Final remarks and research outlook

There are still some questions that remain after the preceding discussions and results and we will address them in this last chapter.

Firstly, one could hope to simplify the main statement for the planar case. The problem so far is that the constructed orbits of negative action are not contractible in the regularised energy hypersurface of the planar problem but only for the hypersurface of the spatial problem. So if one had orbits with negative action which are also contractible for $n = 2$, then one could prove a similarly strong statement for the two-dimensional case as for the three-dimensional case. A way to find these orbits could be to simply add one or several arcs to the current generating orbits, such that the resulting continued orbits in the restricted three-body problem are contractible. The action of the orbits in the sequences of lemma 8.1 would then be modified by a constant term, leaving the limit unchanged. The problem of finding such arcs reduces in some sense to a combinatorial problem but so far the searches for such auxiliary arcs were not successful.

Secondly, it would be interesting to know how large the mass ratios μ in the main theorem actually are. All results on continuing generating orbits to the restricted three-body problem are perturbative, so we can not give a quantitative result with these methods. Numerical evidence suggest that the orbits can be continued and also the negative action remains even for very large mass ratios all the way up to 0.5. There is, however, no analytical proof yet.

Another question is if the lower limit $-\sqrt{2}$ in the main theorem has any meaning or how far down one can rule out contact structures. Since the sequences from lemma 7.11 approach the energies from below, there are certainly orbits with lower energies and negative action. However, it is quite hard to explicitly prove single generating orbits, because one would have to solve the rather complicated equations and not just look at the limits. One could, here as well, look for different generating orbits that could well give lower limits in the energy. The critical value $H_\mu(L_5)$ becomes $-3/2$ for $\mu = 0$, which is the value one could still hope to reach with these methods. For all lower energies between $H_\mu(L_5)$ and $H_\mu(L_1)$ one would have to resort to generating orbits from Hill's lunar problem, which is a difficult dynamical system in its own right.

A different direction could also be to consider different generating orbits all together.

In this work, we only looked at generating orbits as the limit where $\mu \to 0$. However, also other limits would in general be possible and might offer interesting insights. For example, one could investigate the limit as the angular momentum tends to zero. The resulting dynamical system in the limit case would then be Euler's problem of two fixed centres, which is again completely integrable and very well studied. A downside would be that one can not use theorem 6.9 as it stands because in its requirements there is a potential term tending to zero and not a magnetic term.

Bibliography

[AFvKP12] Peter Albers, Urs Frauenfelder, Otto van Koert, and Gabriel P. Paternain. Contact geometry of the restricted three-body problem. *Comm. Pure Appl. Math.*, 65(2):229–263, 2012.

[Alb19] Alain Albouy. Lambert's theorem: Geometry or dynamics? *Celest Mech Dyn Astr*, 131(40), 2019.

[AM78] Ralph Abraham and Jerrold E. Marsden. *Foundations of Mechanics.* Addison-Wesley Publishing Company, Inc., 2 edition, 1978.

[Are63] Richard F. Arenstorf. Periodic solutions of the restricted three body problem representing analytic continuations of keplerian elliptic motions. *American Journal of Mathematics*, 85:27, 1963.

[AU20] Alain Albouy and Antonio J. Ureña. Some simple results about the lambert problem. *Eur. Phys. J. Spec. Top.*, 229, 2020.

[BFvK19a] Edward Belbruno, Urs Frauenfelder, and Otto van Koert. A family of periodic orbits in the three-dimensional lunar problem. *Celestial Mech. Dynam. Astronom.*, 131(2):Paper No. 7, 22, 2019.

[BFvK19b] Edward Belbruno, Urs Frauenfelder, and Otto van Koert. The omega limit set of a family of chords. *Journal of Topology and Analysis*, 02 2019.

[Bir14] George D. Birkhoff. The restricted problem of three bodies. *Rendiconti del Circolo Matematico di Palermo*, 39:265–334, 1914.

[Bir36] George D. Birkhoff. Sur le problème restreint des trois corps (second mémoire). *Annali della Scuola Normale Superiore di Pisa - Classe di Scienze*, 2e série, 5(1):9–50, 1936.

[BM00] Sergey V. Bolotin and Robert S. Mackay. Periodic and chaotic trajectories of the second species for the n-centre problem. *Celestial Mech. Dynam. Astronom.*, 77(1):49–75 (2001), 2000.

[Bru94] Alexander D. Bruno. *The Restricted 3-Body Problem: Plane Periodic Orbits.* De Gruyter, Berlin, New York, 1994.

[Cel06] Alessandra Celletti. Basics of regularization theory. In B. A. Steves, A. J. Maciejewski, and M. Hendry, editors, *Chaotic Worlds: From Order to Disorder in Gravitational N-Body Dynamical Systems*, pages 203–230, Dordrecht, 2006. Springer Netherlands.

[Che89] Alain Chenciner. Le problème de la lune et les systèmes dynamiques. Preprint Université Paris-VII, 1989.

[CJK20] Wanki Cho, Hyojin Jung, and Geonwoo Kim. The contact geometry of the spatial circular restricted 3-body problem. *Abhandlungen aus dem Mathematischen Seminar der Universität Hamburg*, 90(2):161 – 181, 2020.

[CM00] Alain Chenciner and Richard Montgomery. A remarkable periodic solution of the three-body problem in the case of equal masses. *Ann. of Math. (2)*, 152(3):881–901, 2000.

[Con63] Charles Conley. On some new long periodic solutins of the plane restricted three body problem. *Comm. Pure Appl. Math.*, 16:449–467, 1963.

[Flo88] Andreas Floer. Morse theory for Lagrangian intersections. *J. Differential Geom.*, 28(3):513–547, 1988.

[Fra17] Urs Frauenfelder. Lecture notes on symplectic geometry at the university of augsburg, 2017.

[Fra18] Urs Frauenfelder. Lecture notes on J-holomorphic curves at the University of Augsburg, 2017/2018.

[FvK18] Urs Frauenfelder and Otto van Koert. *The Restricted Three-Body Problem and Holomorphic Curves*. Pathways in Mathematics. Birkhäuser Basel, 2018.

[Gei08] Hansjörg Geiges. *An Introduction to Contact Topology*. Cambridge Studies in Advanced Mathematics. Cambridge University Press, 2008.

[GO91] Gerard Gómez and Merce Ollé. Second-species solutions in the circular and elliptic restricted three-body problem. I. Existence and asymptotic approximation. *Celestial Mech. Dynam. Astronom.*, 52(2):107–146, 1991.

[Hag70] Yusuke Hagihara. *Dynamical principles and transformation theory*, volume 1 of *Celestial Mechanics*. MIT Press, 1970.

[Hén69] Michele Hénon. Numerical exploration of the restricted problem. v. *Astronomy & Astrophysics*, 1:223–238, 1969. Hill's Case: Periodic Orbits and Their Stability.

[Hén97] Michel Hénon. *Generating families in the restricted three-body problem*, volume 52 of *Lecture Notes in Physics. New Series m: Monographs*. Springer-Verlag, Berlin, 1997.

[Hil78] George W. Hill. Researches in the lunar theory. *American Journal of Mathematics*, 1(1):5–26, 1878.

[Hof93] Helmut Hofer. Pseudoholomorphic curves in symplectizations with applications to the Weinstein conjecture in dimension three. *Invent. Math.*, 114(3):515–563, 1993.

[HSa11] Umberto Hryniewicz and Pedro A. S. Salomão. On the existence of disk-like global sections for Reeb flows on the tight 3-sphere. *Duke Math. J.*, 160(3):415–465, 2011.

[HWZ98] Helmut Hofer, Kris Wysocki, and Eduard Zehnder. The dynamics on three-dimensional strictly convex energy surfaces. *Ann. of Math. (2)*, 148(1):197–289, 1998.

[KS65] Paul Kustaanheimo and Eduard Stiefel. Perturbation theory of kepler motion based on spinor regularization. *Journal für die reine und angewandte Mathematik*, 218:204–219, 1965.

[Lam61] Johann H. Lambert. *Insigniores orbitae cometarum proprietates*. Eberhard Klett, Augusta Vindelicorum (Augsburg), 1761.

[LC20] Tullio Levi-Civita. Sur la régularisation du problème des trois corps. *Acta Math.*, 42(1):99–144, 1920.

[MHO09] Kennth R. Meyer, Glen R. Hall, and Dan Offin. *Introduction to Hamiltonian Dynamical Systems and the N-Body Problem*. Springer Science+ Buisiness Media, 2 edition, 2009.

[MN95] Jean-Pierre Marco and Laurent Niederman. Sur la construction des solutions de seconde espèce dans le problème plan restreint des trois corps. *Ann. Inst. H. Poincaré Phys. Théor.*, 62(3):211–249, 1995.

[Mos70] Jürgen Moser. Regularization of kepler's problem and the averaging method on a manifold. *Communications on Pure and Applied Mathematics*, 23(4):609–636, 1970.

[MZ05] Jürgen Moser and Eduard Zehnder. *Notes on Dynamical Systems*, volume 12 of *Courant lecture notes in mathematics*. American Mathematical Soc., 2005.

[Poi92] Henri Poincaré. *Les méthodes nouvelles de la mécanique céleste*, volume 1. Gauthier-Villars, Paris, 1892.

[Poi93] Henri Poincaré. *Les méthodes nouvelles de la mécanique céleste*, volume 2. Gauthier-Villars, Paris, 1893.

[Poi99] Henri Poincaré. *Les méthodes nouvelles de la mécanique céleste*, volume 3. Gauthier-Villars, Paris, 1899.

[Str34] Elis Strömgren. Eine Klasse unsymmetrischer librationsähnlicher periodischer Bahnen im Problème Restreint und ihre Entwicklungsgeschichte (Klasse n). *Publikationer og mindre Meddeler fra Kobenhavns Observatorium*, 94:1–I.2, 1934.

[Str35] Elis Strömgren. Connaisance actuelle des orbites dans le problème des trois corps. *Bulletin Astronomique*, 9:87–130, 1935.

[Sze67] Victor G. Szebehely. *Theory of orbits, the restricted problem of three bodies.* Academic Press, 1967.

[Win31] Aurel Wintner. Grundlagen einer genealogie der periodischen bahnen im restringierten dreikörperproblem. *Math. Z.*, 34(3):321–402, 1931.